Molecular interaction of Epap-1 and small molecules with Spike protein: Development of SARS-CoV-2 entry inhibitors

A THESIS SUBMITTED

TO THE UNIVERSITY OF HYDERABAD

FOR THE DEGREE OF DOCTOR OF PHILOSOPHY

By

C V Vidya

(18LTPH08)



Supervisor

Prof. Anand K. Kondapi

Department of Biotechnology & Bioinformatics
School of Life Sciences
University of Hyderabad
Hyderabad-500046
INDIA



Department of Biotechnology & Bioinformatics School of Life Sciences University of Hyderabad Hyderabad-500046. Telangana, India.

CERTIFICATE

This is to certify that the thesis entitled "Molecular interaction of Epap-1 and small molecules with Spike protein: Development of SARS-CoV-2 entry inhibitors" submitted by Ms. C V Vidya bearing registration number 18LTPH08 in partial fulfillment of the requirements for the award of Doctor of Philosophy in the Department of Biotechnology and Bioinformatics, School of Life Sciences is a bonafide work carried out by him under my supervision and guidance.

This thesis is free from plagiarism and has not been submitted previously in part or in full to this or any other University or Institution for the award of any degree or diploma.

Further, the student has the following publication (s) before submission of the thesis/monograph for adjudication and has produced evidence for the same in the form of the acceptance letter or the reprint in the relevant area of his research: (Note: at least one publication in referred journal is required the research)

Voina VC, Swain S, Kammili N, Mahalakshmi G, Muttineni R, Chander Bingi T, Kondapi AK. Effect of Early pregnancy associated protein-1 on Spike protein and ACE2

interactions: Implications in SARS Cov-2 vertical transmission. Placenta. 2024 May 17;152:39-52. doi: 10.1016/j.placenta.2024.05.128. Epub ahead of print. PMID: 38788480.

And Presented in the following conferences/workshops:

S.No. 1	Conferences/Workshops International Conference on Combat HIV 2019	Year
1 2		
2		19-21 January
2	(Participated)	2019
-	35th INTERNATIONAL SOCIETY FOR	21st March
	ANTIVIRAL RESEARCH (ISAR), Seattle, WA,	2022- 25th
	USA. (Poster presentation)	March 2022
3	BioAnveshana: Symposium on Frontiers in	7 th – 8 th Nov
	Biotechnology and Bioinformatics, Department of	2022
	Biotechnology and Bioinformatics, School of	
	Lifesciences, University of Hyderabad. (Poster	
	presentation)	
4	92nd Annual Meet of the Society of Biological	18-20th Dec
	Chemists, BITS Pilani K K Birla Goa Campus (Poster	2023
	presentation)	
5	BioAnveshana: Symposium on Frontiers in	15-18
3	Biotechnology and Bioinformatics, Department of	February 2024
	Biotechnology and Bioinformatics, School of	1 001 daily 2021
	Lifesciences, University of Hyderabad. (Participated)	
6	37th INTERNATIONAL SOCIETY FOR	20 th - 24 th
	ANTIVIRAL RESEARCH (ISAR), Gold Coast,	May, 2024
	Australia. (Poster presentation)	
7	ML & AI Using Covid-19 Virus Data AnalysisML &	20 th -21 th June,
,	AI Using Covid-19 Virus Data Analysis, Finland Labs	2020
	(A Unit of Revert Technology Pvt. Ltd.) In Association	
	with National Social Summit, IIT Roorkee Finland Labs	
I.	(Workshop)	
		1
δ	Statistical Machine Learning for Riologists, CMSD.	19 th -22 nd
8	Statistical Machine Learning for Biologists, CMSD, University of Hyderabad	19 th -22 nd December,
8	Statistical Machine Learning for Biologists, CMSD, University of Hyderabad (Workshop)	1

Further, the student has passed the following courses towards the fulfilment of the coursework requirement for a Ph.D.

COURSE	TITLE OF THE COURSE	CREDITS	RESULTS
NO			
S801	RESEARCH METHODOLOGY/ ANALYTICAL	4	PASS
	TECHNIQUES		
S802	RESEARCH ETHICS, BIOSAFETY, DATA	4	PASS
	ANALYSIS		
S803	RESEARCH PROPOSAL AND SCIENTIFIC	4	PASS
	WRITING		

SupervisorDAPI
ANAND K.
Senior Professor
Senior Professor Senior Professor

spt. of Biotechnology & Bioinformatics

School of Life Sciences

University of Hyderabad

Gechinowil, Hyderabad 198 046.

HEAD

of Department

Dept. of Biotechnology & Bioinformatics University of Hyderabad Hyderabad.

संकाय **PESA Dean** जीव विज्ञान संकाय / School of Life Sciences हैदराबाद विश्वविद्यालय /University of Hyderabad हैदराबाद / Hyderabad-500 046.



Department of Biotechnology & Bioinformatics
School of Life Sciences
University of Hyderabad
Hyderabad-500046. Telangana, India.

DECLARATION

Epap-1 and small molecules with Spike protein: Development of SARS-CoV-2 entry inhibitors" has been carried out by me in the Department of Biotechnology and Bioinformatics, School of Life Sciences, University of Hyderabad, Hyderabad, Telangana under the guidance of Prof. Anand K. Kondapi. I hereby declare that this work is original and has not been submitted in part or full for any other degree or diploma of any other University or Institution.

Name: C V Vidya

Place: Hyderabad

Date: 25/6/2024

Acknowledgements

I am grateful to my supervisor, Prof. Anand K. Kondapi, who has supported me throughout my work with his patience and guidance.

I would like to thank Doctoral Committee members Dr. Sunanda Bhattacharya and Dr. N Prakash Prabhu for their valuable suggestions.

I extend my sincere gratitude to the present Head of the Department of Biotechnology and Bioinformatics, Prof JSS Praksh, and former Head, Prof. K.P.M.S.V. Padmasree, for providing departmental facilities for the smooth conduction of research work.

I am thankful to former Deans Prof. Ramaiah and Prof. Dayananda Siddavattam, and the present Dean, Prof. Anand K Kondapi of the School of Life Sciences, for giving me the opportunity to use the necessary facilities to carry out my work. I especially want to thank Dr. Pankaj Singh Dholaniya for letting me use his cell culture facility whenever needed.

I thank all the faculty members of Life Sciences for their cooperation and their extended help during my work.

I am thankful to the University Grand Commission (UGC) for the financial support as a form of fellowship during the tenure of my PhD and to funding agencies of Govt. of India (DBT, SERB, DST, ICMR) for funding our laboratory and Departments are highly acknowledged.

I thank my past and present lab mates Dr. Akhila, Dr.Jagadeesh, Dr. D.A. Kiran, Dr. Suresh Mallepalli, Dr. Chukhu Muj, Satyajit, Neha, Pritikana, Sarita, Veena, Sandra, Hema, Rithika, Vennala, Soni and Dr. Ravindar Chinapaka for their co-operation, support and cheerful nature all through my research.

I thank Mr. B Sreenivas and Mr. Sreenivas Murthy for their cooperation.

I thank all the lab members of Prof. Sharmistha Banerjee for their help and support.

I am also thankful to my friends Yaseen, Harish Dubey, Sriram, Govind, Anushka, Nandini, Omkar, Siranjeevi, Satrupa, Santhosh, Sawmya, Sushree Sharma, Priyanka Saxena, Gayatri R, Danteshwari akka, Sharma sir, Neha S, Priyambada, Anu bhagat, Indu and Mani for their moral support.

My deepest gratitude goes to my Parents for their love, support, and inspiration throughout my life.

I thank the Almighty for granting me strength, wisdom, and knowledge and showering his blessings.

Last but not least, I offer my regards to all of those who supported me in any aspect of my PhD life.

C V Vidya

Abbreviation

SARS	: Severe Acute Respiratory Syndrome	
COVID-19	: Coronavirus Disease of 2019	
SARS-CoV-2	: SARS-Coronavirus-2	
Epap-1	: Early pregnancy associated protein-1	
S-protein	: Spike protein	
RBD	: Receptor Binding Domain of Spike protein	
ACE2	: Angiotensin Converting Enzyme-2	
PD	: Peptidase domain	
ELISA	: Enzyme-linked immunosorbent assay	
HRP	: Horseradish peroxidase	
BHK-21	: Baby Hamster Kidney-21	
DMEM	: Dulbecco's Modified Eagle Medium	
MEM	: Eagle's Minimum Essential Medium	
FBS	: Fetal bovine serum	
IF	: Immunofluorescence	
μg	: Microgram Concentration	
μΜ	: Micromolar Concentration	
IC ₅₀	: 50% Inhibitory Concentration	
PVDF	: Polyvinylidene Flouride	
НСОН	: Formaldehyde	
Na ₂ S ₂ O ₃	: Sodium thiosulphate	
AgNO ₃	: Silver nitrate	
Na ₂ CO ₃	: Sodium carbonate	
RT	: Room Temperature	
O/N	: Overnight	

CONTENTS

Chapter 1:	Introduction	
1.1 Introduction		2
1.2 SARS-CoV	2 and Pregnancy	7
1.3 Early pregna	ncy associated protein-1 and its role	8
1.4 The placenta	acts as an Anti-viral barrier	8
1.5 Rational of the	he study	10
Chapter 2:	Materials and Methods	
2.1 Materials		12
2.1.1 Antibodies		12
2.1.2 Molecular	Biology Materials	12
2.1.3 Biochemic	als & Cell Culture Materials	12
2.1.4 Instrument	s	13
2.1.5 Software T	Cools	13
2.1.6 Cell types		13
2.2 Methodology	y	13
2.2.1 Cell line		13
2.2.2 Modelling	studies	13
2.2.3 Purification	n of Epap-1 from first trimester placental tissue	15
2.2.4 Silver Stair	ning	15
2.2.5 Cloning of	Spike and RBD proteins	16
2.2.6 Expression	of Spike and RBD in cell lines	16
2.2.7 Western B	lotting	17
2.2.8 Immunoflu	orescence	18
2.2.9 Expression	and Purification of Receptor binding	
domain (RF	BD) in DHα and BL-21 (DE3)	18
2.2.10 Purification	on of IgG from Covid-19 Positive Blood	
sample usi	ing Proteinase A column affinity chromatography	19
2.2.11 Analysis	of the effect of Epap-1 interaction	

with S-protein/RBD protein and ACE2 interaction	
using ELISA	19
2.2.11. A. Analysis of Epap-1 Interaction with S-protein	19
2.2.11. B. Analysis of Epap-1 interaction with RBD-protein	20
2.2.12 Analysis of the effect of Epap-1 interaction with S protein	
and ACE2 interaction using immunofluorescence	21
2.2.13 Analysis of the effect of Epap-1 interaction with RBD	
protein and ACE2 interaction using immunofluorescence	22
2.2.14 Antiviral assay	23
2.2.15 Analysis of Proviral DNA with SK38 and SK39 Primers	24
2.2.16 Analysis of Novel Small Molecules interaction with RBD	
using ELISA	25
2.2.17 Analysis of Novel Small Molecules Interaction with RBD	
using Spectrofluorometer	26
2.2.18 Antiviral Assay of RBD and Spike Pseudovirus with	
Small Molecules	26
2.2.18. A. Antiviral assay	26
2.2.18. B. Analysis of Proviral DNA with SK38 and SK39 Primers	26
Chapter 3: Objective I	
An analysis of effect of Epap-1 on the SARS-Cov-2 Spike protein	
and ACE2 interaction and virus entry	
3.1 Introduction	29
3.2 Results	
3.2.1 Spike protein interacts with Epap-1	29
3.2.2 Interaction of S protein-Epap-1 complex with ACE2	36
3.2.3 Purification of Epap-1 from first trimester placental tissue	37
3.2.4 Cloning and Expression of Spike proteins in pEGFP-C1 vector	38
3.2.5 Cloning and Mammalian Expression of RBD protein in	
pEGFP-C1 vector	39
3.2.6 Cloning and Bacterial Expression of RBD protein in	
pET23d+ vector	40
3.2.7 Purification of IgG from Covid-19 Positive Blood sample	

using Proteinase A column affinity chromatography	41
3.2.8 Analysis of the effect of Epap-1 interaction with	
S-protein/ RBD protein and ACE2 interaction using	
ELISA	42
3.2.9 Analysis of the effect of Epap-1 interaction with	
RBD protein and ACE2 interaction using	
Immunofluorescence	44
3.2.10 Analysis of the effect of Epap-1 interaction with	
Spike protein and ACE2 interaction using	
Immunofluorescence	46
3.2.11 Antiviral assay and analysis of Proviral DNA with	
SK38 and SK39 Primers	49
3.2.12 Discussion	54
3.2.13 Conclusion	55
Chapter 4: Objective II	
Evaluation of efficacy of small molecule mimics of Epap-1	on
Evaluation of efficacy of small molecule mimics of Epap-1 SARS Cov-2 RBD protein and ACE2 interaction and virus	
•	
SARS Cov-2 RBD protein and ACE2 interaction and virus	s entry
SARS Cov-2 RBD protein and ACE2 interaction and virus 4.1 Introduction	s entry 58
SARS Cov-2 RBD protein and ACE2 interaction and virus 4.1 Introduction 4.2 Results and Discussion	s entry 58
SARS Cov-2 RBD protein and ACE2 interaction and virus 4.1 Introduction 4.2 Results and Discussion 4.2.1 Analysis of Novel Small Molecules Interaction with RBD	58 62
SARS Cov-2 RBD protein and ACE2 interaction and virus 4.1 Introduction 4.2 Results and Discussion 4.2.1 Analysis of Novel Small Molecules Interaction with RBD using Spectrofluorometer	58 62
SARS Cov-2 RBD protein and ACE2 interaction and virus 4.1 Introduction 4.2 Results and Discussion 4.2.1 Analysis of Novel Small Molecules Interaction with RBD using Spectrofluorometer 4.2.2 Analysis of small molecule mimics of Epap-1 interaction with	58 62 62
SARS Cov-2 RBD protein and ACE2 interaction and virus 4.1 Introduction 4.2 Results and Discussion 4.2.1 Analysis of Novel Small Molecules Interaction with RBD using Spectrofluorometer 4.2.2 Analysis of small molecule mimics of Epap-1 interaction with RBD using ELISA	58 62 62 64
SARS Cov-2 RBD protein and ACE2 interaction and virus 4.1 Introduction 4.2 Results and Discussion 4.2.1 Analysis of Novel Small Molecules Interaction with RBD using Spectrofluorometer 4.2.2 Analysis of small molecule mimics of Epap-1 interaction with RBD using ELISA 4.2.3 Antiviral assay	58 62 62 64 67
SARS Cov-2 RBD protein and ACE2 interaction and virus 4.1 Introduction 4.2 Results and Discussion 4.2.1 Analysis of Novel Small Molecules Interaction with RBD using Spectrofluorometer 4.2.2 Analysis of small molecule mimics of Epap-1 interaction with RBD using ELISA 4.2.3 Antiviral assay	58 62 62 64 67
SARS Cov-2 RBD protein and ACE2 interaction and virus 4.1 Introduction 4.2 Results and Discussion 4.2.1 Analysis of Novel Small Molecules Interaction with RBD using Spectrofluorometer 4.2.2 Analysis of small molecule mimics of Epap-1 interaction with RBD using ELISA 4.2.3 Antiviral assay 4.3. Conclusion	58 62 62 64 67
SARS Cov-2 RBD protein and ACE2 interaction and virus 4.1 Introduction 4.2 Results and Discussion 4.2.1 Analysis of Novel Small Molecules Interaction with RBD using Spectrofluorometer 4.2.2 Analysis of small molecule mimics of Epap-1 interaction with RBD using ELISA 4.2.3 Antiviral assay 4.3. Conclusion Chapter 5: Objective III	58 62 62 64 67
SARS Cov-2 RBD protein and ACE2 interaction and virus 4.1 Introduction 4.2 Results and Discussion 4.2.1 Analysis of Novel Small Molecules Interaction with RBD using Spectrofluorometer 4.2.2 Analysis of small molecule mimics of Epap-1 interaction with RBD using ELISA 4.2.3 Antiviral assay 4.3. Conclusion Chapter 5: Objective III Development of novel dicoumarol inhibitors of viral entry	58 62 62 64 67

Paper	
References	85
Chapter 6: Overall Summary	82
5.3. Conclusion	81
(dicoumarol) small molecules	80
for Small Molecule Mimics of Epap-1 and Novel	
5.2.4 Analysis of Proviral DNA with SK38 and SK39 Primers	
5.2.3 Antiviral assay	77
with RBD using ELISA	76
5.2.2 Analysis of Novel (dicoumarol) Small Molecules interaction	
with RBD using Spectrofluorometer	74
5.2.1 Analysis of Novel (dicoumarol) Small Molecules Interaction	

CHAPTER-IIntroduction

1.1 Introduction:

SARS-CoV-2 is the causative agent of current pandemic coronavirus disease-2019 (COVID-19). Four genera of coronaviruses (CoVs) are identified, namely, Alphacoronavirus (αCoV), Betacoronavirus (βCoV), Deltacoronavirus (δCoV), and Gammacoronavirus (γCoV) [1]. More than a million people have been infected with SARS-COV-2 across the world. COVID-19 causes an ongoing outbreak of lower respiratory tract disease, which leads to loss of immunity and even death in weak immunity persons. SARS-CoV-2 appears to be efficient for binding to the ACE2 receptor of human. SARS-CoV-2 S protein is a homotrimeric glycoprotein. Receptor-binding Domain (RBD) binds the PD of the human ACE2 receptor protein with higher affinity than the SARS-CoV S protein. ACE2 is a cell surface membrane protein expressed in human alveolar epithelial cells, enabling SARS-CoV-2 infection [2]. ACE2 domains contain a signal peptide, a transmembrane domain, and an intracellular domain [3, 4]. ACE2 is expressed in various tissues, which include the myocardium, upper and lower respiratory tract, and gastrointestinal mucosa.

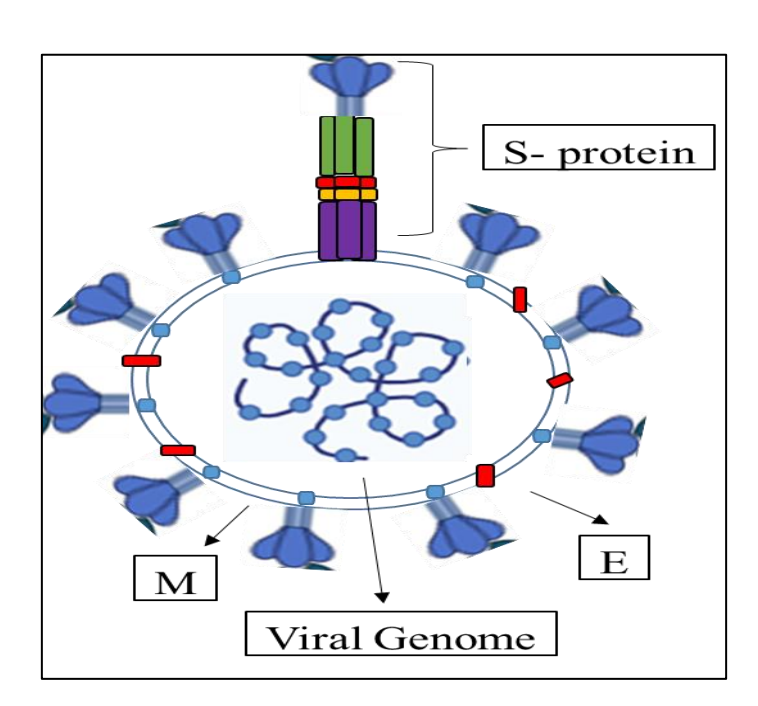


Fig 1.1 Schematic representation of structure of SARS-CoV-2

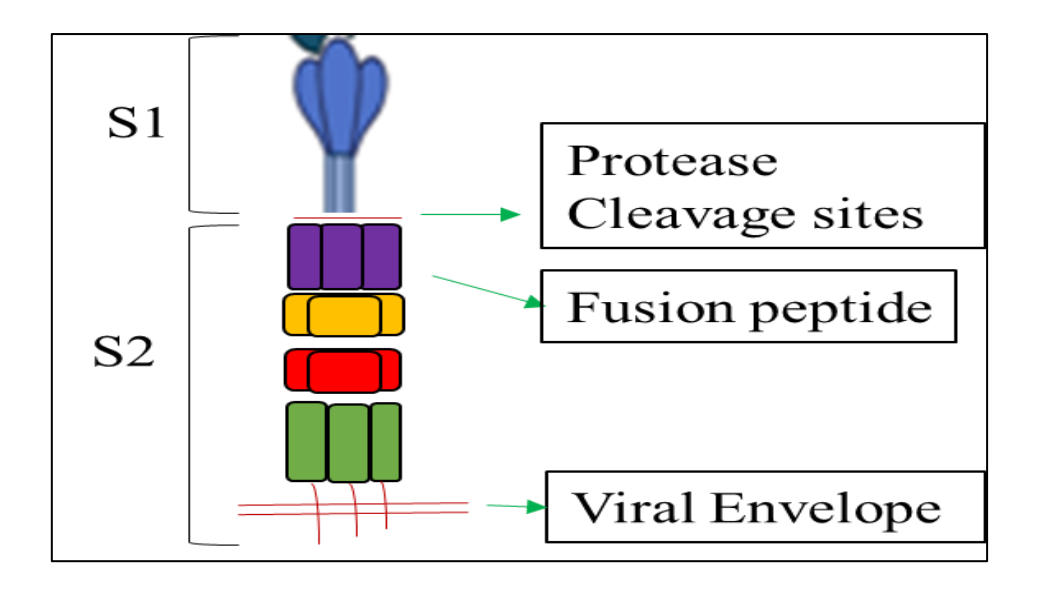


Fig 1.2 Schematics representation of Spike protein sub-units S1 and S2. S1 is surface exposed, which contains a receptor-binding domain (RBD) that binds to the host cell ACE2 receptor, causing pathogenicity. S2 is a transmembrane domain that contains fusion peptides and is involved in fusion machinery: S1 and S2 junction separated by fusion peptide with a protease cleavage site.

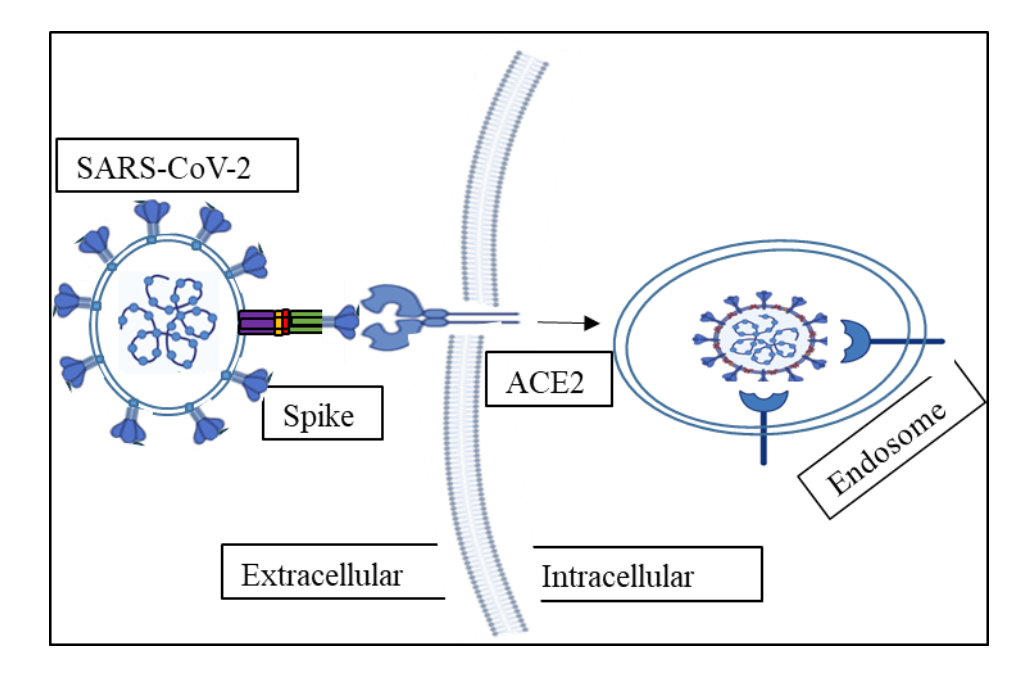


Fig 1.3 Schematics representation of Spike protein (Homotrimeric glycoprotein) binding to the ACE2 receptor. In the presence of the TMPRSS2 a cell protease, it initiates the membrane fusion directly at the cell surface, a part from this, the virion is directly engulfed by endocytosis and fusion occurs in the endosome where cathepsin L or cathepsin B cleave spike.

Coronaviruses possess the largest genomes (30kb) among all known RNA viruses, with 32% to 43% G+C contents. Major structural proteins of genes in all coronaviruses occur in the 5'-3' order as spike (S), envelope (E), membrane (M), and nucleocapsid (N). SARS-CoV-2 is a spherical or pleomorphic enveloped particle with single-stranded (positive sense) RNA associated with a nucleoprotein in a capsid comprised of matrix protein. The S-protein is 1273 amino acids in length and plays a crucial role in viral entry and pathogenesis. It consists of 2 subunits: S1 and S2. The S1 subunit binds to the ACE2 receptor on the host cell through RBD, whereas the S2 subunit is membrane-anchored and involved in the fusion machinery. SARS-CoV-2 RBD is 223 amino acids and is located in the S1 subunit of S protein between 331-524 residues. It was reported that the S protein might be activated by cleavage in the basic argininerich region between S1 and S2 by furin to facilitate membrane fusion of the virus and unable cell-cell transmission of the virus [5, 6]. Furin is abundantly present in the respiratory tract, and may be involved in cleaving the S protein during leaving the lung epithelial cells, thereby successfully infecting other cells. During infection, the extracellular PD of ACE2 binds to the S-protein's RBD and is a surface protein on SARS-CoV-2 [7]. The replication of this virus happens in the epithelial cells of the respiratory tract with cellular necrosis in the stage of early infection, which later leads to eventual pulmonary tissue repair due to an inflammatory response with viral clearance and focal consolidation in pulmonary tissue [8, 9].

The SARS-CoV-2 genome consists of 10 to 12 open reading frames (ORFs). The envelope bears club-shaped glycoprotein projections. Its replication is mediated by RNA-dependent RNA polymerase (RdRp), which has nonstructural proteins (nsps) for transcription and replication through multisubunit [10]. The 30Kb long SARS-CoV-2 genome contains a hefty 21Kb portion attributing to non-structural proteins (NSPs) that cater to viral replication and translation. NSP 12, or RNA-dependent RNA polymerase (RdRp), is the key player, and Nsp8 and Nsp10 regulate RdRp. Mutations in RdRp occur prior to S-protein, and differential RdRp

mutations were associated with geographical locations, suggesting a possible role of RdRP in virus evolution [11]. It contains (nsp12) as a catalytic subunit among nsp7, nsp8, and the complex of nsp12-nsp7-nsp8 [12, 13]. Among all ORFs, 67% of the entire genome represented by ORF1ab with 15 or 16 nsps. Non-structural proteins (nsps) are encoded by ORF1ab, ORF1ab are involved in viral processing and replication. Meanwhile, viral structural proteins are encoded by remaining ORFs (S, E, M, and N). Viral envelopes are formed by the M and E proteins, while the helical ribonucleocapsid complex with positive-strand viral genomic RNA by formed N protein and during the assembly of virions interacts with viral membrane protein. The exclusive proof-reading capacity of SARS-CoV-2 is promoted by the NSPs coded by ORF1ab. A replication and transcription complex (RTC) is a multiprotein NSP complex comprising NSP 7, NSP-8, NSP 12, NSP 13.1, and 13.2(RTC). Transcription is initiated on genomic RNA template for synthesis of a sub-genomic anti-sense strand of RNA by a complex of NSP7, NSP8, NSP12, NSP13.1 (backtracking complex; BTC), which serves an mRNA and full-length genomic RNA. Replication of genomic RNA is promoted by RTC, while a complex of NSP14 and NSP 10 (PRC) provide a proof-reading activity that corrects the replication errors, while a complex of NSP 13, 14, 16, and 10 perform capping of RNA at the final step [14]. Since the template anti-sense strand synthesis takes place in the presence of BTC, it is unknown if this complex has proofreading activity. Furthermore, RTC not in association with vesicles was reported to exhibit poor proofreading activity [15]. It is not clear if BTC or PRC devoid of non-vascular RTC introduces errors during the synthesis of sub-genomic and genomic RNA.

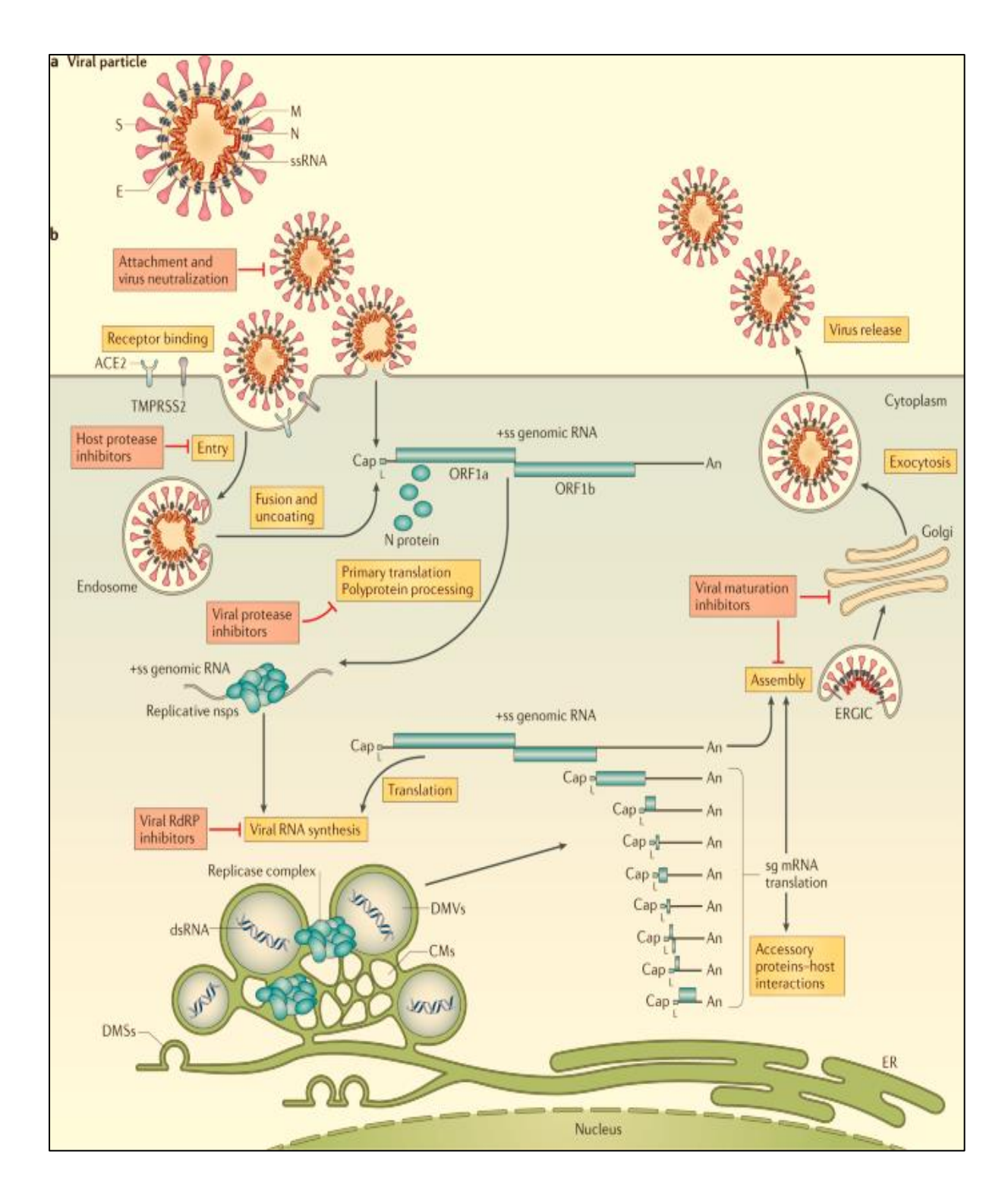


Fig 1.4 Schematic representation of the Life cycle of the SARS-CoV-2 genomic RNA (gRNA) (Nature Reviews Microbiology (Nat Rev Microbiol) ISSN 1740-1534 (online) ISSN 1740-1526 (print))

1.2 SARS-CoV 2 and Pregnancy:

The interaction between SARS-CoV-2 and pregnancy has been an area of significant research and concern since the onset of the pandemic. Pregnant women are more likely to be susceptible to SARS-CoV-2 infection than non-pregnant women [16]. However, pregnancy can lead to changes in the immune system and physiology that might affect the severity and outcome of the infection. Most pregnant women who contract COVID-19 experience mild to moderate symptoms similar to non-pregnant women. However, a small proportion may develop severe illness requiring hospitalization, intensive care, or mechanical ventilation. Advanced maternal age, obesity, preeclampsia, preterm birth, stillbirth, and pre-existing medical conditions (such as diabetes or hypertension) are known risk factors for severe COVID-19 in pregnant women [16]. While studies for vertical transmission (transmission of SARS-CoV-2 from mother to fetus during pregnancy) are possible, they are relatively rare. The majority of the studies showed that third-trimester pregnant women were more prone to severe infection compared to first and second trimesters [17, 18]. Studies have shown that SARS-CoV-2 can infect placental cells, although the implications of this infection for pregnancy outcomes are still being studied. In some cases, placental inflammation and injury have been observed, which could potentially affect fetal development. Few neonates born to mothers with COVID-19 infection were asymptomatic, and those symptomatic were admitted to the neonatal intensive care unit (NICU). Virus-specific antibodies such as IgM, IgG, and cytokines (Il-6, IL-10) levels were elevated in neonate blood sera samples born to mothers infected with COVID-19 [19]. IgM antibodies do not generally pass through the placenta to the fetus [20]. SARS-COV 2 infection reports in neonates are still unclear, and there is no direct evidence of SARS-CoV 2 infection occurrence during the delivery process (vaginal delivery or cesarean) or after birth, as there are no positive reports of RT-PCR of the umbilical cord blood, amniotic fluid, breast milk, placenta, or vaginal secretions.

1.3 Early pregnancy associated protein-1 and its role:

The expression of Epap-1, a 90 kDa anti-HIV-1 active glycoprotein, in the first trimester placental tissue suggests that it is one of the major innate immune factors/proteins protecting the fetus from HIV infections [21]. Epap-1 can be a very efficient natural protection mechanism against cell-free and cell-associated viral infections during early pregnancy. Its role in interaction with other viral proteins and viruses is not understood.

1.4. The placenta acts as an Anti-viral barrier:

During the development process of the fetus, the placenta supplies continuous nutrients. This requires a continuous supply of maternal blood to transport the surface to the multinucleate syncytiotrophoblast layer [22]. The trophoblast layer acts as a major barrier between Hofbauer cells and maternal fluids. Several reasons make recognizing the cellular mechanisms controlling transplacental viral transmission essential.

Fetal Health Protection: The placenta separates the mother and fetal circulations. One of the major functions of the placenta is to act as a barrier, keeping dangerous substances from entering the developing fetus, like viruses.

Transmission: Viruses can reach the fetus either by crossing the placenta directly (vertical transmission) or by infecting the mother, resulting in systemic effects that indirectly impact on the placenta and fetus.

Cellular Barriers: Cell barriers against viral entry are created by specialized cells in the placenta, such as syncytiotrophoblasts, cytotrophoblasts, and Hofbauer cells. Knowing the best is crucial for understanding how such cells eliminate, or indeed permit, the transmission of the virus.

Immune Responses: Placenta also possesses immune responses of its own in order to defend against infections. For example, the production of antiviral proteins and cytokines and the detection of viral threats due to innate immune responses.

Infections: Viral infections during pregnancy can have severe outcomes such as miscarriage, preterm birth, congenital anomalies, and developmental neurological disability. Further, it is important to know how viruses escape or are kept at bay by placental defenses to manage these risks.

Public Health Implications: Knowledge from studies of placental viral transmission will be critical for public health efforts to prevent and treat infections in pregnancy.

This research area involves studying of viral-host interactions, placental structure-function relationships, immunological responses, and the impact of infections on placental function. Understanding these mechanisms would enhance our knowledge of pregnancy biology and contribute to the development of therapies and preventive measures to protect maternal and fetal health.

1.5 Rationale of the Study:

During pregnancy, women express an ambit of innate immune factors in circulation to protect the fetus against pathogens [23]. Most of the SARS-CoV-2 infected pregnant women showed asymptomatic (64.71%) [24, 25] when compared to pregnant women who were symptomatic (35.29%). There is a very low frequency of virus transmission to a fetus when the mother is infected in the second trimester [26]. While there is a report that when a mother is infected in the third trimester, transmission may occur [27, 28], this could be due to the thinning of vascular endothelial cell layers during the third trimester [29]. Further, vascular endothelial cells were reported to express ACE2 [30] and harbor SARS-CoV-2 infection [31, 32]. Epap-1, a 90 kDa protein, is one of the innate immune factors involved in neutralizing viruses, specifically HIV [21]. If Epap-1 shows interaction with Spike protein activity, it may form a potential anti-viral factor modulating both HIV-1 and SARS-CoV-2. Further, an evaluation of the action of small molecular mimics of Epap-1 protein and novel small molecules will throw light on the potential molecular interactions associated with RBD interaction in interfering with ACE2 binding.

The following objectives were framed based on the above rationale:

- 1) An analysis of effect of Epap-1 on the SARS Cov-2 Spike protein and ACE2 interaction and virus entry.
- 2) Evaluation of efficacy of small molecule mimics of Epap-1 on SARS-Cov-2 RBD protein and ACE2 interaction and virus entry.
- 3) Development of novel dicumarol inhibitors of viral entry through RBD interaction.

CHAPTER-II Materials and Methods

2.1 Materials:

2.1.1 Antibodies:

- S2 Monoclonal Antibody (Invitrogen 1A9)
- SARS-CoV-2 Spike Protein (RBD) Antibody (MA5-38033)
- Anti-ACE2 antibody (Sigma Aldrich SAB3500346)
- Alexa flora 594 (Rabbit and mouse)
- Secondary antibodies Goat anti-mouse HRP and Goat Anti-rabbit HRP were used.
- Hoescht 33342 (Catalog number: H3570)

2.1.2 Molecular Biology Materials:

- Sambucus nigra Agarose lectin was procured from Labmate
- 0.22 μm and 0.45 μm syringe filters, Polyvinylidene Flouride (PVDF) membrane
 (PALL Life Scientific, USA and Sartorius, Germany).
- Nitrocellulose Membrane from PALL Life Sciences, USA.
- SuperSignal chemiluminescent substrate (Pierce, Rockford, IL)
- Protein A agarose beads (B. Genei).
- PCR Master mix from Thermo Fischer manufacturers
- HIV-1 p24 Antigen Capture Assay was performed with an ABL (Advanced Bioscience Laboratories) ELISA kit purchased from Kensington, MD, USA.
- TMB substrate

2.1.3 Biochemicals & Cell Culture Materials:

- DMEM –high glucose and MEM was purchased from Gibco Thermo Fischer
- Trypsin in Dulbecco's Phosphate Buffered Saline w/o Phenol red (TCL006)
- Lipofectamine 3000 (Thermo fisher Catalog number: L3000001)

- Cell culture dishes, bottles, plates, and flasks were procured from Tarson and Corning.
- **2.1.4** <u>Instruments:</u> Vortexer, Centrifuge (REMI C30BL and Hermle Z36HK), UV & visible spectrophotometer (Jasco v550), ELISA reader (Teccan), Ultrasonic homogenizer or sonicator, (300V/T, Biologics Inc., Manassas, Virginia, USA), Confocal microscope (Carl Zeiss), Gel electrophoresis apparatus (Medoxbiotech), SDS-PAGE running and transfer unit (Biorad).
- **2.1.5** Software Tools: Graphpad Prism 9.0, Sigma Plot v11.0, Image lab, Zen 3.0.

2.1.6 <u>Cell types:</u>

- BHK-21 was obtained from NCCS PUNE, INDIA.
- HEK293T

2.2 Methodology

2.2.1 *Cell line*:

The cell lines BHK-21 and HEK293T were cultured in MEM and DEMEM, respectively, in the presence of 0.01% FBS in an incubator with 5% CO2, 37°C.

2.2.2 Modelling studies:

The 3D structure of the S-protein of Wuhan, delta, and omicron was retrieved from RCSB PDB (https://www.rcsb.org/) of PDB ID: 6VXX, 7W9E, 7WK2. The resolution of the S-protein of Wuhan was 2.80A, and Delta, Omicron was 3.10A. The 3D structure of ACE2 was retrieved from RCS PDB of PDB ID 1R42. The resolution of the structure was 2.20A. The structure of Epap-1 was modeled using MODELLER software and refined using GROMACS software for 100ns. The docking of Epap-1 with S-protein of Wuhan, delta, and omicron was carried out using HADDOCK. The active region selected for S-protein is from 331-526, and for Epap-1 is from 1-50, 321-360, and 521-560 in the input parameters. All the docking parameters, such as distance restraints, sampling parameters, clustering parameters, dihedral and hydrogen bond

restraints, restraint energy constant, scoring parameters, energy and interaction parameters, solvated docking parameters, and analysis parameters, were set as default. The complex of Epap-1 with the S-protein of Wuhan, delta, and omicron was subjected to molecular dynamics simulation through GROMACS software using CHARMM36 forcefield. To carry out the simulation, a cubic box was built using the SPC/E water model, and the complexes were placed in the center of the box. Negatively charged chlorine ions replaced seven water molecules to neutralize the system. The systems were minimized using the steepest descent minimization algorithm for 50000 steps. The systems were equilibrated at constant pressure, volume, and temperature. The simulation of the systems was processed for 100ns.

The simulated structure of Epap-1 and S-protein of Wuhan, delta, and omicron complexes were docked with ACE2 receptors using the ClusPro server (https://cluspro.bu.edu/). The complexes were refined through GROMACS software using CHARMM36 forcefield for 100ns. Epap-1, ACE2, and S-protein interaction of Wuhan, delta, and omicron was visualized using pymol and ligplot software.

For validation, amino acid arginine at position 453 was substituted to alanine in Wuhan S-protein and docked with Epap-1. Likewise, Amino acid lysine and proline at position 449, 548 was substituted to alanine and docked with Epap-1. Similarly, asparagine, arginine, and glutamine at positions 345, 440, and 549 were substituted to alanine for Delta S-protein, and arginine, serine, and glutamic acid at positions 328, 340, and 452 were substituted to alanine for Omicron S-protein, then docked with Epap-1 using Cluspro server. The interaction of Epap-1 complexed with the S-protein of mutated S-protein of Wuhan, Delta, and Omicron was visualized and analyzed using pymol and Discovery Studio software [33].

2.2.3 <u>Purification of Epap-1 from first trimester placental tissue:</u>

Epap-1 was purified from first-trimester placental tissue following procedure of Kondapi et al. (2002). The placental tissue was washed and homogenised 1xPBS and fractionated with ammonium sulfate at 0-80% saturation. The pellet was discarded and proteins present in the supernatant were refractionated with 80% saturation of ammonium sulfate. 60-80% fractionated proteins were dissolved in the minimum volume of 1xPBS and dialyzed extensively against 1xPBS of pH 7.3 overnight at 4°C. The dialyzed fraction was used for further purification and binding studies. The dialysate was centrifuged at 8000x g/10,000rpm for 10 min at 4°C. The proteins in the supernatant were estimated using the Bradford colorimetric method (Bradford, 1976). 10mg of total protein from 60-80% ammonium sulfate precipitated fraction was loaded onto 5ml immobilized Sambucus nigra agglutinin lectinagarose (Broekaetet. al. 1984) affinity column. Collected the flow-through and washed the column with 50-bed volumes of 1xPBS until OD 280 of the flow-through reached below 0.01. The protein was eluted with 1xPBS, pH 7.3, containing 50mM D (+) galactose in 1 ml fractions. The eluted protein was dialyzed extensively and analyzed immediately using 10% SDS-PAGE, followed by silver staining. A high molecular weight protein standard marker was used [33].

2.2.4 Silver staining:

After electrophoresis, 10% SDS-PAGE gel was fixed in a fixing reagent (50% Methanol, 12% Glacial Acetic acid, 100μl HCOH) for 1 hour. After 1 hr, the gel was washed twice with 20% methanol for each 20 sec. The gel was pre-treated with 0.02% Na₂S₂O₃ for 1-2 mins; after that, the gel was rinsed with double distilled water thrice each 20 sec. The gel was impregnated in 200mg AgNO3 and 100μl HCOH for 30 mins. The gel was again rinsed with double distilled water thrice each 20 sec. A developing solution (3% Na₂CO₃ with 100μl HCOH) was added to

the gel and incubated until it developed. Once developed, a Stop solution containing 5% acetic acid was added to the gel. The gel was preserved in double distilled water [33].

2.2.5 Cloning of Spike and RBD proteins:

Spike and RBD protein from SARS Cov-2 was amplified using specific primers based on the nucleotide sequences from the Gen Bank (accession number MT415320, MT415321, MT415322, MT415323, MT457402, MT457403, MT477885) and cloned into a pEGFP-C1 vector for cell line expression. RBD protein cloned into pET23d+ vector for bacterial expression.

Table 1: Primer Sequences of Spike and RBD

S.No	Oligo Name	Sequence 5'-3'	Primer size(bp)
1	Spike prtn_F	ATGTTTGTTTTTCTTGTTTTATTGC	25 bp
2	Spike prtn_R	TTATGTGTAATGTAATTTGACTCCT	25 bp
3	RBD_F	AGAGTCCAACCAACAGAATCTATTG	25 bp
4	RBD_R	TTGACACATTTGTTTTTAACCAA	25 bp

Table 1: The above table shows the primers used for PCR experiments.

2.2.6 Expression of Spike and RBD in cell lines:

HEK293T cells 10⁵ were suspended in DMEM supplemented with 10% FBS and were seeded in a 35mm dish. The cells were incubated for 24 hrs at 37°C in a 5% CO 2 incubator to reach 70% confluency. After incubation, the cells were transfected with the standard protocol of lipofectamine3000 (Thermo Fisher **Catalog number:** L3000001). After 6 hours of Transfection, complete media was added to the cells. Cell lysate was collected at 48 hrs and 72 hrs [33].

2.2.7 Western Blotting:

The cell lysate was suspended in RIPA buffer (25 mM Tris-HCl, pH 7.6, 150 mM NaCl, 1% NP-40, 1% Sodium deoxycholate, 0.1% SDS). Total protein (20 µg) was resolved on 8% SDS-PAGE. The samples were processed as per standard protocol. Electrophoresis was carried with 1X Running buffer [0.025 M Tris HCl, 192 mM Glycine, and 1% SDS (pH 8.3)] electrode running at 120 V. After electrophoresis, the PVDF membrane was placed on the gel for the protein transfer by Towbin et al. method [34]. Initially, PVDF membranes were equilibrated in 100% Methanol for 10 mins. The gel and PVDF membrane were placed in a transfer unit with buffer containing (0.025 M Tris HCl, 192 mM Glycine, and 20% methanol) for overnight transfer at 35 V under 4°C. The next day, the blot is blocked with a blocking solution containing (5% Skim milk powder w/v) in 0.02 % Tween 20 (1xTBST) at RT for 2 h. Then, the blot was rinsed with 1xTBST (TBS containing 0.02 % Tween-20). Primary antibody of SARS-CoV-2 Spike Protein S2 Monoclonal Antibody (Invitrogen- 1A9) and Primary antibody of SARS-CoV-2 Spike Protein (RBD) Antibody (MA5-38033) incubated overnight at 4 °C. The next day, the blot was washed twice in 1xTBST for 10 minutes, and a single wash in 1xTBS, and the blot was incubated with a secondary anti-mouse antibody conjugated to HRP (horseradish peroxidase) used for Spike protein and Anti-Rabbit secondary antibody was used for RBD protein detection for 2 h at room temperature. After incubation, the blot was washed again with 1xTBST (twice) and 1xTBS (single). Substrate ECL from Thermo Scientific, USA used to develop the blots, and the chemiluminescence was developed in the chemidoc instrument (Bio-Rad).

2.2.8 Immunofluorescence:

HEK293T, 10^5 cells grown on coverslips and suspended in DMEM supplemented with 10% FBS were seeded in a 35mm dish. The cells were incubated for 24 hrs at 37°C in a 5% CO 2 incubator to reach 70% confluency. After incubation, the cells were transfected with the standard protocol of lipofectamine3000 (Thermo Fisher **Catalog number:** L3000001). After 24 hrs of Transfection, complete media was added to the cells. Cells were washed with 1x phosphate buffer saline (PBS). The cells were fixed in 4% paraformaldehyde and permeabilized in 0.1% Triton X-100 in 1x PBS for 15 min at room temperature. Then gently washed thrice with 1x PBS and cells were blocked with 3% BSA in 1xPBS for 2 h at room temperature. The cells were washed thrice with 1x PBS. The coverslips were mounted onto glass slides with 40% glycerol. Finally, the slides were viewed under a confocal microscope, and images were captured [33].

2.2.9 Expression and Purification of Receptor binding domain (RBD) in DHa and BL-21 (DE3):

RBD was cloned into pET23d (+) using SacI and NotI restriction sites to produce pET23d (+)-RBD-HisX6. pET23d (+)-RBD-HisX6 was expressed in E.coli BL21 (DE3) cells. After transformation, the positive colony was inoculated into LB-broth with Ampicillin 12-16hr or overnight at 37°C, 180rpm. After 12-16hr, the primary culture is inoculated into secondary culture at 37°C, 180rpm, till it reaches OD₆₀₀ value 0.4-0.6. After the culture reached the desired OD, 1mM IPTG was added to the secondary culture and further incubated for 4hr at 28°C, 180rpm. The culture was centrifuged at 6,800 rpm, 4°C to pellet down and resuspended the pellet in lysis buffer (50 mM Tri-HCl, pH-8.0, 200 mM NaCl, 1 mM PMSF, Lysozyme (5μg/ml), 10% Glycerol). Sonication was done at 35% amplitude for 15mins with 10 On and 10 Off pulse. After sonication, cell lysate was centrifuged at 10,000 rpm for 15 minutes at 4°C

to separate cell debris. The Supernatant was loaded onto the NTA-Ni2+ column previously equilibrated with equilibration solution 50 mM Tris—HCl, 200 mM NaCl, 10% glycerol, pH 8.0. The flow-through was reloaded thrice, and the column was washed with a wash buffer containing 10 mM imidazole. RBD was eluted with an elution buffer containing 250 mM imidazole. The eluted protein was dialyzed thrice, initially with 50 mM Tris-HCl, 0.2 mM NaCl, 10%Glycerol, 1 mM PMSF, and twice followed by 1xPBS with 10%glycerol and 1 mM PMSF and quantified the protein using the Bradford method and stored at -80°C.

2.2.10 <u>Purification of IgG from Covid-19 Positive Blood sample using Proteinase A column</u> affinity chromatography:

Blood samples from COVID-19-positive patients were drawn carefully under medical practitioner guidelines from Gandhi Medical College and Hospital and centrifuged at 2,000 rpm for 10 mins to separate serum and blood cells. The supernatant serum was collected and loaded on the protein A column affinity chromatography. The serum was incubated in protein A column overnight at 4°C. The next day, serum was passed through the column thrice, and Igg was eluted using 0.1M glycine. The purified Cov-2 IgG reactivity to Spike and RBD protein samples was analyzed using Western blotting using Human IgG (Gamma chain) Cross-Adsorbed Secondary Antibody (62-8420) [33].

2.2.11 Analysis of the effect of Epap-1 interaction with S-protein/RBD protein and ACE2 interaction using ELISA:

2.2.11. A. Analysis of Epap-1 interaction with S-protein:

2.2.11. A1. HEK293T Cells were seeded in 96 well plates in triplicate at a density of 0.15 x 10⁵ cells per well in100μL of complete media. Cells were grown overnight at 37°c, with 5% CO₂. The next day, cells were washed once with 1xPBS and fixed with 1% PFA for 15 mins. Cells were rinsed thrice with 1xPBS. Cells were incubated with Anti-ACE2 antibody overnight

at 4°c. The next day, cells were washed thrice with 1xPBS. Cells were incubated with an Anti-Rabbit HRP secondary antibody for 1 hour at room temperature. Cells were rinsed thrice with 1xPBS. 100μL of TMB was added to wells and incubated in the dark for 20 mins. 100μL of 2N H2SO4 (Stop solution) was added to these wells, and readings were taken at 450nm.

2.2.11. A2. HEK293T Cells were seeded and fixed as mentioned above. Cells were rinsed thrice with 1xPBS after fixing. Cells were incubated with only S-protein (100 μg), Spike-Epap1 (Epap1- 50μg, 100μg) complex for 1 hour at 37°c. Cells were rinsed thrice with 1xPBS. Cells were incubated with Anti-ACE2 antibody overnight at 4°c. The next day, cells were washed thrice with 1xPBS. Cells were incubated with a secondary Anti-Rabbit HRP antibody for 1 hour at room temperature. Cells were rinsed thrice with 1xPBS. 100μL of TMB was added to wells and incubated in the dark for 20 mins. 100μL of 2N H2SO4 (Stop solution) was added to these wells, and readings were taken at 450nm.

2.2.11. A3. HEK293T Cells were seeded and fixed as mentioned above. Cells were rinsed thrice with 1xPBS after fixing. Cells were incubated with only S-protein (100 μg), Spike-Epap1 (Epap1- 50μg, 100μg) complex for 1 hour at 37°c. Cells were rinsed thrice with 1xPBS. Cells were incubated with an Anti-Spike antibody overnight at 4°c. The next day, cells were washed thrice with 1xPBS. Cells were incubated with a secondary Anti-Mouse HRP antibody for 1 hour at room temperature. Cells were rinsed thrice with 1xPBS. 100μL of TMB was added to wells and incubated in the dark for 20 mins. 100μL of 2N H2SO4 (Stop solution) was added to these wells, and readings were taken at 450nm.

2.2.11. B. Analysis of Epap-1 interaction with RBD protein:

2.2.11. B1. HEK Cells were seeded in 96 well plates in triplicates at a density of 1.5 x 10⁶ cells per well in 100μL of complete media. Cells were grown overnight at 37°C, with 5% CO₂. The next day, cells were washed once with 1xPBS and fixed with 1% PFA for 15 mins. Cells were

rinsed thrice with 1xPBS. Cells were incubated with only RBD-protein (100 μg), RBD-Epap1 (Epap1- 50μg, 100μg) complex for 1 h at 37°c. Cells were rinsed thrice with 1xPBS. Cells were incubated with Anti-ACE2 antibody overnight at 4°c. The next day, cells were washed thrice with 1xPBS. Cells were incubated with a secondary Anti-Rabbit HRP antibody for 1 h at room temperature. Cells were rinsed thrice with 1xPBS. 100μL of TMB was added to wells and incubated in the dark for 20 mins. 100μL of 2N H2SO4 (Stop solution) was added to these wells. Absorbance was recorded at 450nm.

2.2.11. B2. HEK293T Cells were seeded and fixed as mentioned above. Cells were rinsed thrice with 1xPBS after fixing. Cells were incubated with RBD-protein, RBD-Epap1 (Epap1- 50μg, 100μg) complex for 1 h at 37°c. Cells were rinsed thrice with 1xPBS. Cells were incubated with Rabbit Anti-RBD antibody overnight at 4°c. The next day, cells were washed thrice with 1xPBS. Cells were incubated with a secondary Anti-Rabbit HRP antibody for 1 h at room temperature. Cells were rinsed thrice with 1xPBS. 100μL of TMB was added to wells and incubated in the dark for 20 mins. 100μL of 2N H2SO4 (Stop solution) was added to these wells. Absorbance was recorded at 450nm [33].

2.2.12. <u>Analysis of the effect of Epap-1 interaction with S protein and ACE2 interaction</u> using immunofluorescence:

2.2.12.1. HEK293T 10⁵ cells suspended in DMEM media supplemented with 10% FBS and seeded on coverslips in a 35mm dish. The cells were incubated at 37°C for 24 hrs in a 5% CO₂ incubator to reach 70% confluency. After incubation, the cells were fixed with 4% PFA for 20 mins. Cells were rinsed thrice with 1xPBS. Spike- Epap1 complex incubated at 37°C for 1 hour. In the negative control, cells were incubated with 1xPBS, whereas, in the positive control, cells were incubated with 100 μg Cov-2 IgG for 4 hours at 37°C. Cells were incubated with only Spike protein (100 μg) and Spike- Epap1 complex (50μg, 100 μg) for 4 hours at 37°C.

After 4 hours of incubation, the cells were gently washed thrice with 1x PBS. Cells were incubated with Anti-ACE2 antibody overnight at 4°c. The next day, cells were washed thrice with 1xPBS. Cells were incubated with a secondary Anti-Rabbit HRP antibody for 1 hour at room temperature. Cells were washed thrice with 1xPBS. The coverslips were mounted onto glass slides with 50% glycerol. Finally, the slides were viewed under a confocal microscope, and images were captured.

2.2.12.2. HEK293T 10⁵ cells grown on coverslips and fixed as mentioned above. Cells were rinsed thrice with 1xPBS. Spike- Epap1 complex incubated at 37°C for 1 hour. In the negative control, cells were incubated with 1xPBS, whereas, in the positive control, cells were incubated with 100 μg Cov-2 IgG for 4 hours at 37°C. Cells were incubated with only Spike protein (100 μg) and Spike- Epap1 complex (50μg, 100 μg) for 4 hours at 37°C. After 4 hours of incubation, the cells were gently washed thrice with 1x PBS. Cells were incubated with an Anti-Spike antibody overnight at 4°c. The next day, cells were washed thrice with 1xPBS. Cells were incubated with a secondary Anti-Mouse HRP antibody for 1 hour at room temperature. Cells were washed thrice with 1xPBS. The coverslips were mounted onto glass slides with 40% glycerol. Finally, the slides were viewed under a confocal microscope, and images were captured [33].

2.2.13. <u>Analysis of the effect of Epap-1 interaction with RBD protein and ACE2 interaction</u> using immunofluorescence:

2.2.13.1. HEK293T 10⁵ cells suspended in DMEM media supplemented with 10% FBS and seeded on coverslips in a 35mm dish. The cells were incubated for 24 h at 37°C in a 5% CO 2 incubator to reach 70% confluency. After incubation, the cells were fixed with 4% PFA for 20 mins. Cells were rinsed thrice with 1xPBS. RBD- Epap1 complex incubated at 37°C for 1 h. In the negative control, cells were incubated with 1xPBS, whereas, in the positive control, cells

were incubated with 100 μg Cov-2 IgG for 4 hours at 37°C. Cells were incubated with only RBD protein (100 μg) and RBD- Epap1 complex (50μg, 100 μg) for 4 hours at 37°C. Cells were incubated with Rabbit Anti-ACE2 antibody overnight at 4°C. The next day, cells were washed thrice with 1xPBS. Cells were incubated with a secondary Anti-Rabbit HRP antibody for 1 h at room temperature. Cells were washed thrice with 1xPBS. The coverslips were mounted onto glass slides with 40% glycerol. Finally, the slides were viewed under a confocal microscope, and images were captured.

2.2.13.2. HEK293T 10⁵ cells grown on coverslips and fixed as mentioned above. Cells were rinsed thrice with 1xPBS. RBD- Epap1 complex incubated at 37°C for 1 h. In the negative control, cells were incubated with 1xPBS, whereas, in the positive control, cells were incubated with 100 μg Cov-2 IgG for 4 hours at 37°C. Cells were incubated with only RBD protein (100 μg) and RBD- Epap1 complex (50μg, 100 μg) for 4 hours at 37°C. After 4 h of incubation, the cells were gently washed thrice with 1x PBS. Cells were incubated with Rabbit Anti-RBD antibody overnight at 4°c. The next day, cells were washed thrice with 1xPBS. Cells were incubated with a secondary Anti-Rabbit HRP antibody for 1 h at room temperature. Cells were washed thrice with 1xPBS. The coverslips were mounted onto glass slides with 40% glycerol. Finally, the slides were viewed under a confocal microscope, and images were captured [33].

2.2.14. Antiviral assay:

In a 12-well plate, HEK293T 10⁵ cells suspended in DMEM supplemented with 10% FBS were seeded on coverslips. The cells were incubated for 24 h at 37°C in a 5% CO 2 incubator to reach 70% confluency. The cells were then infected with 100µl pseudovirus (HIV-1 strain Indie delEnv d2EFP S-protein/RBD protein) (100pg/ml each) of Spike or RBD expressing pseudovirus in the absence and presence of 50µg, 100µg Epap1, respectively. Cells were incubated at 37°C in a humidified incubator with 5% CO₂ for 6 h. After 6 h post-infection,

Cells were rinsed thrice with 1xPBS. The cells were fixed with 4% PFA for 20 mins. Cells were rinsed thrice with 1xPBS. The coverslips were mounted onto glass slides with 40% glycerol. Finally, the slides were viewed under a confocal microscope, and images were captured [33].

2.2.15. Analysis of Proviral DNA with SK38 and SK39 Primers:

HEK293T 10⁵ cells were seeded in DMEM supplemented with 10% FBS in each well of a 12-well plate. The cells were incubated for 24 h at 37°C in a 5% CO 2 incubator to reach 70% confluency. After incubation, the cells were then infected with 100μl pseudo virus of RBD alone, pseudovirus of RBD with each 50μg, 100μg Epap1, and pseudovirus of Spike alone, with pseudovirus of Spike each 50μg, 100μg Epap1 (100pg/ml each) respectively. Cells were incubated at 37°C in a humidified incubator with 5% CO₂ for 6 h. After 6 h post-infection, the plate was centrifuged for 10 mins at 1200 rpm, and the supernatant was safely discarded into Sodium hypochlorite solution. The cells were re-suspended in 1xPBS and pelleted at 1200 rpm for 5 mins. From the cell pellet, genomic DNA was isolated using a standard protocol of the phenol/chloroform method. DNA was used as the template for PCR. The primer details are given in Table 2. The PCR was carried out in a thermal cycler with the following PCR conditions: 1 cycle, 95°C for 10 min; 35 cycles, 95°C for 1 min; 60°C for 30 sec, and 72°C for 1 min; 1 cycle, 72°C for 7 min. The PCR products were separated on a 2% agarose gel stained with ethidium bromide at 100V, and the gel image was obtained using Chemidoc. [33]

Table 2: Primer Sequences of Proviral DNA

S.No	Oligo Name	Sequence 5'-3'	Primer	Purpose of
			size(bp)	Primers
1	Sk38_FP	ATAATCCACCTATCCCAGTAGG	28 bp	Proviral
		AGAAAT		DNA
				synthesis
2	Sk39_RP	TTTGGTCCTTGTCTTATGTCCAG	28 bp	Proviral
		AATGC		DNA
				synthesis
3	GAPDH_FP	GTCGGAGTCAACGGATTTGGT	21 bp	Standard
				Control
4	GAPDH_RP	CTTGACGGTGCCATGGAATTTGC	23 bp	Standard
				Control

Table 2: The above table shows the primers used for PCR experiments to analyze Proviral DNA.

2.2.16. Analysis of Novel Small Molecules interaction with RBD using ELISA:

In a 96-well plate, HEK293T Cells were seeded in triplicates at a density of 1.5 x 10⁶ cells per well in 100μL of DMEM media and 10% FBS. Cells were grown O/N at 37°c, 5% CO2. The following day, cells were washed once with 1xPBS and fixed with 4% PFA for 15 mins. Cells were rinsed thrice with 1xPBS. Cells were incubated with RBD-protein, RBD-small molecules (100μM) complex for 1 h at 37°c. Cells were rinsed thrice with 1xPBS. Cells were incubated with Rabbit Anti-RBD antibody overnight at 4°c. The next day, cells were washed thrice with 1xPBS. Cells were incubated with a secondary Anti-Rabbit HRP antibody for 1 h at room temperature. Cells were rinsed thrice with 1xPBS. 100μL of TMB was added to wells and incubated in the dark for 20 mins. 100μL of 2N H2SO4 (Stop solution) was added to these wells. Reading was taken at 450nm.

2.2.17. Analysis of Novel Small Molecules Interaction with RBD using Spectrofluorometer:

Spectrafluoromteric analysis were performed using Jasco FP-8550 equipped with a thermostated cell holder connected to a circulating water bath set at 20 °C. The excitation and emission wavelength for RBD protein were set to 295 nm and 310–450 nm, respectively. The slits-width were set at 5nm each [35]. The RBD protein concentration used was 27.77 μ M with different concentrations of small molecules.

2.2.18. Antiviral Assay of RBD and Spike Pseudovirus with Small Molecules:

2.2.18. A. Antiviral assay:

In a 12-well plate, HEK293T 10⁵ cells grown on coverslips suspended in DMEM supplemented with 0.01% FBS were seeded. The cells were incubated O/N at 37°C in a 5% CO 2 incubator to reach 70% confluency. The cells were then infected with 100μl pseudovirus of RBD alone, pseudovirus of Spike alone, and pseudovirus of RBD/Spike with 100μM each small molecule, respectively. Cells were incubated at 37°C in a humidified incubator with 5% CO₂ for 6 h. After 6 h post-infection, Cells were rinsed thrice with 1xPBS. The cells were fixed with 4% PFA for 20 mins. Cells were rinsed thrice with 1xPBS. The coverslips were mounted onto glass slides with 40% glycerol. The slides were focused under a confocal microscope, and images were viewed.

2.2.18. B. Analysis of Proviral DNA with SK38 and SK39 Primers:

In each well of a 12-well plate, HEK293T 10⁵ cells were seeded in DMEM supplemented with 0.01% FBS. The cells were incubated O/N at 37°C in a 5% CO 2 incubator to reach 70% confluency. The cells were then infected with 100μl pseudovirus of RBD alone, pseudovirus of Spike alone, and pseudovirus of RBD/Spike with 100μM each small molecule, respectively. Cells were incubated at 37°C in a humidified incubator with 5% CO₂ for 6 h. After 6 h post-infection, the plate was centrifuged for 10 mins at 1200 rpm, and the supernatant was safely

discarded into Sodium hypochlorite solution. The cells were re-suspended in 1xPBS and pelleted at 1200 rpm for 5 mins. From the cell pellet, genomic DNA was isolated using a standard protocol of the phenol/chloroform method. DNA was used as the template for PCR. The primer details are mentioned in Table 2, and PCR details are in Section *2.2.15*.

Chapter III

An analysis of effect of Epap-1 on the SARS-Cov-2 Spike protein and ACE2 interaction and virus entry

3.1 Introduction:

Studies on vertical transmission of the virus reported mixed results, though the majority of studies were during the third trimester of pregnancy [36, 37]. Neonates from Cov-2 infected women showed positive for the virus at 16 hours [38], 30 h [39], and 36 h [40], and after delivery and on the first day of life after delivery [41, 39], while it is unclear if the transmission from the mother or environment. A study reported that longer virus exposure may contribute to neonatal infection [42], while the virus transmission is seen irrespective of the severity of infection [43, 44]. There is no evidence of the presence of infected cells in the feto-maternal interface [45]. However, placenta samples were shown to be positive for the virus [46, 47, 48, 49, and 50]. Higher viral load was detected in placental tissue compared to the amniotic fluid or maternal or neonatal blood, umbilical stump, and nasopharyngeal aspirate of the neonate [51, 52]. Virions were detected in the syncytiotrophoblast and in the fetal capillary endothelium [53].

Indeed, IgM and IgG antibodies against SARS Cov-2 were reported in neonate blood, suggesting possible in-utero exposure to the virus [54, 45]. IgG may be transferred through the placenta, while virus exposure through the placenta may lead to IgM secretion in the infant [55]. N-protein antibodies were correlated with the severity of maternal infection [56]. Thus, it suggests that host defense mechanisms are associated with a protective environment.

3.2 Results:

3.2.1 Spike protein interacts with Epap-1:

The Wuhan Spike protein and Epap-1 structure were modeled as described in the methods; the structure was optimized using molecular dynamics simulation using GROMACS at 100ns. As shown in **Fig 3.1A**, an optimized structure was used to determine their interactions using Pymol and ligplot. The results of these studies show that the Spike-protein binds with Epap-1 at

position ASN381, LYS449, ARG453, THR457, GLU458, PRO548 of S-protein hydrogen bonded with LEU346 TYR355, ILE358, ASN457, HIS465, ARG570, HIS573 of Epap-1 with docking score of -12.0 (Fig 3.1B). Further, a comparison of Epap-1 interaction of delta and omicron variants of S protein showed that the Spike-protein of Delta variant binds with Epap-1 at positions ARG331, ARG340, ASN345, ARG451, ALA507, GLN549, ARG562 of Spikeprotein hydrogen bonded with ASN1, ARG5, THR23, ALA389, THR390, LYS392, ALA393, TYR555, ARG564 of Epap-1 (Fig 3.2A). While the Spike-protein of Omicron variant binds with Epap-1 at position GLU321, THR326, ARG328, PHE328, ALA329, SER330, ASN335, SER340, ILE449, GLU452 of Spike-protein hydrogen bonded with LEU346, ASN347, ARG570, HIS573, PRO587, SER591, PHE718, LEU721, GLY722, LEU728, GLN729, GLY730, ASN731 of Epap-1 (Fig 3.2B). The docking score of Epap-1 with Spike-protein of SARS CoV-2 delta and omicron is -16.6 and -15.2, suggesting a stronger interaction of these variants compared to the Wuhan variant. The interaction studies shows that mutation in arginine at 453 of Wuhan S-protein interact with Epap-1 at position K28, N108, L163 D165, R177, S192, K193, N198, E211, T271, I272, T273, K293, D732, Q823, Y824, D826, G829, S961, S962, N965, D966 of S-protein hydrogen bonded with R299, E300, L346, R359, R363, K564, R568, R570, L571, L574, R588, G719, L723, F724 of Epap-1 (Fig 3.3(A)) with binding energy of -17.6 kJ/mol. The mutation in lysine at 449 of Wuhan S-protein interact with Epap-1 at position K28, D96, N198, T271, I272, T273, D723, Q823, D826, G829, S961, S962, N965 of S-protein hydrogen bonded with R299, E300, L346, R359, L441, R570, L574, S577, R580, R588, G719, L723, F724, N731 of Epap-1 (Fig 3.3(B)) with energy of -17.6 kJ/mol. The mutation in proline at 548 of Wuhan S-protein interact with Epap-1 at position K28, V107, N108, L163, S192 K193, N198, E217, S259, T271, T273, I272, D723, Q823, D826, S961, S962, N965, D966 of S-protein hydrogen bonded with R299, E300, L346, R359, L441, V565, R568, W569, R570, L574, S577, R580, R588, G719, F724, L723, N781 of Epap-1 (**Fig 3.3(C**))

with binding energy of -18.2 kJ/mol. Similarly, the mutation in asparagine at 345 of Delta Sprotein interact with Epap-1 at position S1108, L1126, E1129, N899, E903, T897, E1096, Q1098, E1072, Q886, Q1021, E1016, Y889, W871, T872 of S-protein hydrogen bonded with R299, N781, R463, N466, S444, R359, H573, R570, V565, D356, P563, R364, R568, R363 Epap-1 (Fig 3.4(A)) with binding energy of -14.0 kJ/mol. The mutation in arginine at 440 of Delta S-protein interact with Epap-1 at position T807, W871, T872, Q886, Y889, N892, N899, E1016, Q1021, E1077, E1096, Q1098, S1108, E1126, L1129, S1132 of S-protein hydrogen bonded with R299, D356, R359, R463, N466, G467, P563, V565, R568, R570, H573, N731, S944 of Epap-1 (Fig 3.4(B)) with binding energy of -14.1 kJ/mol. The mutation in glutamine at 549 of Delta S-protein interact with Epap-1 at position N882, Q886, Y889, N892, N899, E903, E1077, Q1091, E1096, Q1098, E1106, S1108, L1126, E1129 of S-protein hydrogen bonded with R299, D354, D356, R359, R363, R364, S444, N466, P563, R564, V565, R568, R570, N731 of Epap-1 (Fig 3.4(C)) with binding energy of -14.0. Likewise, the mutation in arginine at 328 of Omicron S-protein interact with Epap-1 at position Y401, F410, E497, D408, T411, R548, D532, D562, S444, R300, E600, T599, R627, A628, N592, S640, S638, A682 of S-protein hydrogen bonded with K261, T424, D422, D32, G31, Q33, S27, T440, N298, L442, V361, R363, Y546, H362, R359, E354, S353, R580, G730, N731 of Epap-1 (Fig 3.5(A)) with binding energy of -21.9 kJ/mol. The mutation in serine 340 of Delta S-protein interact with Epap-1 at position Y402, D408, F410, D488, E497, Q625, R67, A628, Y636, N638, S640, A682, N697, Y737, F740, Q743, E754, Q989, T990 of S-protein hydrogen bonded with Q47, K48, Y293, S353, L354, N357, R359, N402, R414, D415, R416, R422, T424, H465, R570, R580, G730, N731 of Epap-1 (Fig 3.5(B)) with binding energy of -22.7 kJ/mol. The mutation in glutamic acid at 452 of Omicron S-protein interact with Epap-1 at position N298, Y402, D408, E497, R548, D549, D552, N597, Q599, Q625, R627, A628, Y737, S739, Q743, E754, Q983, T990 of S-protein hydrogen bonded with D32, Q33, R41, Q47, K48, K261, H353, E354,

N357, S358, R359, H362, R363, R414, D415, R422, T424, T440, S444, H465, R578 of Epap-1 (**Fig 3.5(C**)) with binding energy of -23.0 kJ/mol [33].

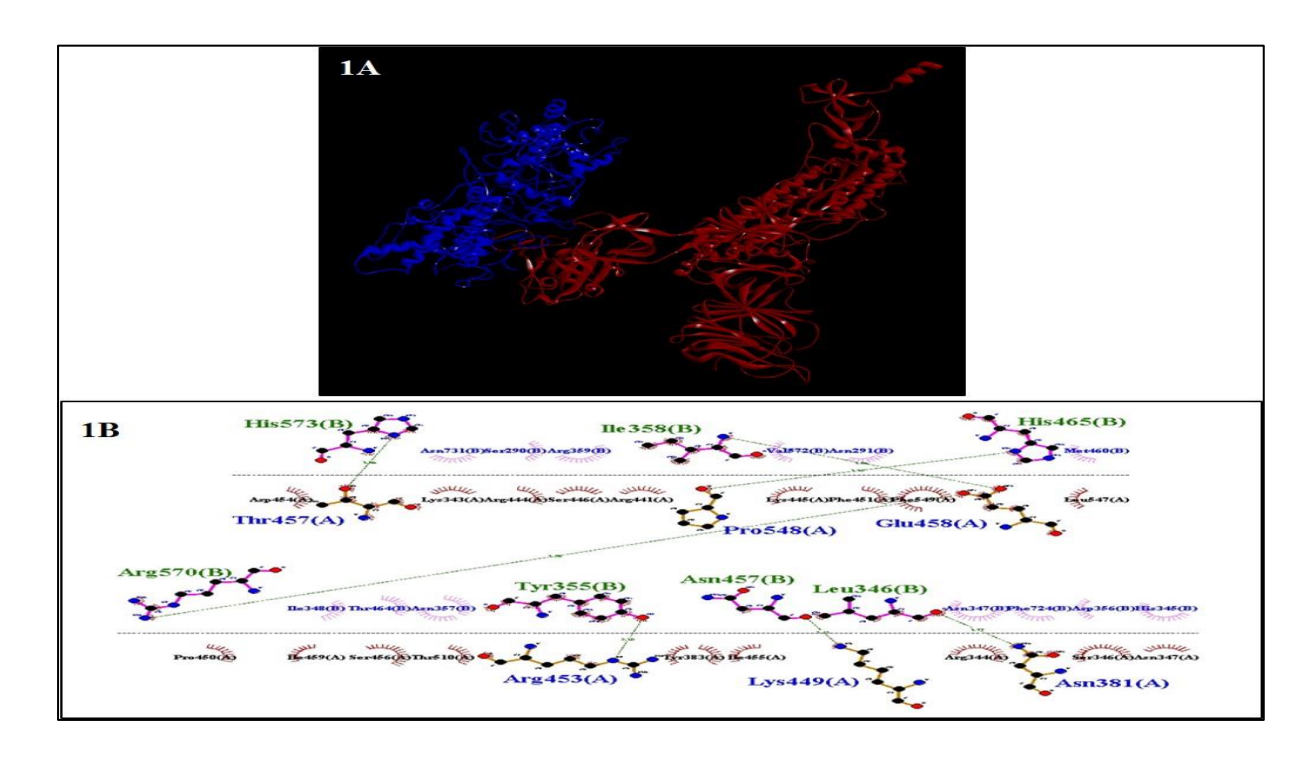


Fig 3.1 A: 3D Structure of Wuhan Spike-protein and Epap-1 complex Blue represents Epap-1, and red represents Wuhan Spike-protein; **B:** 2D representation of Wuhan Spike-protein and Epap-1 complex

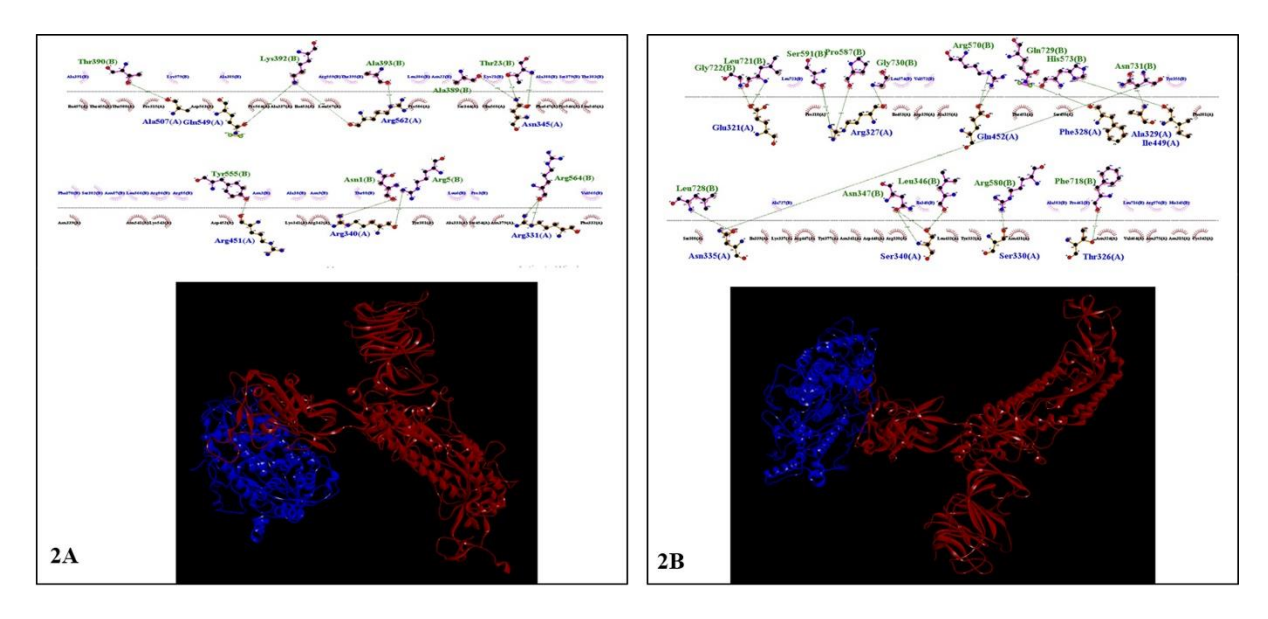


Fig 3.2A: Structure of Delta Spike-protein and Epap-1 complex Blue represents Epap-1, and red represents Delta Spike-protein; **B:** Structure of Omicron Spike-protein and Epap-1 complex Blue represents Epap-1, and red represents Omicron Spike-protein

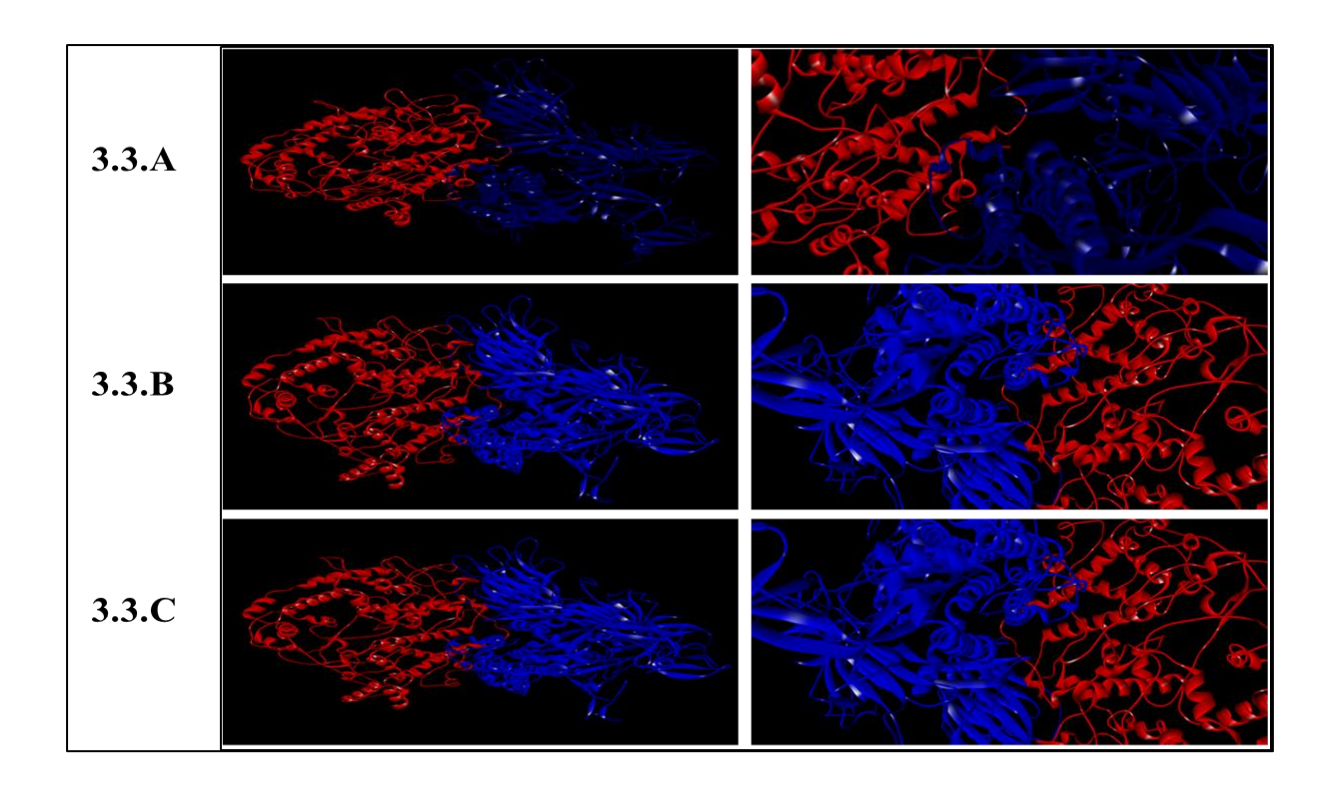


Figure 3.3: (A) Interaction of S-protein having mutation ARG453 with Epap-1. Blue represents S-protein, and red represents Epap-1. (B) Interaction of S-protein having mutation LYS449 with Epap-1. Blue represents S-protein, and red represents Epap-1. (C) The interaction of S-protein has a mutation PRO548 with Epap-1. Blue represents S-protein, and red represents Epap-1.

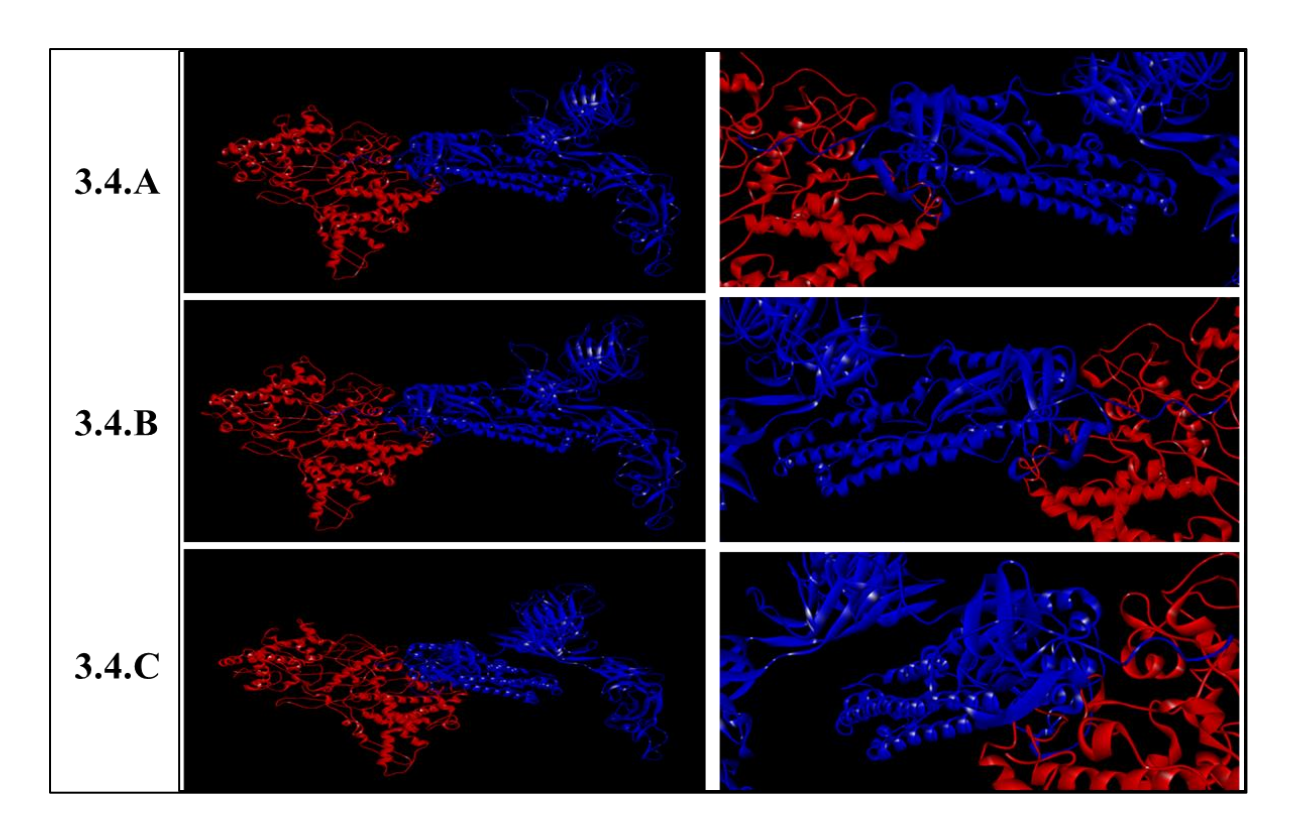


Figure 3.4: (A) Interaction of Delta S-protein having mutation ASN345 with Epap-1. Blue represents S-protein, and red represents Epap-1. (B) Interaction of Delta S-protein having mutation ARG440 with Epap-1. Blue represents S-protein, and red represents Epap-1. (C) Interaction of Delta S-protein having mutation GLN549 with Epap-1. Blue represents S-protein, and red represents Epap-1.

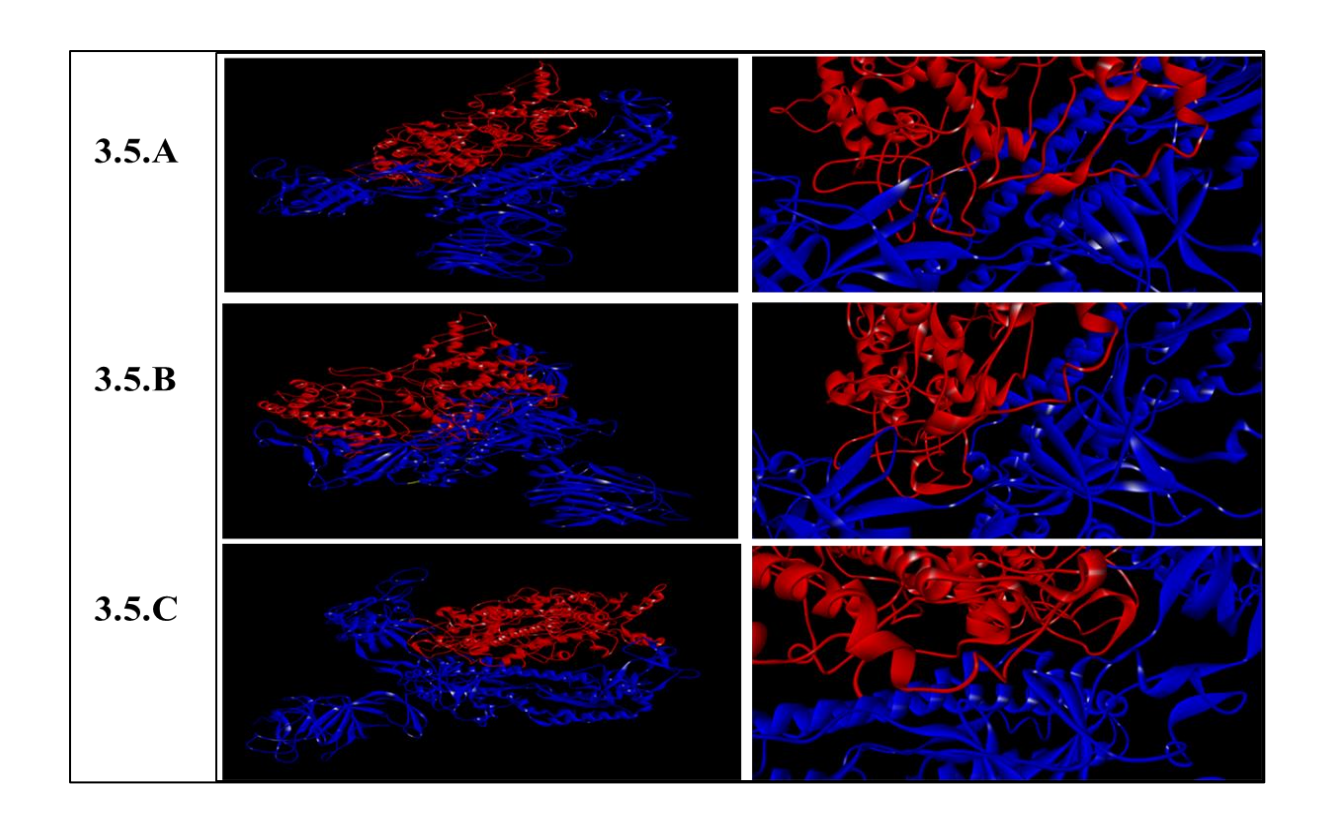


Figure 3.5: (A) Interaction of Omicron S-protein having mutation ARG328 with Epap-1. Blue represents S-protein, and red represents Epap-1. (B) Interaction of Omicron S-protein having mutation SER340 with Epap-1. Blue represents S-protein, and red represents Epap-1. (C) Interaction of Omicron S-protein having mutation GLU452 with Epap-1 Blue represents S-protein, and red represents Epap-1.

3.2.2 Interaction of S protein-Epap-1 complex with ACE2

Spike protein and Epap-1 complex, as formed in **Fig 1B**, was studied for its interaction with ACE2; the results in Fig 4 show that the Spike-protein and Epap-1 complex interaction with ACE2 at position THR9 of Spike-protein and ARG4, ARG5, ARG363, SER511, TRP548, TYR555, ARG559, VAL565, ARG568, LYS683, SER684, CYS687, LYS695 of Epap-1 hydrogen bonded with ASN134, ASP136, ASN137, ASP157, TYR158, ASN159, GLU160, TYR255, SER257, LYS600, ASP609, ASP615 of ACE2 (**Fig 3.6**), these interactions weaken Spike-protein binding to ACE2 with a binding score of -5.9 suggesting that Epap-1 is weakening interaction Spike protein with ACE2. While Spike-protein interact with ACE2 at the position Y449, Y453, N487, Y489, G496, T500, G502, Y505, L455, F456, F486, Q493, Q498, and N501 in the absence of Epap-1, it interacts at the position ASP553, ILE554, ARG631, MET682, GLU687, TYR692, ASN694, GLN747, GLU745, ARG1004, GLU1016, ARG1024 in the presence of Epap-1 which indicates that the Spike-protein Epap-1 interaction may interfere the interaction of ACE2 with Spike-protein [33].

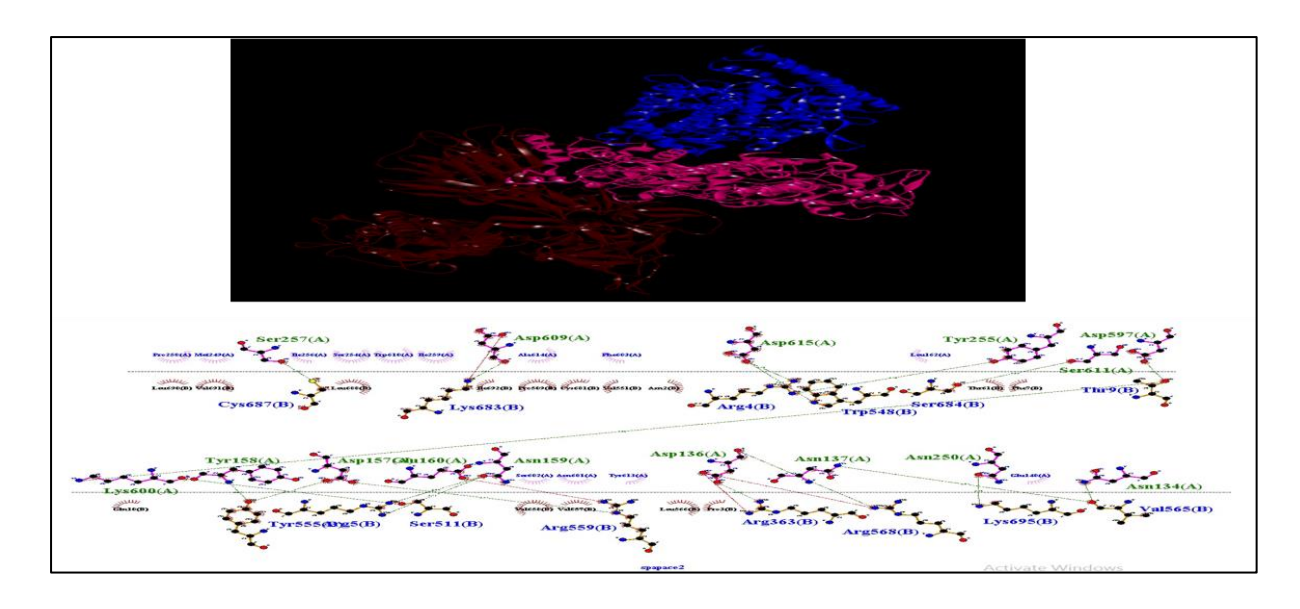


Fig 3.6: Wuhan Spike-protein and Epap-1 complex with ACE2 interaction Red: Spike-protein Blue: Epap-1 Pink: ACE2

3.2.3 Purification of Epap-1 from first trimester placental tissue:

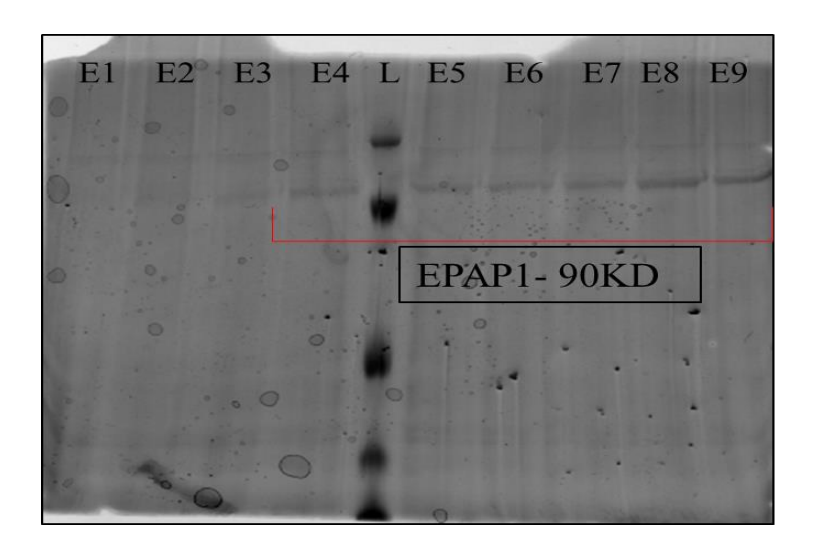


Fig 3.7. Purification of Epap-1 from first-trimester placental tissue using SNA affinity chromatography.

3.2.4 Cloning and Expression of Spike proteins in pEGFP-C1 vector:

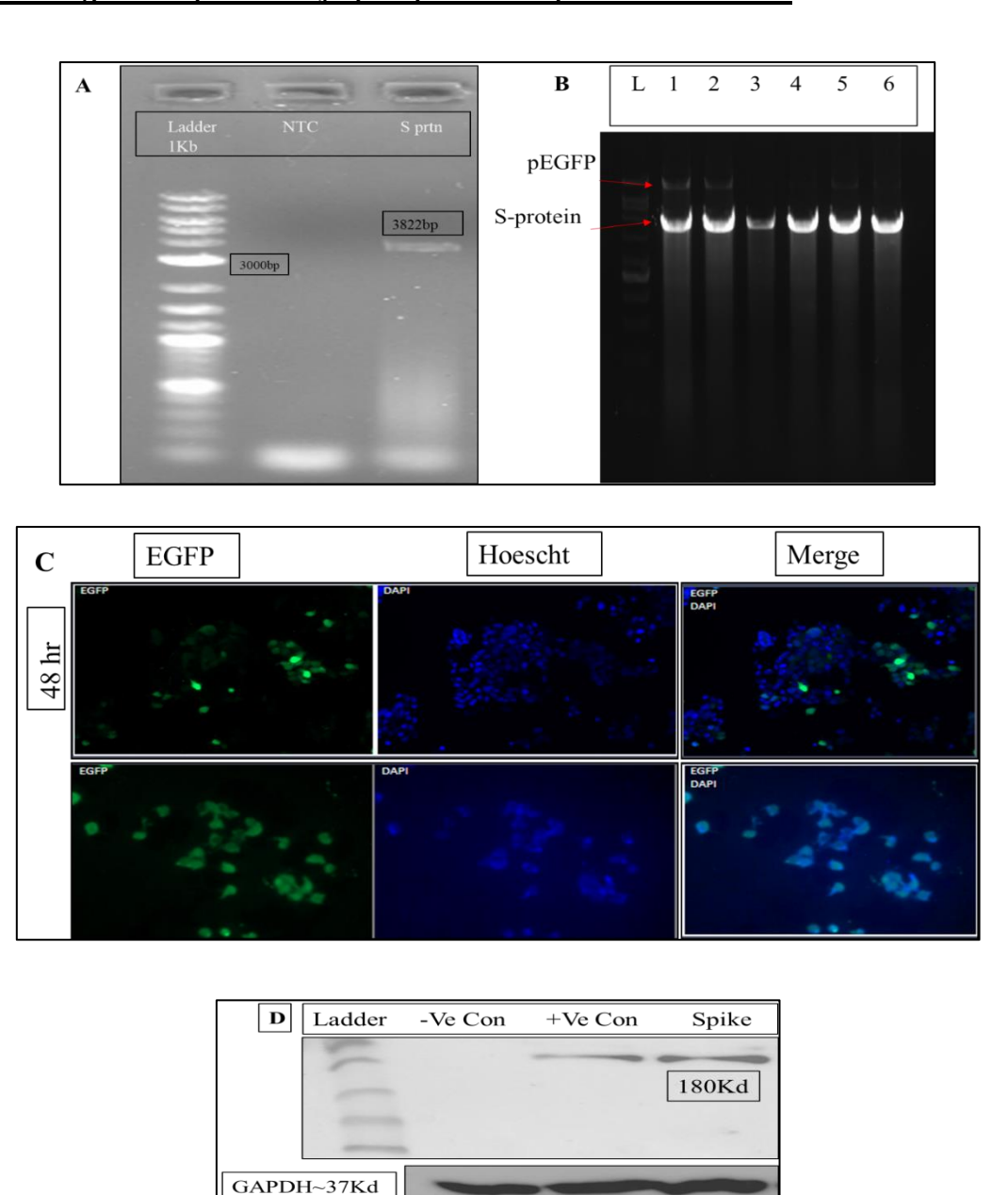


Fig 3.8 Above results show cloning and expression of Spike protein in pEGFP-C1. **Fig 3.8A.** Shows PCR amplification of a fragment of Spike protein (3822bp) using iProof Highfidelity master mix. **Fig 3.8B.** Shows double digestion of pEGFP-Spike clone using Xho1 and Kpn1 restriction digestion enzymes. **Fig 3.8C.** Shows transfection of pEGFP-Spike clone in HEK293T cells. **Fig 3.8D.** The Western blot analysis of Spike protein was confirmed using a mouse anti-spike 180kDa antibody, and GAPDH was used as the standard control.

3.2.5 Cloning and Mammalian Expression of RBD protein in pEGFP-C1 vector:

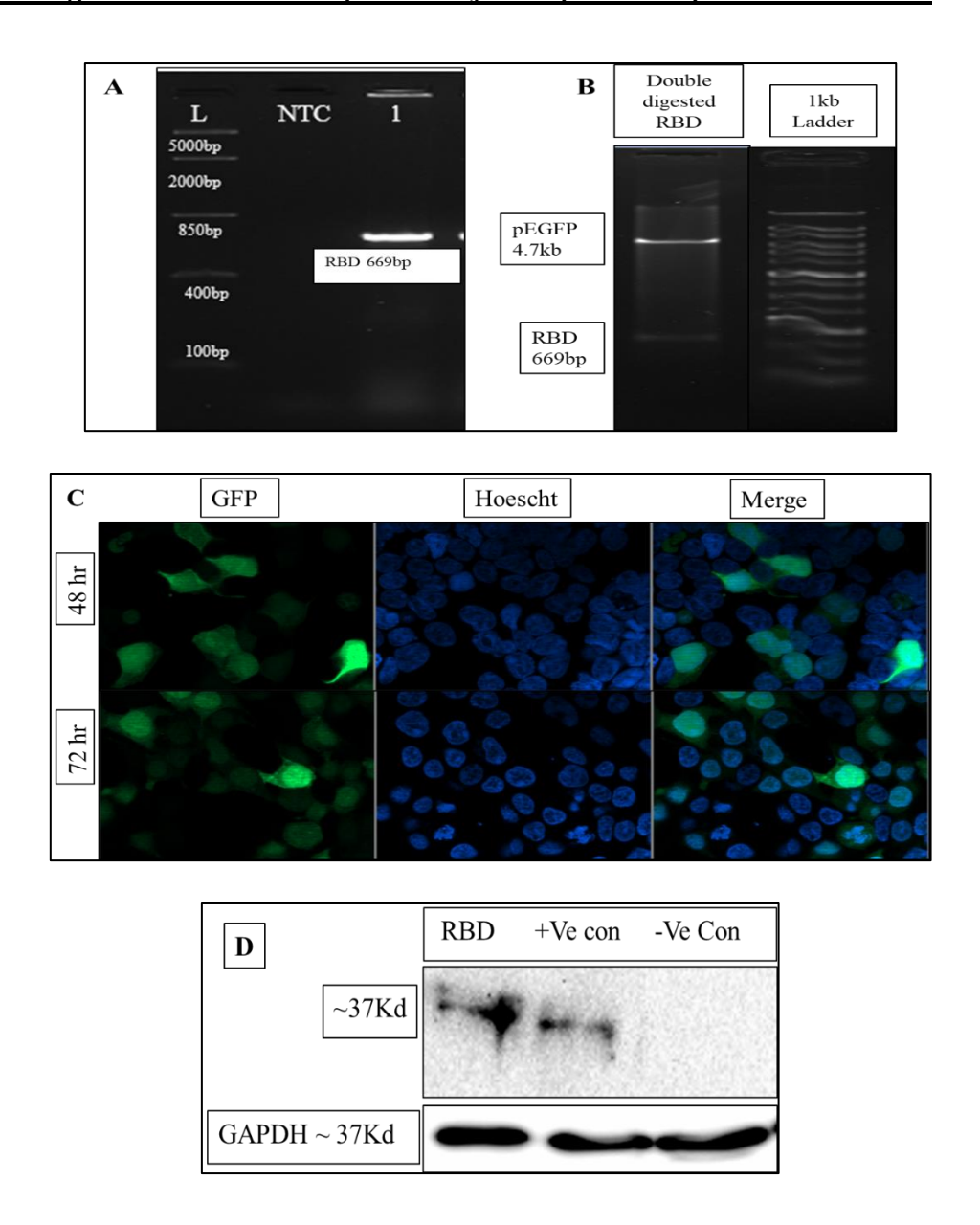


Fig 3.9 The results above show the cloning and expression of RBD protein in pEGFP-C1. **Fig 3.9A.** Shows PCR amplification of a fragment of RBD protein (669bp) using Thermo Fisher 2X Green Taq master mix. **Fig 3.9B.** It shows double digestion of the pEGFP-RBD clone using Xho1 and Kpn1 restriction digestion enzymes. **Fig 3.9C.** Shows transfection of pEGFP-RBD clone in HEK293T cells. **Fig 3.9D.** The Western blot analysis of the RBD protein was confirmed using a rabbit anti-RBD 37kDa antibody, and GAPDH was used as the standard control.

3.2.6 Cloning and Bacterial Expression of RBD protein in pET23d+ vector:

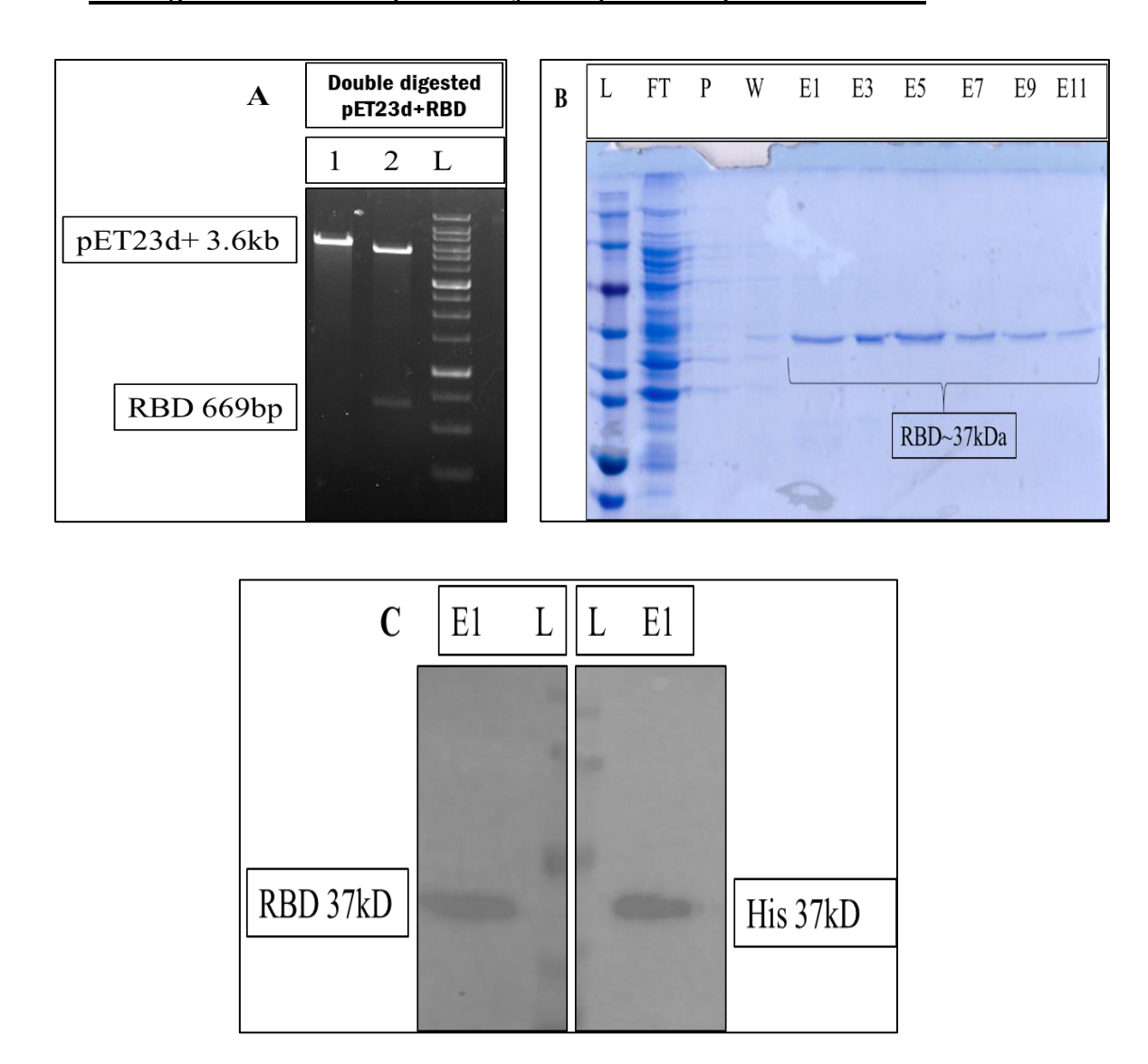


Fig 3.10 The Above results show cloning and bacterial expression of RBD protein in pET23d+. **Fig 3.10A.** Shows double digestion of pET23d+-RBD clone using Sac1 and Not1 restriction digestion enzymes (L- ladder, 1- Ligated pET23d-RBD clone, 2-Double digested products of pET23d+ and RBD). **Fig 3.10B.** pET23d+RBD clone was transformed into BL21 (DE) cells for purification of RBD protein. Purified protein was loaded onto 10% SDS gel analyzed by Coomassie Brilliant Blue stain. Results confirmed by RBD protein bands at 37kDa (FT- Flow through, P- pellet, W- wash, E- elutions). **Fig 3.10C.** Shows a Western blot analysis of RBD protein confirmed by using rabbit anti-RBD 37kDa antibody and as a control primary antibody against His-tag antibody was used.

3.2.7 <u>Purification of IgG from Covid-19 Positive Blood sample using Proteinase A column affinity chromatography:</u>

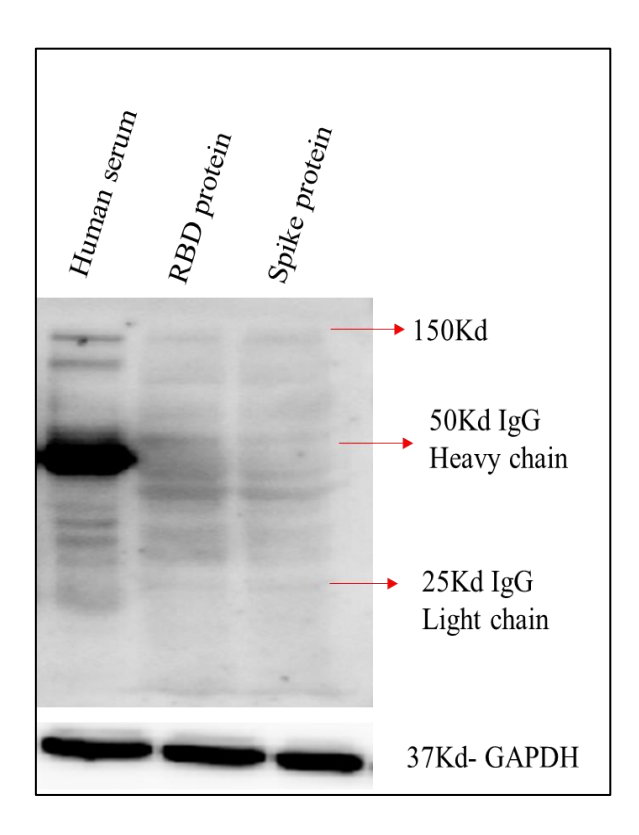


Fig 3.11. It shows the purified human anti-sera from positive COVID-19 patient samples. Western blot analysis of human anti-sera, RBD protein, and spike protein was confirmed by using human IgG (Gamma chain) cross-adsorbed secondary antibody (62-8420).

3.2.8 <u>Analysis of the effect of Epap-1 interaction with S-protein/RBD protein and ACE2</u> interaction using ELISA:

HEK cells were incubated with only RBD protein and RBD - Epap1 protein complexes and were assessed by Rabbit Anti- ACE2 antibody. When compared to the control HEK cells, the absorbance of the ACE2 antibody decreased due to the strong interaction of only RBD protein (100μg) when RBD-Epap-1 complexes are formed in the presence of increasing concentrations of Epap1 protein (50μg, 100μg) complex, the ACE2 exposed thus increasing recognition of ACE2 antibody. Thus suggesting a strong interaction between RBD and Epap-1 (**Fig-3.12A**). A similar experiment was carried out using S protein; the results of these experiments are shown in (**Fig 3.12B**), confirming that Epap-1 interferes with S protein-ACE interaction.

HEK293T cells were incubated with only RBD protein, RBD protein- Epap1 complex, and were assessed by Rabbit Anti-RBD antibody. HEK cells incubated with only RBD protein (100μg) showed more intensity to RBD antibody when compared to the RBD- Epap1 complex (50μg, 100μg) complex (**Fig 3.12C**). These results suggest that the binding of RBD is inhibited in the presence of Epap-1. HEK293T cells were incubated with only S protein, S protein- Epap1 complex, and bound S protein was probed with Mouse Anti-Spike antibody. HEK cells incubated with only S protein (100μg) showed higher intensity to Mouse Anti-Spike antibody when compared to Spike- Epap1 complex (50μg, 100μg) complex, suggesting that the binding of S protein to ACE2 was inhibited by Epap-1 (**Fig 3.12D**) [33].

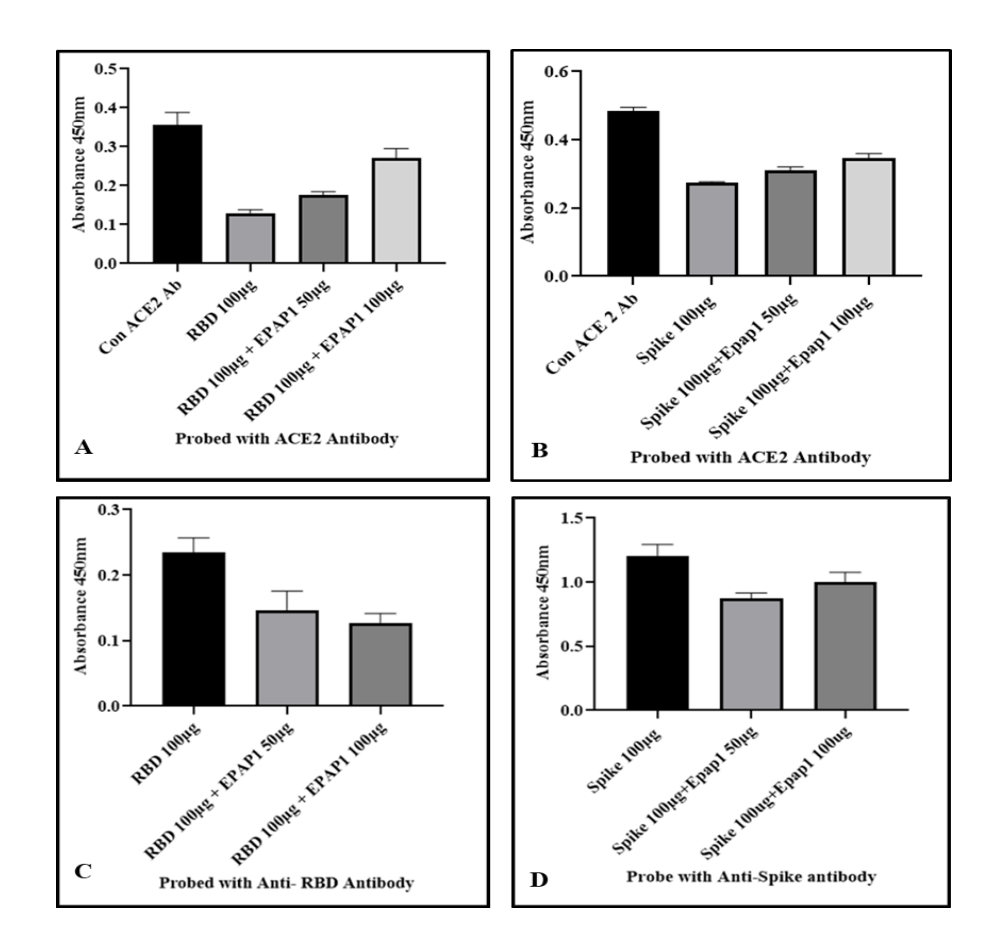
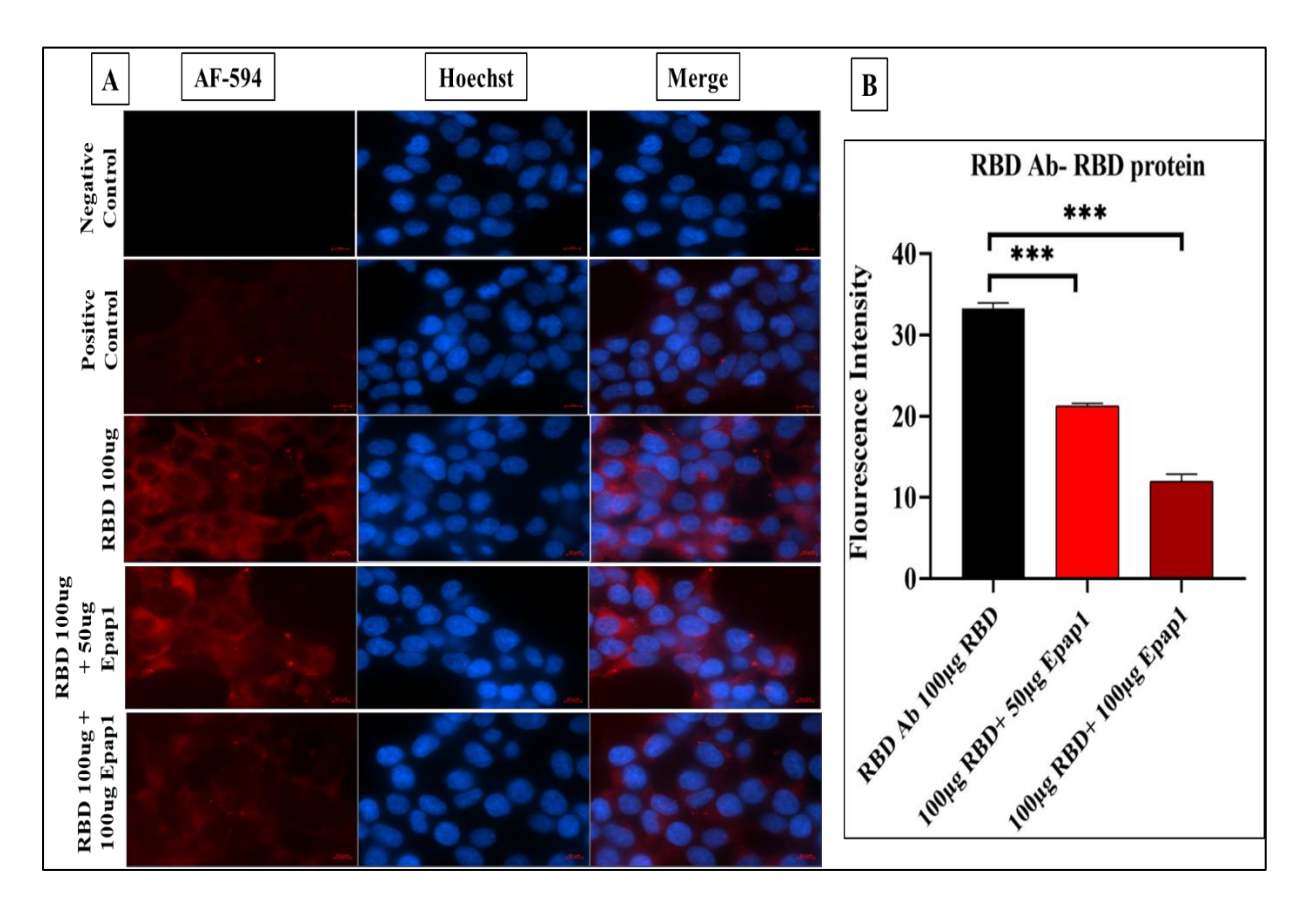


Fig 3.12A. RBD protein- Epap1 (50, 100 μg) complexes interaction with ACE2 expressing HEK293T cells; cells were seeded and fixed on 96 wells and incubated with RBD-Epap-1 complexes, probed with Rabbit Anti-ACE2 antibody and quantified. **3.12B.** Spike-Epap1 protein (50, 100 μg) complexes interaction with ACE2 expressing HEK293T cells; cells were fixed on 96 wells, incubated with Spike-Epap-1 protein complexes, probed with anti-ACE2 antibody, and quantified. **3.12C.** RBD protein- Epap1 (50, 100 μg) complexes interaction with ACE2 expressing HEK293T cells; cells were fixed on 96 wells, incubated with RBD –Epap-1 complexes, and probed with Rabbit Anti- RBD antibody and quantified. **3.12D.** Spike protein-Epap1 (50, 100 μg) complexes interaction with ACE2 expressing HEK293T cells; cells were fixed on 96 wells and incubated with Spike-Epap-1 complexes and probed with anti-Mouse Anti- Spike antibody and quantified.

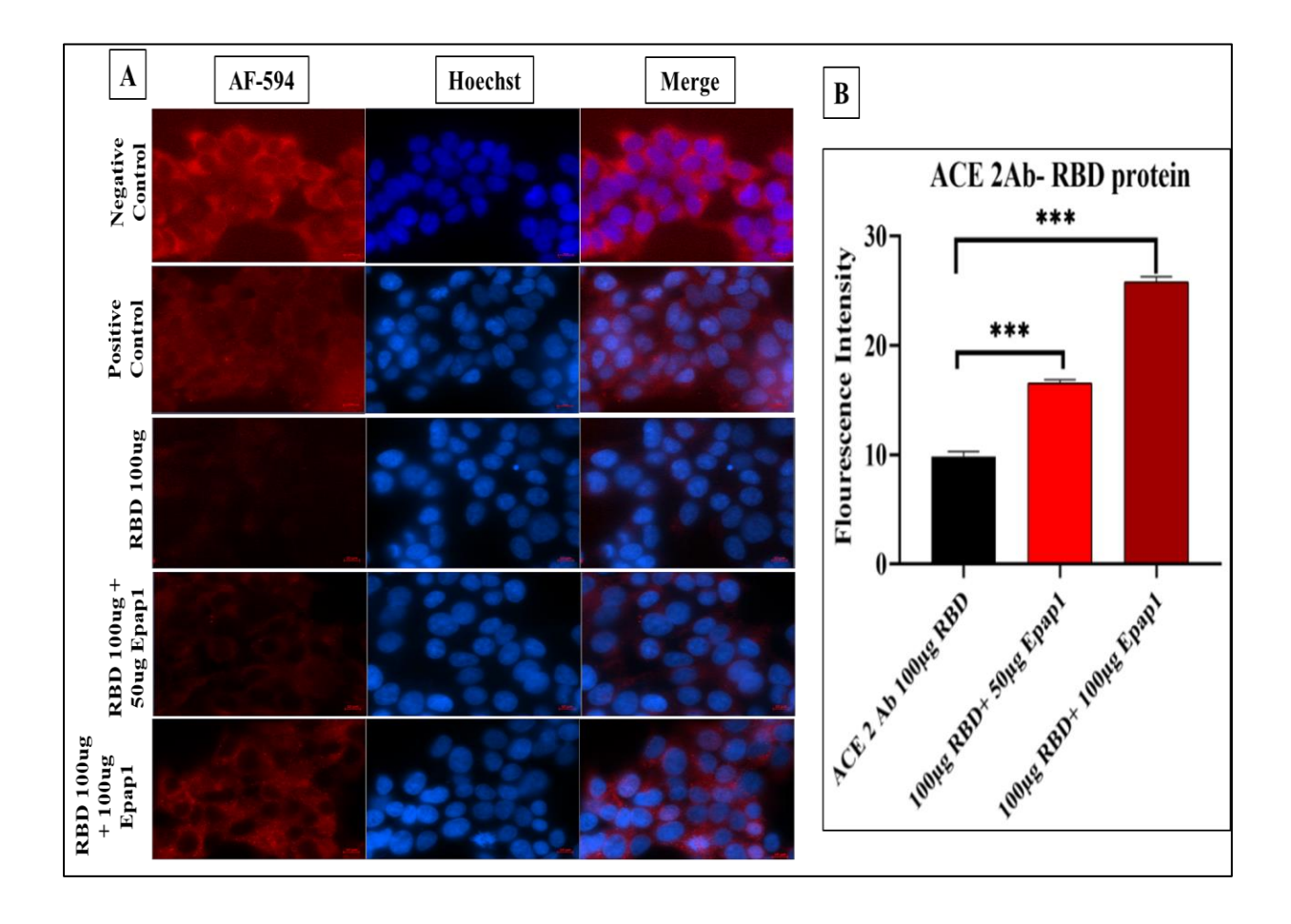
3.2.9 <u>Analysis of the effect of Epap-1 interaction with RBD protein and ACE2 interaction</u> using immunofluorescence:

ACE2-expressing cells were measured using the fluorescent dye Alexa Flora 594. This result shows a significant decrease in the intensity of Alexa flora 594 in the presence of Epap-1 when probed with Rabbit Anti-RBD antibody, suggesting the ACE2 receptor does not recognize Epap-1 bound RBD (**Fig 3.13A**). When ACE2 and RBD protein interaction was analyzed using Rabbit Anti-ACE2 antibody in the presence of increasing concentrations of Epap-1, the results showed that at higher Epap-1 concentrations, ACE2 is accessible to Rabbit Anti-ACE2 antibody (**Fig 3.14A**). In positive control, cells were incubated with RBD protein (100μg) in the presence of Cov-2 IgG (100μg); the results of these experiments showed that Cov-2 IgG significantly inhibits RBD protein binding to ACE2 receptors of HEK 293T cells [33].



3.13A. Negative control cells, the experiments were conducted in PBS. In positive control, cells were treated with RBD protein (100µg) with Human anti-sera from COVID-19 positive

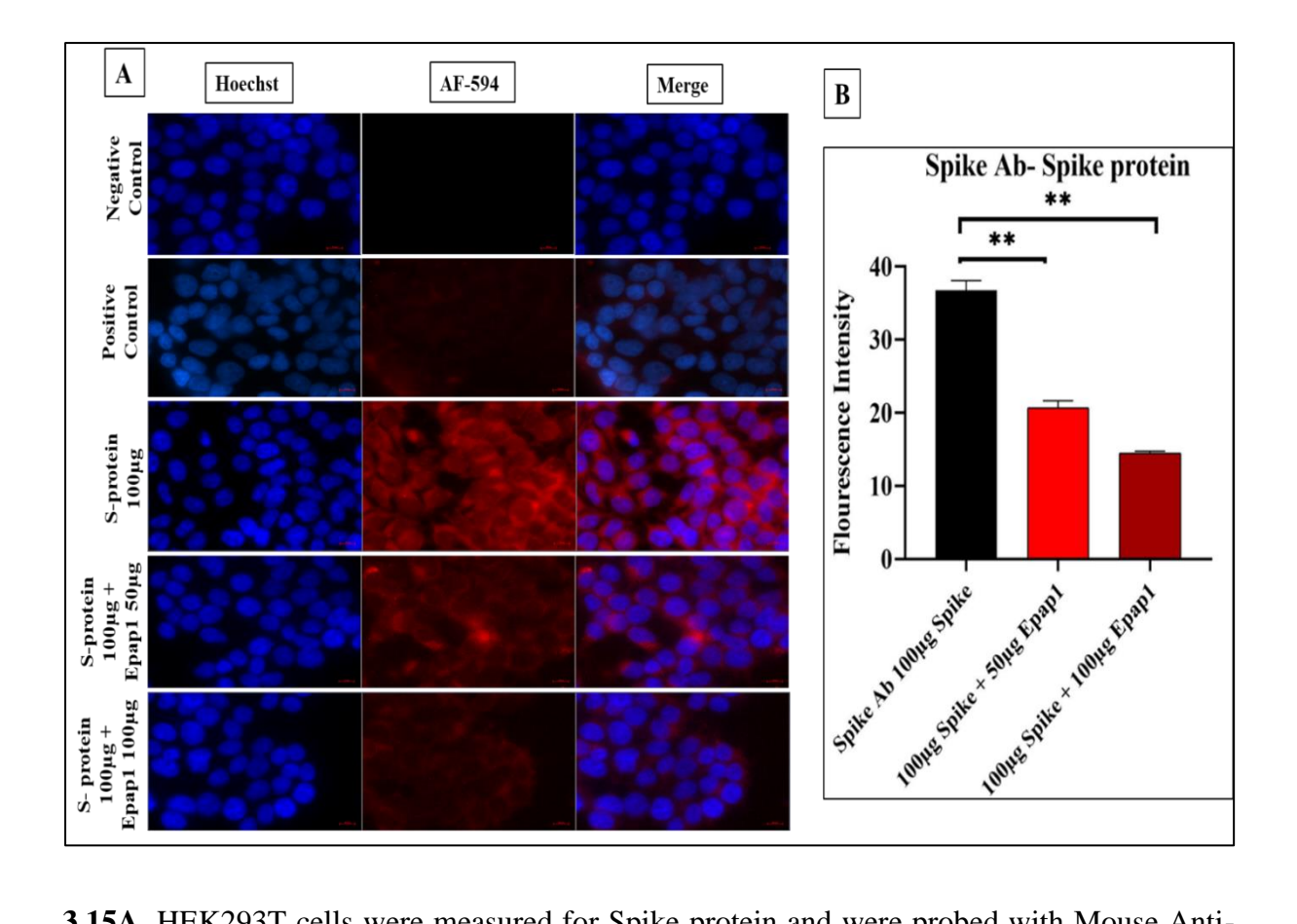
patient ($100\mu g$), RBD protein ($100\mu g$) and Epap-1 (0, 50, $100\,\mu g$) complexes were formed and incubated with ACE2 expressing HEK293T cells.HEK293T cells were measured for RBD protein and were probed with Rabbit Anti-RBD antibody. The results show that RBD-protein binding to ACE2 is significantly inhibited by Epap-1. 63x image is presented; Red: RBD antibody coupled with alexfluor-594, Blue: Hoechst. **3.13B.** Using Image J software, Fluorescent intensity was quantified and represented as a bar diagram. Two-tailed unpaired student's t-test was used to calculate P-values; * indicates P < 0.05, ***P< 0.001.



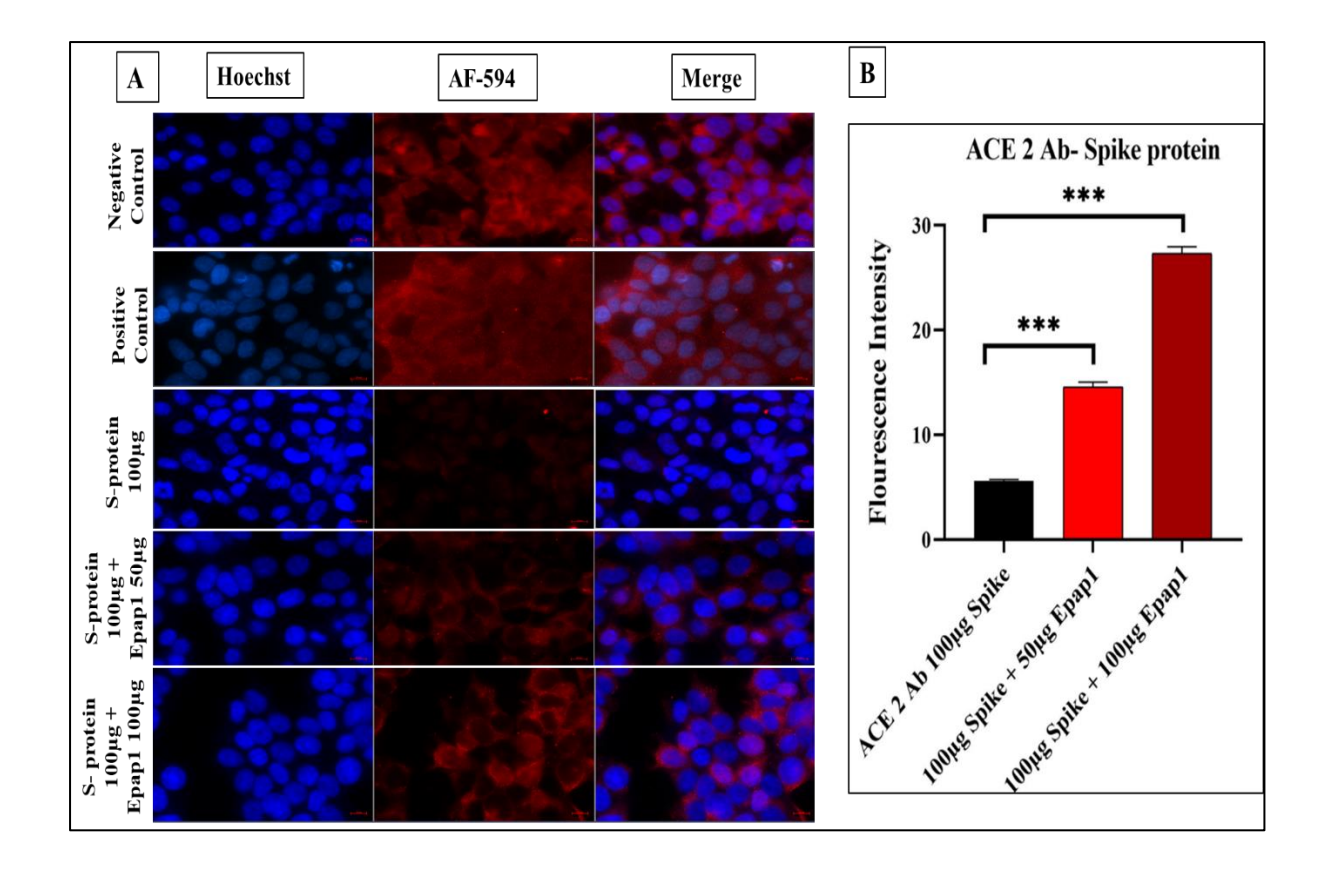
3.14A. HEK293T cells were measured using the fluorescent dye Alexa Flora 594. This result shows a significant increase in the intensity of Alexa flora 594 when probed with Rabbit Anti-ACE2 antibody, suggesting that ACE2 is exposed when Epap-1 inhibits RBD protein and ACE2 interaction. 63x image is presented; Red: Anti-ACE antibody coupled with alexfluor-594, Blue: Hoechst. **3.14B.** Using Image J software, Fluorescent intensity was quantified and represented as a bar diagram. Two-tailed unpaired student's t-test was used to calculate P-values; * indicates P < 0.05, ***P < 0.001.

3.2.10 <u>Analysis of the effect of Epap-1 interaction with Spike protein and ACE2 interaction</u> using immunofluorescence:

ACE2 expressing cells were incubated with Spike protein and Spike-Epap-1 protein complex, the Spike protein was probed with Mouse Anti-Spike antibody, and the Spike protein antibody was detected with secondary antibody conjugated with Alexa flora 594. This result shows a significant decrease in the intensity of Alexa flora 594 when Spike protein (100μg) was incubated with 50 and 100μg Epap1, suggesting Epap-1 inhibits Spike protein and ACE2 interaction (**Fig 3.15A**). In the same experiments when ACE2 and Spike protein interaction was analyzed using Rabbit Anti-ACE2 antibody in the presence of increasing concentrations of Epap-1, the results showed that at higher Epap-1 concentrations, ACE2 is accessible to Rabbit Anti-ACE2 antibody (**Fig 3.16A**). The results showed that Spike protein binding to ACE2 receptors on HEK 293T cells was inhibited in the presence of Cov-2 IgG (positive control) [33].



3.15A. HEK293T cells were measured for Spike protein and were probed with Mouse Anti-Spike antibody. The results show that Spike protein binding to ACE2 is significantly inhibited by Human serum and Epap-1. 63x image is presented; Red: Mouse Anti-Spike antibody coupled with alexfluor-594, Blue: Hoechst. **3.15B.** Using Image J software, Fluorescent intensity was quantified and represented as a bar diagram. Two-tailed unpaired student's t-test was used to calculate P-values; * indicates P < 0.05, ***P < 0.001.



3.16A. HEK293T cells were measured using the fluorescent dye Alexa Flora 594. This result shows a significant increase in the intensity of Alexa flora 594 when probed with Rabbit Anti-ACE2 antibody to detect exposed ACE2 receptors in the presence of S-protein-Epap-1 complexes. The results show that the Spike protein blocks ACE2 antibody detection; when Spike and Epap-1 protein complexes are used, the ACE2 is exposed, as evidenced by the binding of the Rabbit Anti-ACE2 antibody. **3.16B.** Using Image J software, Fluorescent intensity was quantified and represented as a bar diagram. Two-tailed unpaired student's t-test was used to calculate P-values; * indicates P < 0.05, ***P< 0.001.

3.2.11 Antiviral assay and analysis of Proviral DNA with SK38 and SK39 Primers:

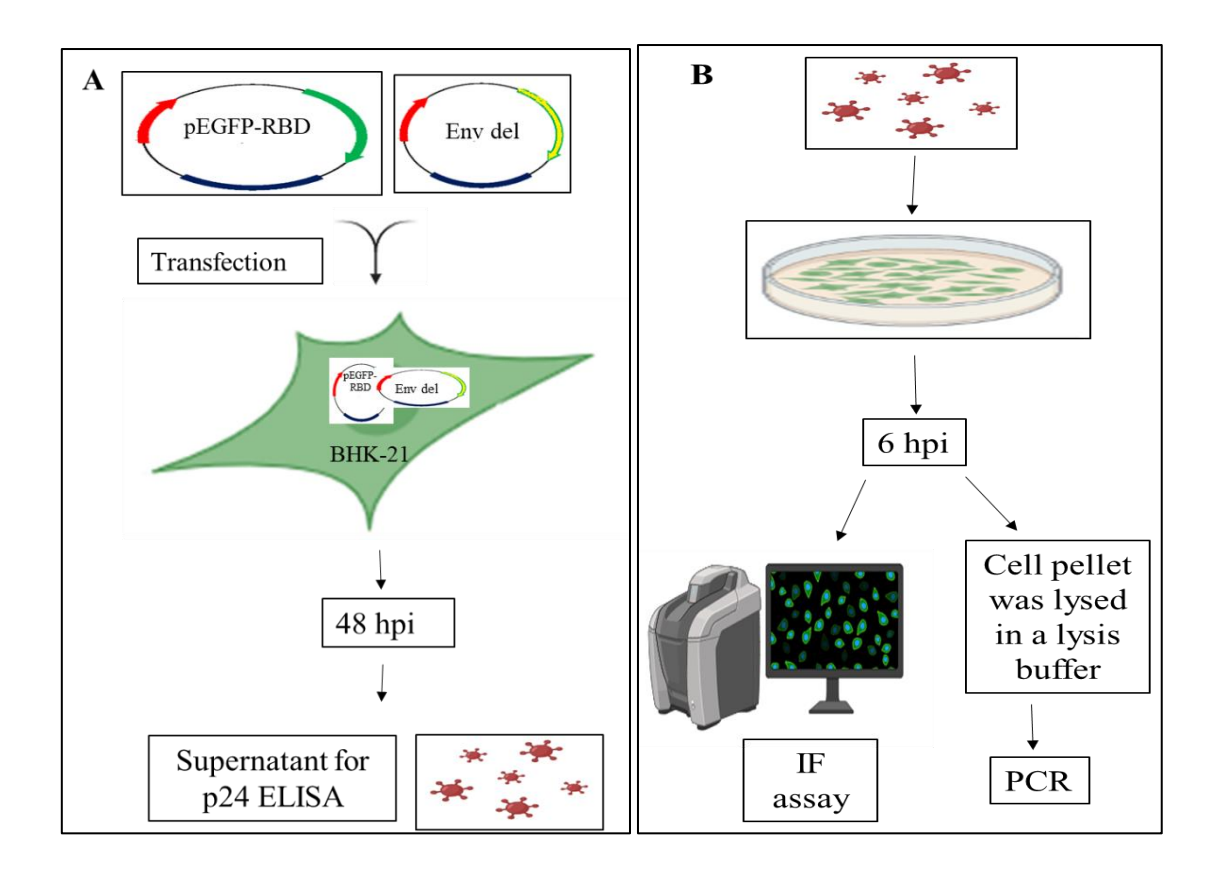
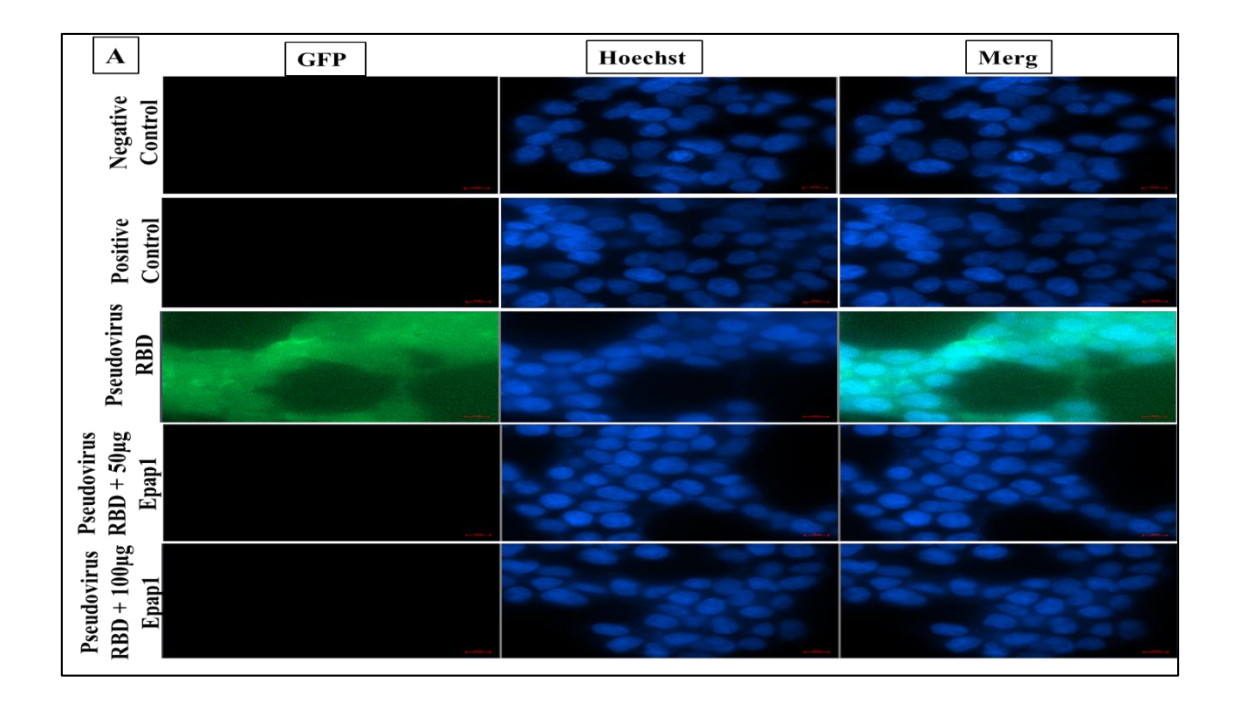


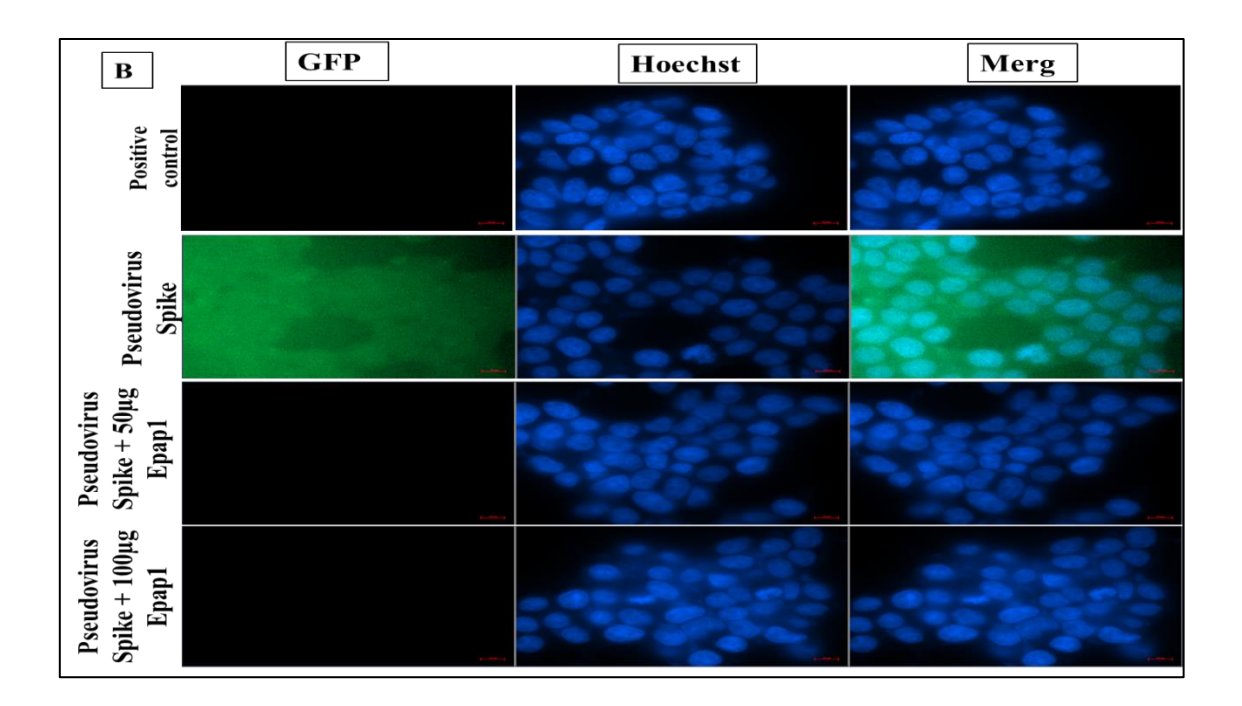
Fig 3.17. Schematic representation to understand if virus surface conformation of RBD and Spike protein has a potential interaction with Epap-1, neutralizing entry of RBD/Spike anchored HIV-1 pseudovirus, entered virus in HEK293T cells was analyzed by GFP-expression of RBD and Spike and further confirmed by gag DNA synthesis using PCR.

HEK293T cells were incubated with pseudovirus expressing RBD protein, pseudovirus of RBD- Epap1 (50μg, 100μg) complex and the pseudovirus entry was monitored using a fluorescence microscope using a GFP tag of RBD protein; the results in **Fig 3.18A** show that Epap-1 inhibited the pseudovirus. In another experiment, HEK293T cells were incubated with pseudovirus anchored with Spike protein in the presence of increasing concentrations of the Epap1 (50μg, 100μg); the pseudo viral entry was monitored by the expression of GFP-tag of Spike protein, the results in **Fig 3.18B** show that Epap-1 significantly inhibits Spike protein anchored pseudovirus. These results confirm that Epap-1 interferes with RBD and Spike protein-mediated virus entry. In positive control, cells were incubated with RBD/Spike pseudovirus (100μg) in the presence of Cov-2 IgG (100μg); the results of these experiments showed that Cov-2 IgG significantly inhibits RBD/ Spike Pseudovirus binding to ACE2 receptors of HEK 293T cells [33].



3.18A. HEK293T cells were measured using GFP expression. In negative control cells, the experiments were conducted in PBS, while in positive control, 100µg Cov-2 IgG was used with pseudovirus of RBD in the experiments. The results of these experiments showed that Cov-2 IgG significantly inhibits RBD Pseudovirus binding to ACE2 receptors of HEK 293T cells. In

Pseudovirus RBD, HEK293T cells were infected with pseudovirus without Epap-1. In the presence of Epap-1 (50, 100 µg), Epap-1 inhibits the pseudovirus of RBD infection in ACE2-expressing HEK293T cells compared to cells infected with the pseudovirus of RBD alone.



3.18B. HEK293T cells were measured using GFP expression. In negative control cells, the experiments were conducted in PBS, while in positive control, 100µg Cov-2 IgG was used with pseudovirus of Spike in the experiments. The results of these experiments showed that Cov-2 IgG significantly inhibits Spike Pseudovirus binding to ACE2 receptors of HEK 293T cells. In Pseudovirus Spike, HEK293T cells were infected with pseudovirus without Epap-1. In the presence of Epap-1, Epap-1 inhibits the pseudovirus of Spike infection in ACE2-expressing cells compared to cells infected with the pseudovirus of Spike alone.

Further confirmation of Epap-1 effect on viral entry, infected cells in the presence of Epap-1 were analyzed for gag DNA synthesis using SK38/SK39 primers; the results presented in **Fig 3.19** show that the gag synthesis significantly inhibited in Epap-1 treated infected HEK cells. These results confirm that Epap-1 inhibits RBD and Spike protein-mediated pseudovirus infection in HEK cells [33].

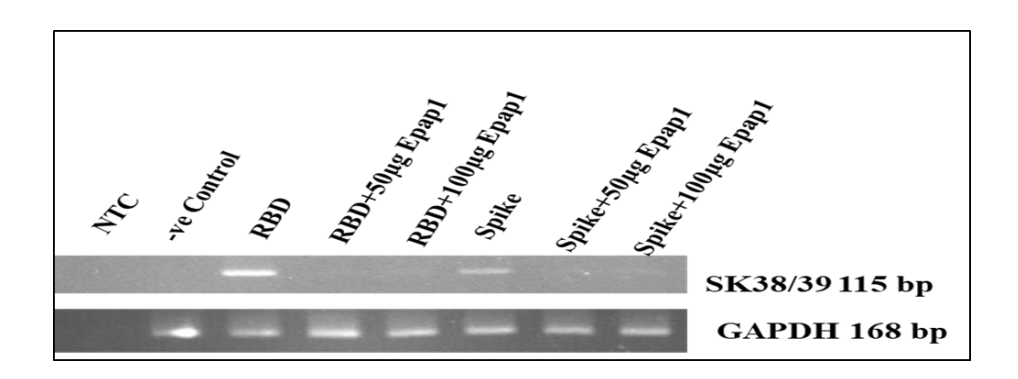


Fig 3.19. The cells were collected after 6 hpi, and DNAs were extracted using phenol/chloroform. PCR was carried out according to the Thermo Fischer 2X Green Taq manufacturers' instructions, and amplified products of the gag region (115 bp), and GAPDH (168 bp, control) were visualized in 2% agarose gel stained with ethidium bromide. The gag synthesis was significantly reduced in Epap-1 treated with infected HEK293T cells. These results confirm that Epap-1 inhibits RBD and Spike protein-mediated pseudovirus infection in HEK293T cells.

3.2.12 Discussion:

Infection through vertical transmission includes intrauterine transmission, transmission during the delivery process (cesarean or vaginal delivery), during breastfeeding, and coming in contact with a child after birth. However, intrauterine vertical transmission can be a major route for maternal-fetal transmission. Although the reports of SARS-COV-2 infection in neonates it is still unclear. There is no direct evidence of infection occurring during delivery or after birth, as there are no positive reports of RT-PCR of the amniotic fluid, placenta, cord blood, vaginal secretions, or breast milk [57]. In a review of 22 studies, 9 out of 83 neonates showed positive RT-PCR results for SARS-COV-2 infection, and Virus-specific antibodies such as IgG and IgM were elevated in serum samples. In contrast, inflammatory cytokines were elevated in the fetus [57, 58]. Viral load among pregnant women was higher in sputum, followed by oral, saliva, and nasal swabs.

ACE2 is abundantly expressed in the ovaries and the oocytes. Therefore, it could be possible that SARS-CoV-2 may target the ovaries and oocytes [59]. Also, in some previous reports, ACE2 mRNA was detected in the uterus and vagina [60]. Further, an increase in ACE2 receptor expression closer to the end of gestation was correlated with enhanced infectivity of coronaviruses in a study [61] and also reported variability of ACE2 expression in the placenta in women could be one of the reasons for transmission variability [62]. In the first trimester, ACE2 is preferentially expressed in STB and TMPRES2 in EVT and CTB, while during the second and third trimesters, ACE2 is also expressed in EVT, whereas TMPRES2 is equally expressed in all cells of trophoblast lineage [63]. In addition, Spike and Nucleocapsid protein expression was reported in STB [49]. In spite of the abundance of receptors in placental tissue, it was observed that the case of 2nd-semester miscarriage showed no evidence of virus infection in the fetus [49]. Thus, a repertoire of the anti-viral environment in the placenta may play a role in reducing the transmission rate. Epap-1 could be one such recruit from the women in

reducing Spike protein and ACE2 interaction for virus entry. The results of the present study show that Epap-1 interaction with S proteins and RBD region inhibits Spike protein interaction with ACE2, thus protecting the fetus from Spike protein-mediated virus innovation. The results using pseudovirus anchored with RBD and Spike protein clearly demonstrate the virus-neutralization activity of Epap-1. Further, silico studies indicate the enhanced affinity of Epap-1 to delta and omicron variants, suggesting Epap-1 possesses multiple epitopes for RBD interactions [33].

3.2.13 Conclusion:

- Epap-1 shows a strong interaction with the ACE2 region of the Cov-2 spike protein; the region reported being involved in Cov-2 interaction with the host cells.
- Spike protein and Epap-1 complex interaction with ACE2 at position THR9 of Spike-protein and ARG4, ARG5, ARG363, SER511, TRP548, TYR555, ARG559, VAL565, ARG568, LYS683, SER684, CYS687, LYS695 of Epap-1 hydrogen bonded with ASN134, ASP136, ASN137, ASP157, TYR158, ASN159, GLU160, TYR255, SER257, LYS600, ASP609, ASP615 of ACE2 receptor.
- Spike-protein interact with ACE2 at the position Y449, Y453, N487, Y489, G496,
 T500, G502, Y505, L455, F456, F486, Q493, Q498, and N501 in the absence of Epap-1, it interacts at the position ASP553, ILE554, ARG631, MET682, GLU687, TYR692,
 ASN694, GLN747, GLU745, ARG1004, GLU1016, ARG1024 in the presence of Epap-1 which indicates that the Spike-protein Epap-1 interaction may interfere the interaction of ACE2 with Spike-protein
- The results of ELISA and IF show that the RBD/Spike protein blocks ACE2 antibody
 detection; when RBD/Spike and Epap-1 protein complexes are used, the ACE2 receptor
 is exposed, as evidenced by the binding of the Anti-ACE2 antibody.
- The results of ELISA and IF show that RBD/Spike protein binding to ACE2 is significantly inhibited by Epap-1.
- The results of the anti-viral analysis confirm that Epap-1 interferes with RBD and Spike protein-mediated virus entry.

Chapter IV

Evaluation of efficacy of small molecule mimics of Epap-1 on SARS Cov-2 RBD protein and ACE2 interaction and virus entry

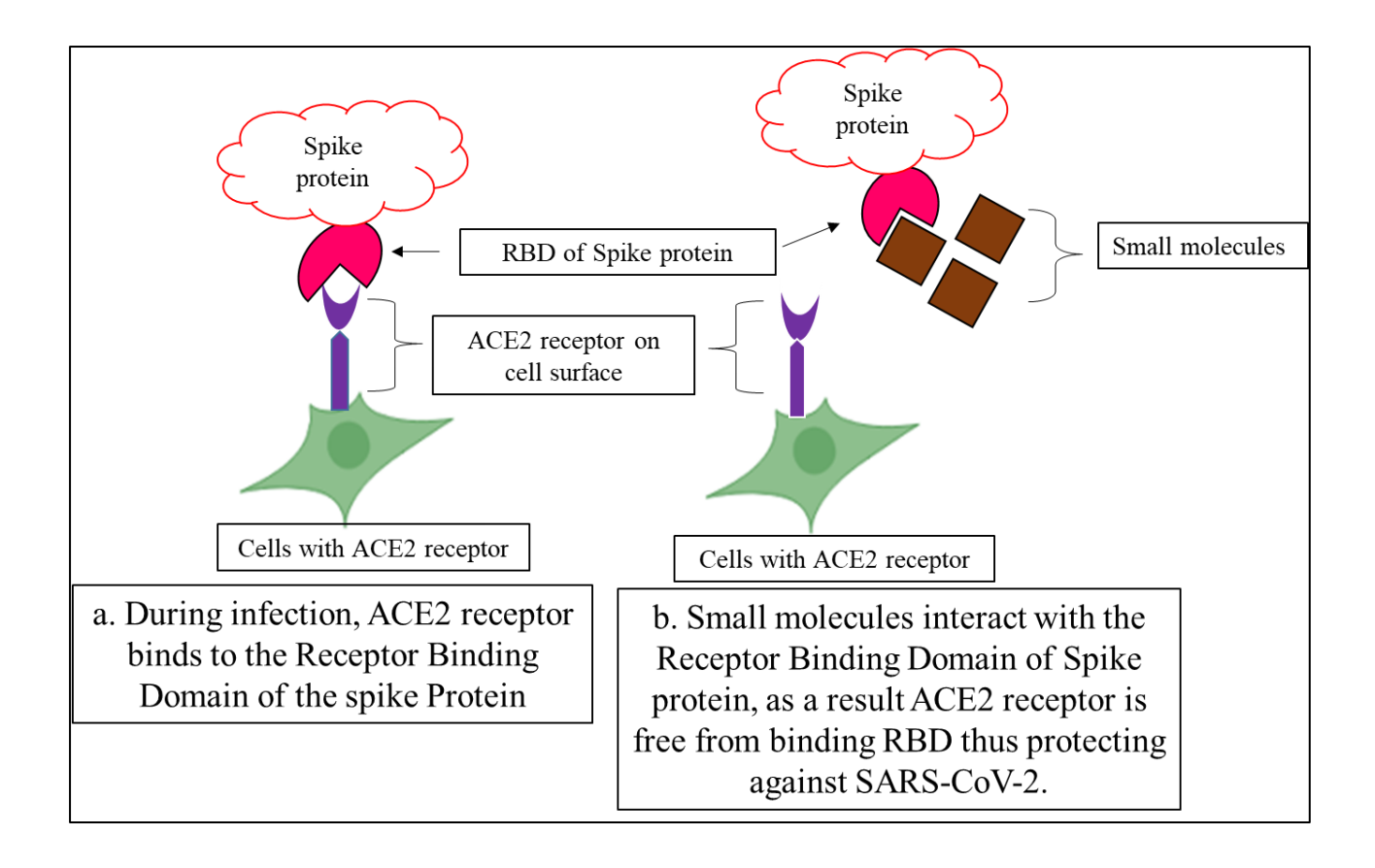
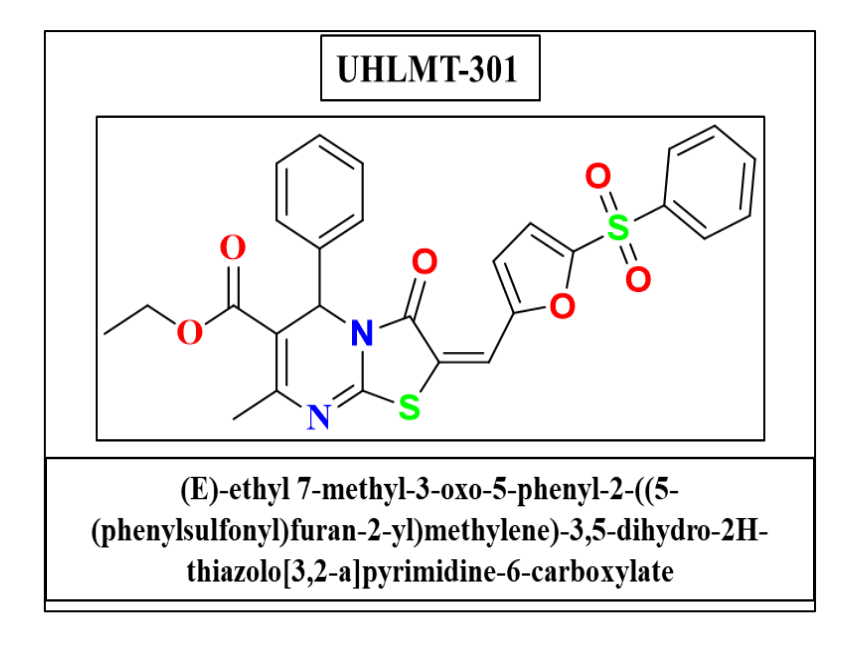


Fig 4.1. Hypothetical model for understanding the interaction of small molecules to the Receptor binding domain (RBD) of Spike protein. As a result, RBD of spike protein is inhibited from binding to ACE2 receptor on the cell surface.

4.1 <u>Introduction:</u>

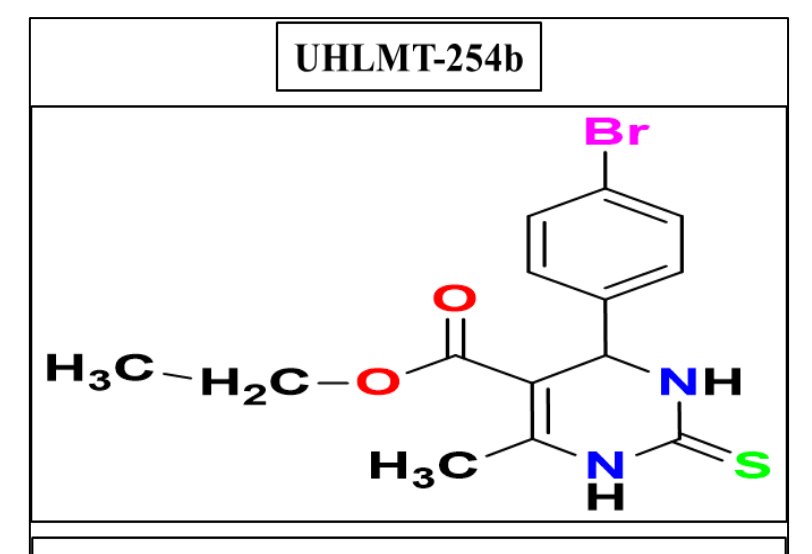
A 90 kDa protein, Epap-1, showed interaction with the RBD region of Spike protein by inhibiting the RBD binding to the ACE2 receptor. Our research group designed various small molecular mimics of Epap-1 [64]. These Epap-1 mimics small molecules were docked against the RBD region of Spike protein. Molecular docking of these Epap-1 mimics with RBD protein showed that Epap-1 mimics small molecules inhibit interaction with the RBD region of Spike protein to ACE2 receptor. Various Epap-1 small molecule mimics were synthesized [64].

Fig 4.2: Structures of small molecule mimics of Epap-1



H₃C-H₂C-ONH H₃CNS

ethyl 4-(4-hydroxyphenyl)-6-methyl-2-thioxo-1,2,3,4tetrahydropyrimidine-5-carboxylate



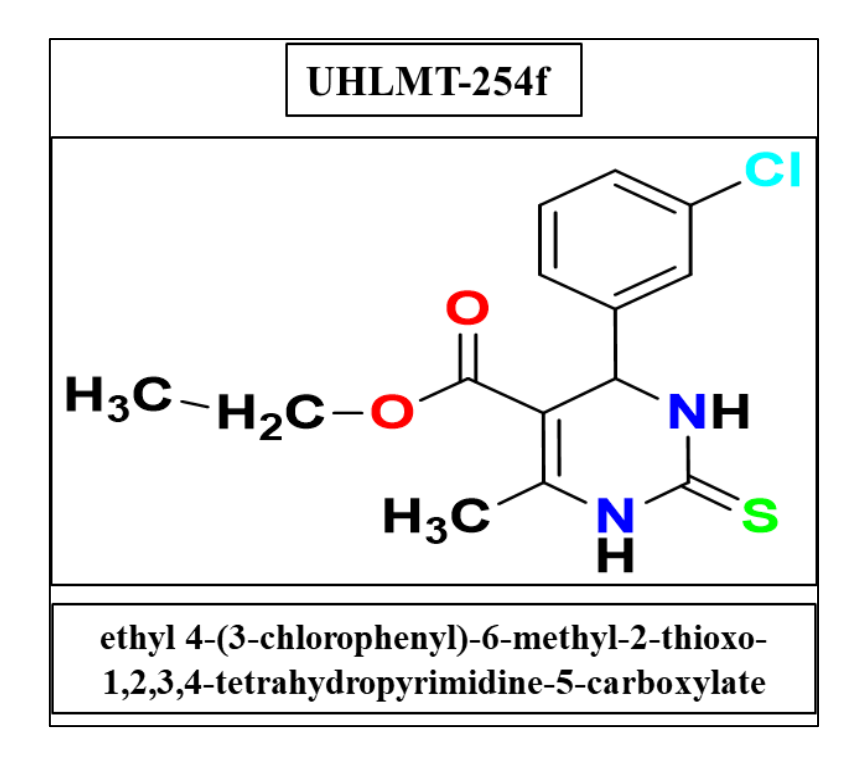
ethyl 4-(4-bromophenyl)-6-methyl-2-thioxo-1,2,3,4tetrahydropyrimidine-5-carboxylate

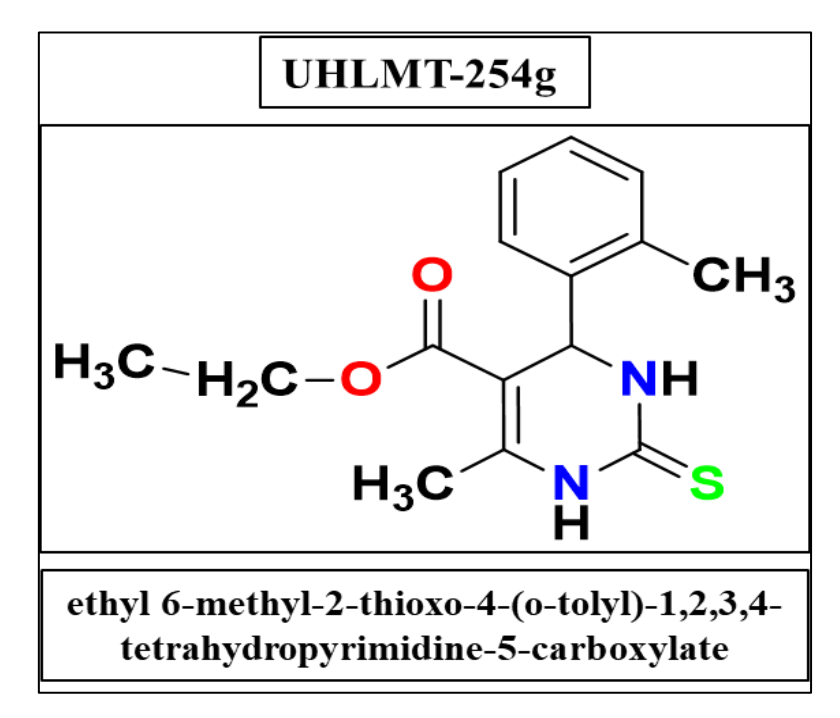
H₃C-H₂C-ONH H₃CNS

ethyl 4-(4-methoxyphenyl)-6-methyl-2-thioxo-1,2,3,4tetrahydropyrimidine-5-carboxylate

H₃C-H₂C-ONH H₃CNS

ethyl 4-(4-hydroxy-3-methoxyphenyl)-6-methyl-2-thioxo-1,2,3,4-tetrahydropyrimidine-5-carboxylate



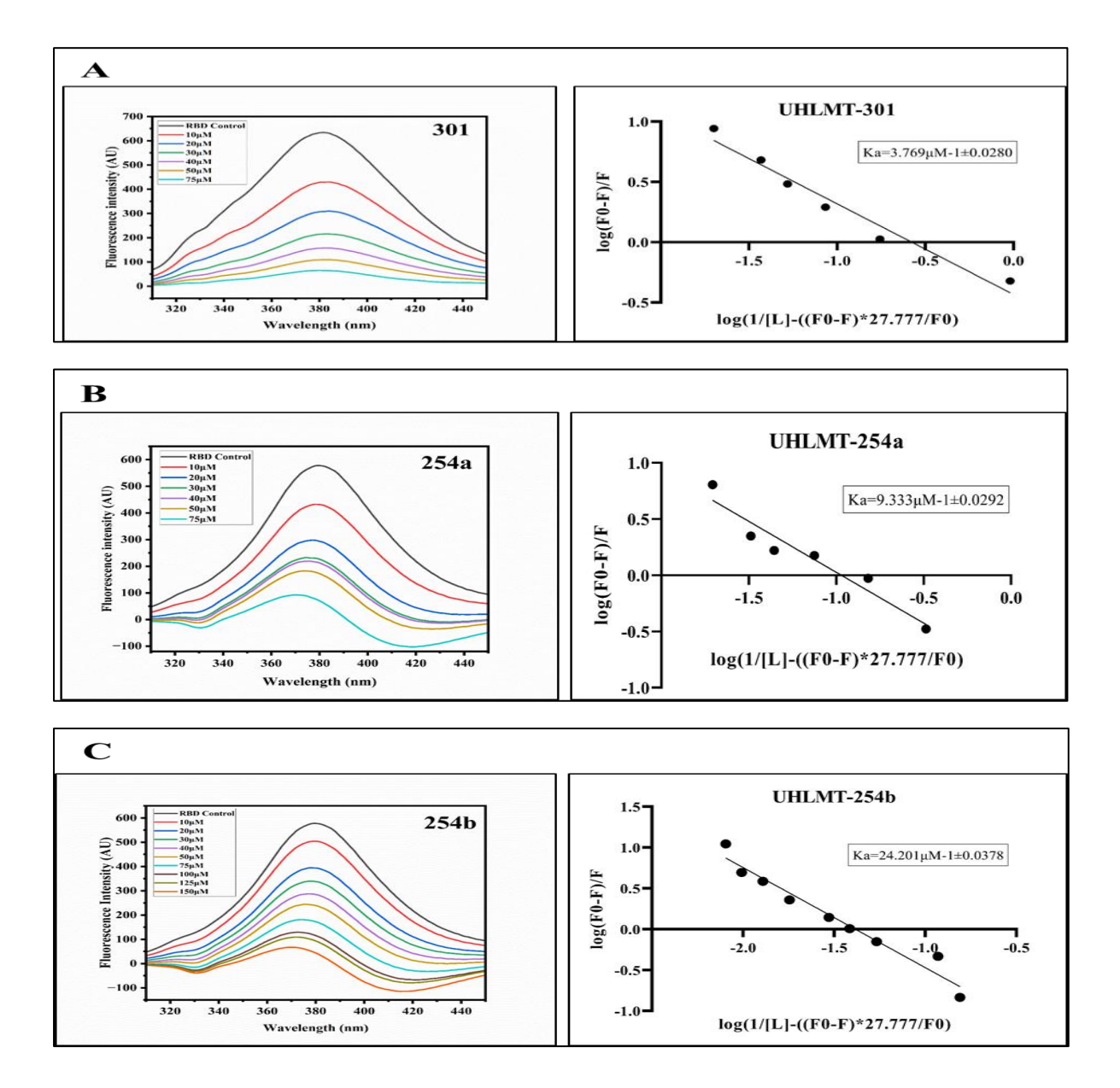


UHLMT-301, UHLMT-254a to UHLMT-254g Molecules were synthesized as per Jagdeesh et al. (2021), and further molecular action and biological characterization for antiviral were carried out.

4.2 Results and Discussion:

4.2.1 Analysis of Novel Small Molecules Interaction with RBD using Spectrofluorometer:

Small molecule and RBD interaction were studied using spectrofluorimetric analysis. In spectrofluorometric analysis, results showed that RBD protein was quenched at different concentrations of Epap-1 small molecule mimics (**Fig 4.3.1**), and binding constants were analyzed using the Stern-Volmer equation [38]. The results showed compound #254e (4-hydroxy and 3-methoxy phenyl substitution on pyridine) possesses higher affinity, followed by the other molecules (**Table 4.2.1**).



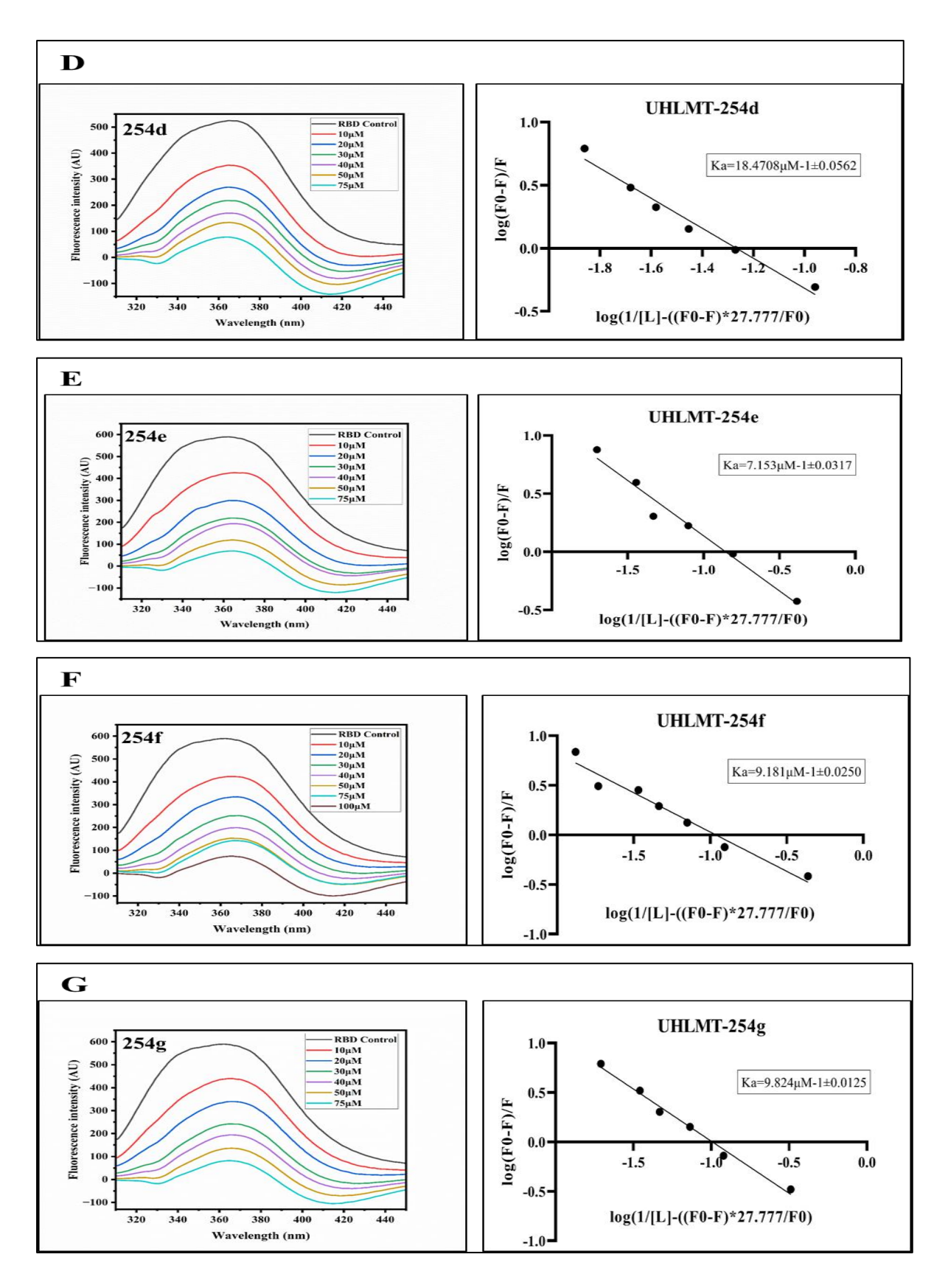


Fig 4.3. Spectrofluorimetric analysis was performed with different concentrations of small molecule mimics of Epap-1 ($10\mu M$ to $100\mu M$) with RBD protein ($100 \mu g$) in HEK293T cells. Results showed that the RBD protein ($100 \mu g$) was inhibited with increasing concentrations of

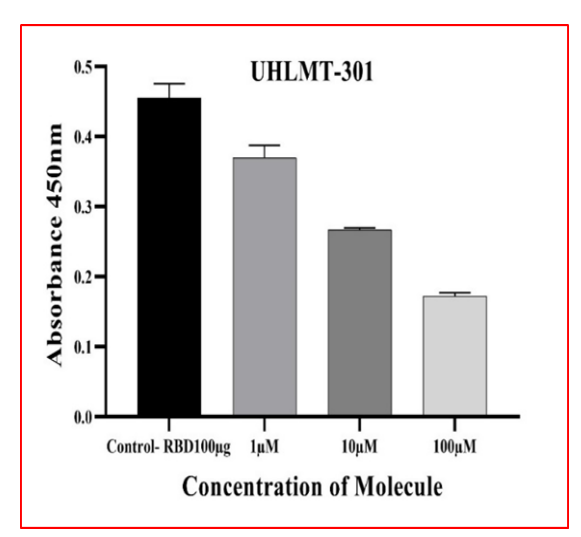
small molecule mimics of Epap-1. Fluorescence emission wavelength for RBD protein was monitored at 295 nm in 1xPBS, pH 7.4 at 20°C and 310–450 nm, respectively. (F0-fluorescence intensities in the absence of ligand, F- Fluorescence intensities in the presence of ligand, L- Concentration of Ligand, 27.777µM is the concentration of RBD protein, AU-Arbitrary Unit).

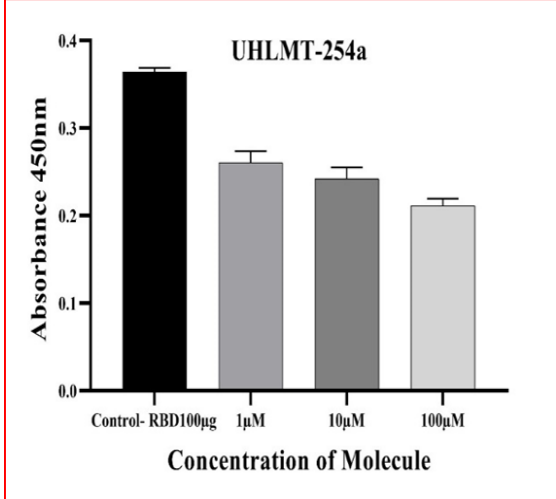
Small molecular mimics of Epap-1	Ка (µМ)	Kd (µM)
UHLMT-301	3.769±0.028	0.265
UHLMT-254a	9.333±0.029	0.107
UHLMT-254b	24.201±0.037	0.041
UHLMT-254d	18.4708±0.059	0.054
UHLMT-254e	7.153±0.031	0.139
UHLMT-254f	9.181±0.025	0.108
UHLMT-254g	9.824±0.012	0.101

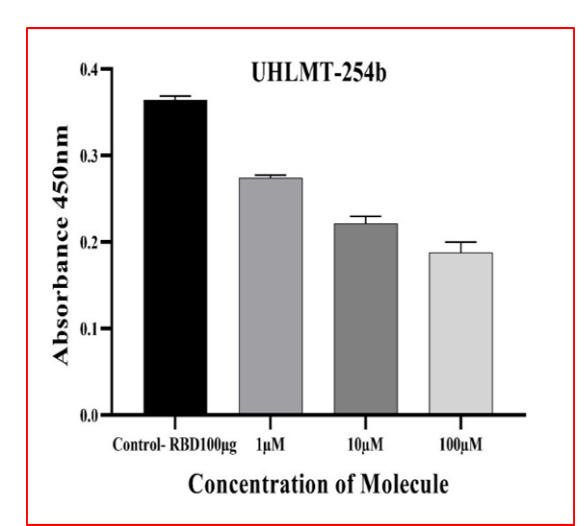
Table 4.2.1. Indicates the Ka and Kd values of small molecule mimics of Epap-1.

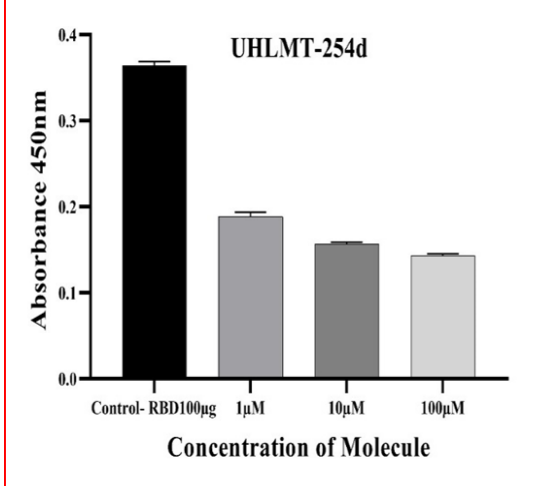
4.2.2 Analysis of small molecule mimics of Epap-1 interaction with RBD using ELISA:

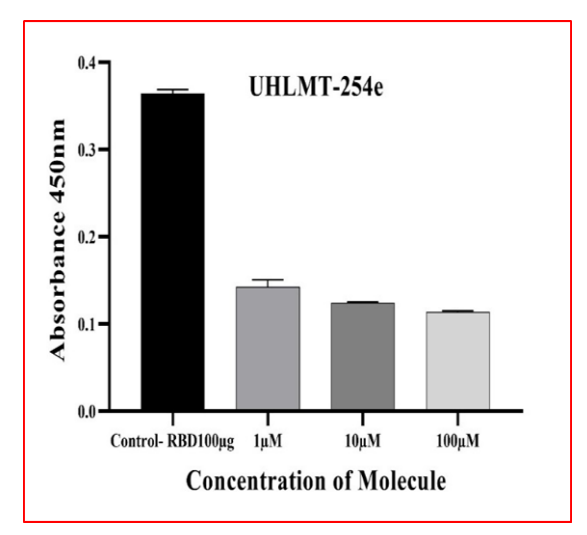
Since Epap-1 small molecule mimics show significant binding to RBD, we have analyzed the activity of these molecules on the RBD protein and ACE2 interaction. In the analysis using ELISA, HEK293T incubated with RBD (100 μ g) and RBD-Small molecules complexes at different concentrations of small molecules (1 μ M, 10 μ M, and 100 μ M). When cells were probed using an Anti-RBD antibody, the RBD protein was inhibited with increasing concentration of small molecules (**Fig 4.4**). The results of the ELISA assay show that Epap-1 small molecule mimics significantly inhibits RBD protein binding to ACE2. IC50 values are presented in Table 4.2.2; the results show that 254e is the highest inhibitory activity.

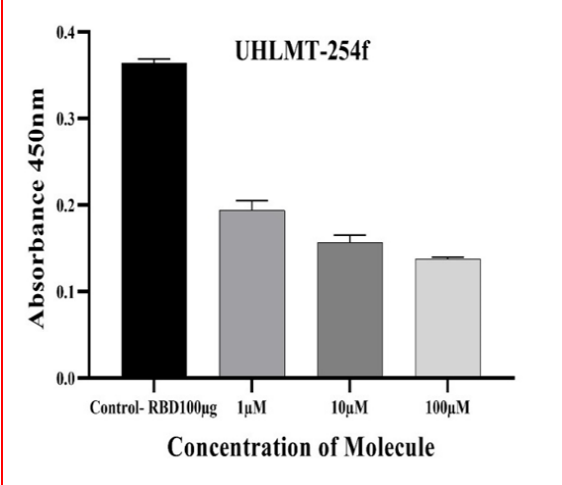












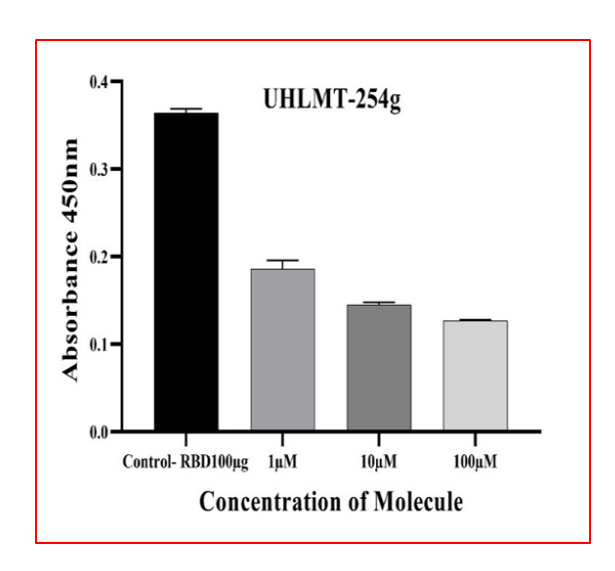


Fig 4.4. ELISA was performed with different concentrations of small molecule mimics of Epap-1 ($1\mu M$, $10\mu M$, and $100\mu M$) with RBD protein ($100~\mu g$) in HEk293T cells. Results showed that the RBD protein ($100~\mu g$) was inhibited with increasing concentrations of small molecule mimics of Epap-1.

Small molecular	IC _{50 (µM)}
mimics of Epap-1	
301	3.466±0.132
254a	2.513±0.099
254b	2.996±0.124
254d	2.327±0.080
254e	1.929±0.073
254f	2.43±0.073
254g	2.45±0.109

Table 4.2.2 Indicates the IC₅₀ values. 254e showed higher activity, followed by the rest of the molecules.

4.2.3 Antiviral assay:

Since Epap-1 small molecule mimics showed significant interaction with RBD protein and also shown to inhibit RBD and ACE-2 binding, we have evaluated their effect on infection conducted using pseudo-virus. In an antiviral assay, HEK293T cells were incubated with pseudo-virus RBD-GFP, pseudo-virus Spike-GFP, and pseudo-virus RBD/Spike-GFP in the presence of 100 μM concentration of Epap-1 small molecule mimics, and results were analyzed in terms of GFP expression in host ACE2 cells (HEK cells) when the virus enters the cells. Cells incubated with Pseudovirus RBD (**Fig 4.5**) / Spike (**Fig 4.6**) alone showed high GFP expression in the infection conducted in the presence of 100 μM concentrations of Epap-1 small molecules mimics; virus entry was inhibited, leading to decreased GFP expression with 100 μM concentrations of Epap-1 small molecules mimics. Thus, Epap-1 small molecule mimics affect RBD and Spike protein-mediated virus entry.

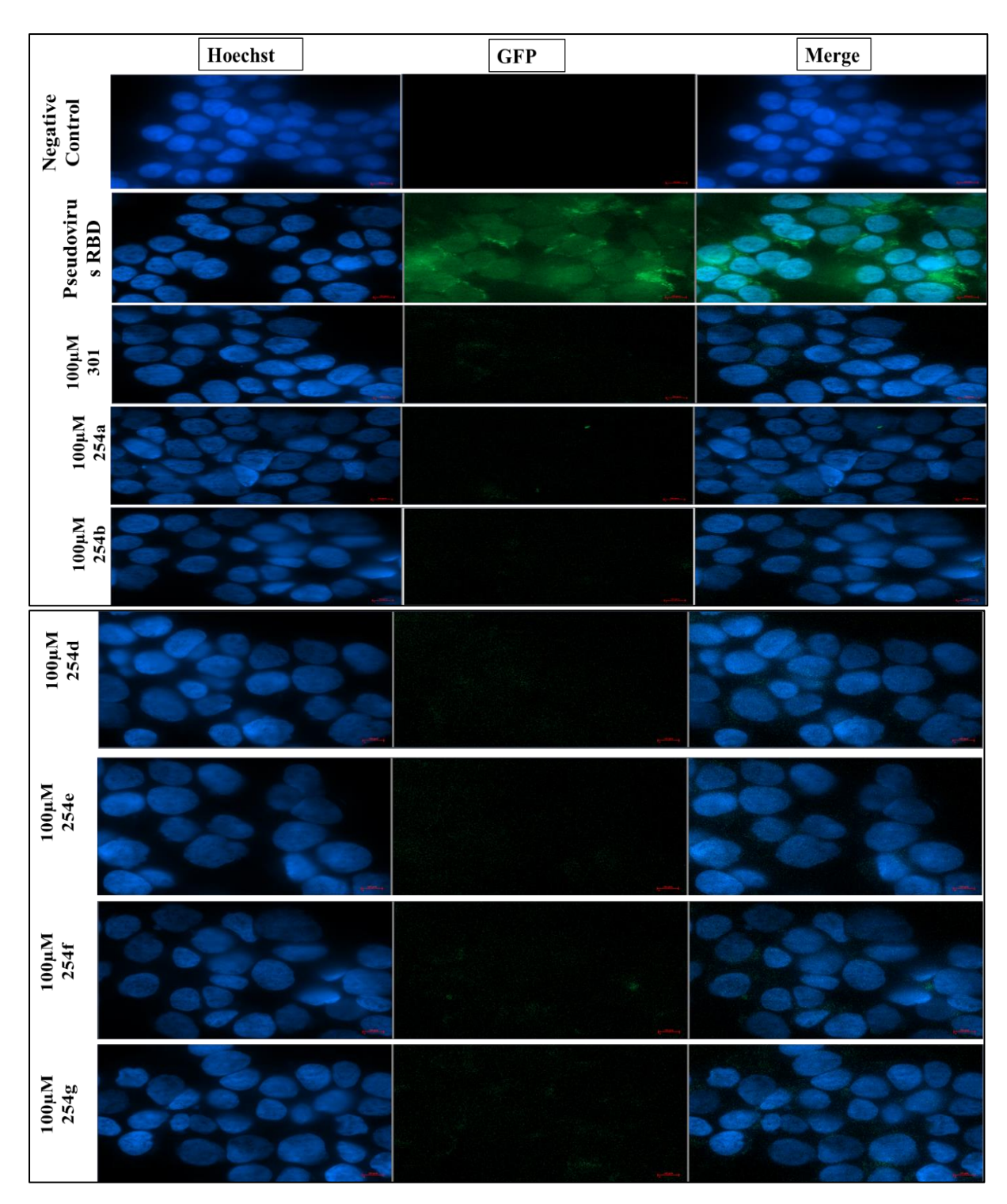


Fig 4.5. HEK293T cells were measured using GFP expression. The experiments were conducted in PBS in negative control cells. In Pseudovirus RBD, HEK293T cells were infected with pseudovirus without small molecule mimics of Epap-1. The presence of small molecule mimics of Epap-1 (100μM) inhibits the pseudovirus of RBD infection in ACE2-expressing cells compared to cells infected with the pseudovirus of RBD alone.

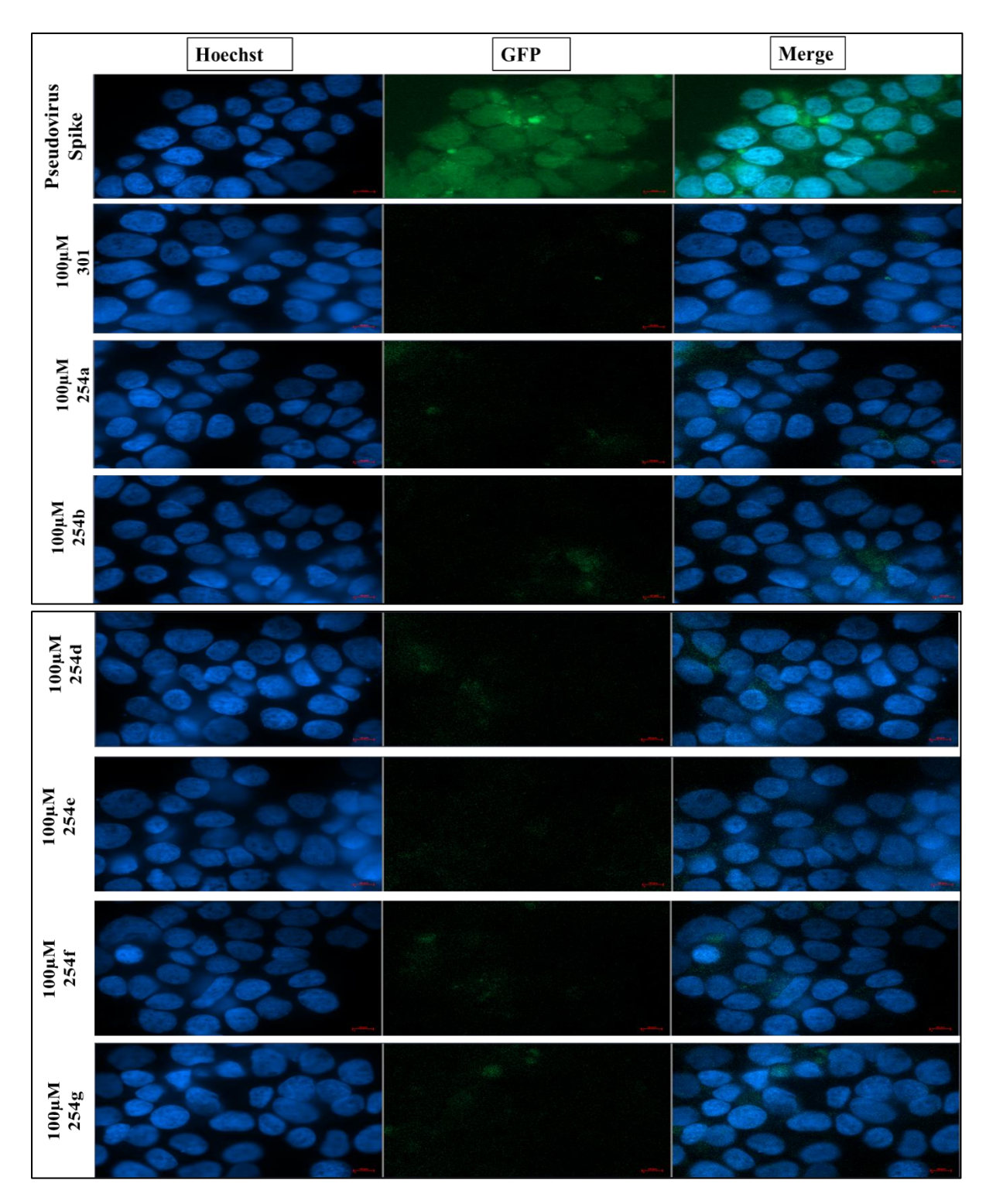


Fig 4.6. HEK293T cells were measured using GFP expression. The experiments were conducted in PBS in negative control cells. In Pseudovirus Spike, HEK293T cells were infected with pseudovirus without small molecule mimics of Epap-1. The presence of small molecule mimics of Epap-1 (100μM) inhibits the pseudovirus of Spike infection in ACE2-expressing cells compared to cells infected with the pseudovirus of Spike alone.

4.3 Conclusion:

- Spectrofluorimetric analysis of small molecule mimics of Epap-1 shows significant interaction of these molecules with RBD protein.
- An analysis of the action of small molecule mimics of Epap-1 on RBD and ACE2 interaction shows that these molecules inhibit in a dose-dependent manner. The compounds exhibit activity in the order of 254e>254d>254f>254g>254a>254b>301;
 4-hydroxyl and 3-methoxy may be involved in interaction.
- The confirmatory analysis of the action of small molecule mimics of Epap-1 on RBD /
 S protein-expressed pseudovirus infection to ACE2 expressing HEK293T cells shows
 that these molecules inhibit both RBD as well as S protein-mediated infection in
 HEK293T cells.

Future Perspective:

This study demonstrates that Epap-1 mimic small molecules can be a potential pharmacophore that can target RBD protein of Spike. These Epap-1 mimic small molecules results shown compounds have shown high potential RBD protein inhibition and anti-SARS-CoV 2 activity. In this objective, we have observed that 4-hydroxyl and 3-methoxy have shown the highest RBD protein inhibition and anti-SARS-CoV-2 activity.

Chapter V

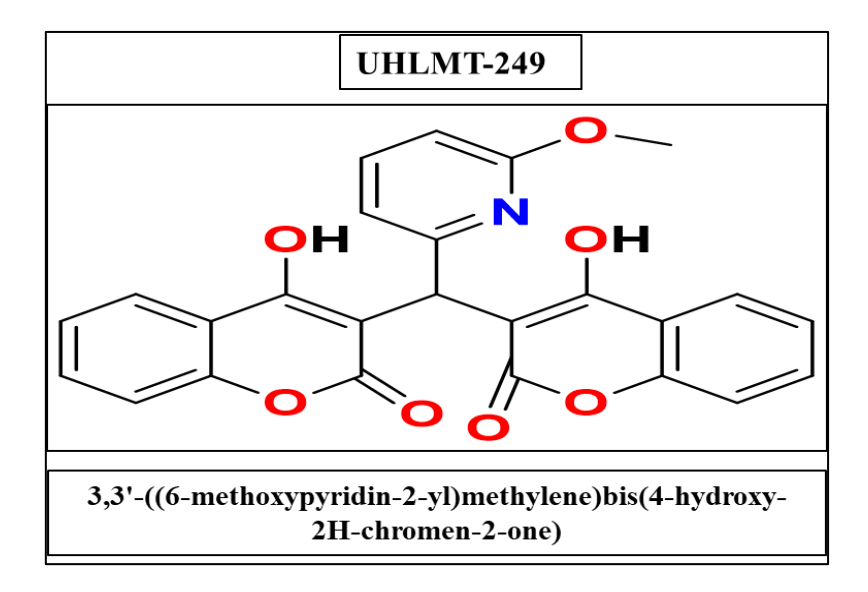
Development of novel dicoumarol inhibitors of viral entry through RBD interaction.

5.1 Introduction:

Various anti-viral compounds are designed and synthesized to block the activity of the viral protein entry. SARS-CoV-2 Spike protein RBD region plays an important role in viral entry. Spike protein has S1 and S2 sub-units; the S1 sub-unit plays an important role in binding to the viral expressing receptor, i.e., the ACE2 receptor, and the S2 sub-unit has fusion peptide, which is involved in fusion machinery. The Receptor Binding Domain (RBD) region of the surface exposed S1 sub-unit is involved in binding to the ACE2 receptors.

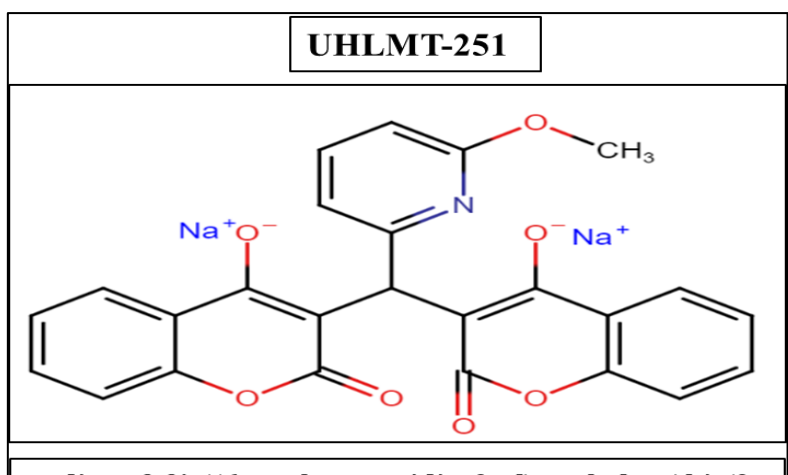
Since Epap-1 small molecular mimics, which possess an interaction with HIV-1 gp120 (Jagadeesh et al. 2021), have shown significant interaction with RBD protein (Chapter 4), we have analyzed the affinity of novel (dicoumarol) small molecules having significant affinity to HIV-1 gp120, we have chosen four molecules with significant affinity to RBD as per Fig 5.1 for further analysis in this chapter.

Fig 5.1: Structures of Novel (dicoumarol) Small Molecules. Molecules were synthesized as per Kurumurthy K and Anand K Kondapi (**Indian Patent No. 385140 (2021)**), and further molecular action and biological characterization for antiviral were carried out.

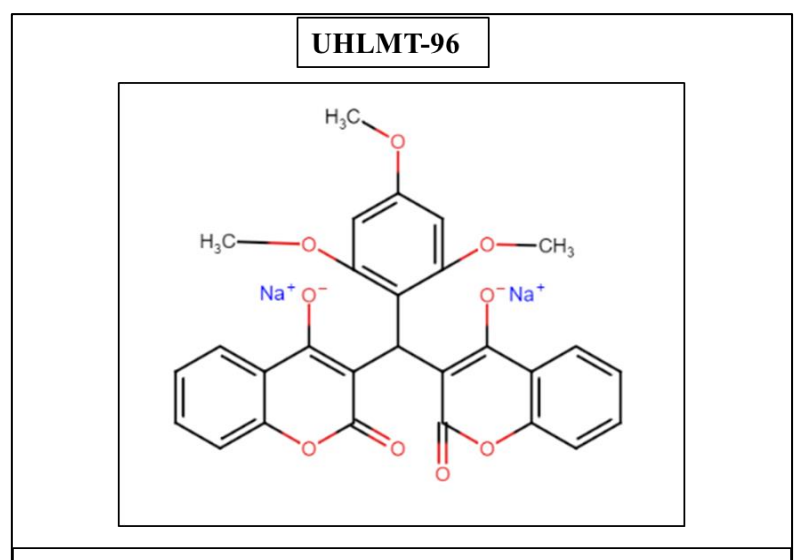


UHLMT-250

7-(6-methoxypyridin-2-yl)-6H-pyrano[3,2-c:5,6-c']dichromene-6,8(7H)-dione



sodium 3,3'-((6-methoxypyridin-2-yl)methylene)bis(2-oxo-2H-chromen-4-olate)

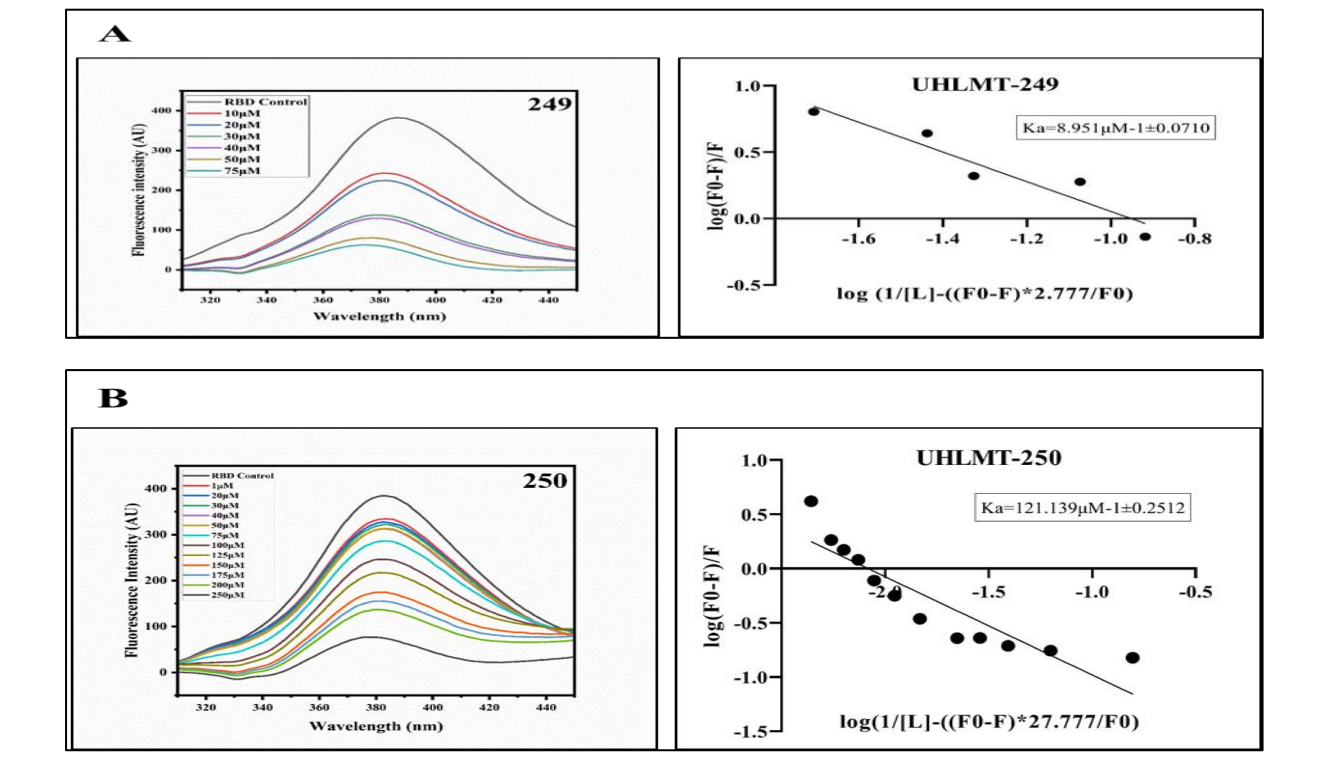


sodium 3,3'-((2,4,6-trimethoxyphenyl)methylene)bis(2-oxo-2H-chromen-4-olate)

5.2. Results and discussion:

5.2.1 <u>Analysis of Novel (dicoumarol) Small Molecules Interaction with RBD using Spectrofluorometer:</u>

The molecules selected as per Table 5.1 were analyzed for their affinity to RBD protein using spectrofluorimetric analysis. The results of spectrofluorimetric analysis showed that RBD protein was quenched at different concentrations of dicoumarol derivatives (**Fig 5.2.1**), and binding constants were analyzed using the Stern-Volmer equation [38]. The results showed compound #96: Trimethoxybenzene substitution of dicoumarol shows higher affinity to RBD compared to other substitutions, followed by the other dicumarol derivatives studied (**Table 5.2.1**).



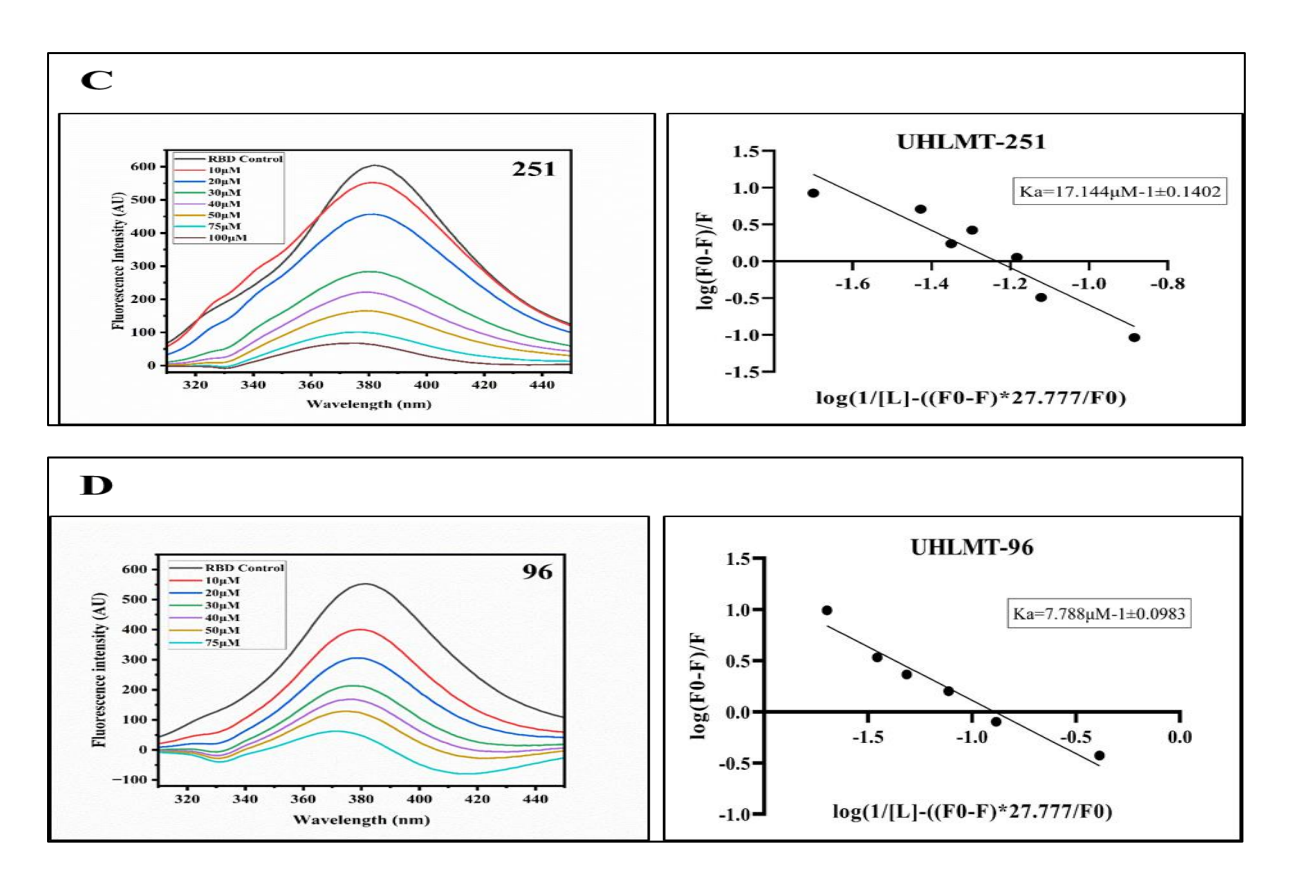


Fig 5.2.1. Spectrofluorimetric analysis was performed with different concentrations of Novel (dicoumarol) small molecule ($10\mu M$ to $100\mu M$) with RBD protein ($100\mu g$) in HEk293T cells. Results showed that the RBD protein ($100\mu g$) was inhibited with increasing concentrations of small molecule mimics of Epap-1. Fluorescence emission wavelength for RBD protein was monitored at 295 nm in 1xPBS, pH 7.4 at 20°C and 310–450 nm, respectively. (F0-fluorescence intensities in the absence of ligand, F- Fluorescence intensities in the presence of ligand, L- Concentration of Ligand, 27.777μM is the concentration of RBD protein, AU-Arbitrary Unit).

Novel Molecules	Ka (µM)	Kd (µM)
UHLMT-249	8.951±0.071	0.111
UHLMT-250	121.139±0.251	0.008
UHLMT-251	17.144±0.14	0.058
UHLMT-96	7.78±0.098	0.128

Table 5.2.1. Indicates the Ka and Kd values of Novel (dicoumarol) small molecule.

5.2.2 Analysis of Novel (dicoumarol) Small Molecules interaction with RBD using ELISA:

Since dicumarol derivatives showed significant affinity to RBD protein (Table 5.2.1), the action of these compounds on RBD and ACE-2 was studied. In the analysis using ELISA, HEK29T was incubated with RBD (100 µg) and RBD- dicumarol complexes with different concentrations of dicumarol derivatives (1 µM, 10 µM, and 100 µM). When cells were probed using an anti-RBD antibody, the RBD protein was inhibited with increasing concentration of dicumarol derivatives. The results showed that dicumarol derivatives showed a dose-dependent decrease in RBD protein and ACE2 interaction (**Fig 5.2.2**). Compound #96 showed the highest activity among the compounds, followed by 250, 251, and 249 (**Table 5.2.2**). In summary, dicumarol derivatives significantly inhibit the binding of RBD protein to ACE2.

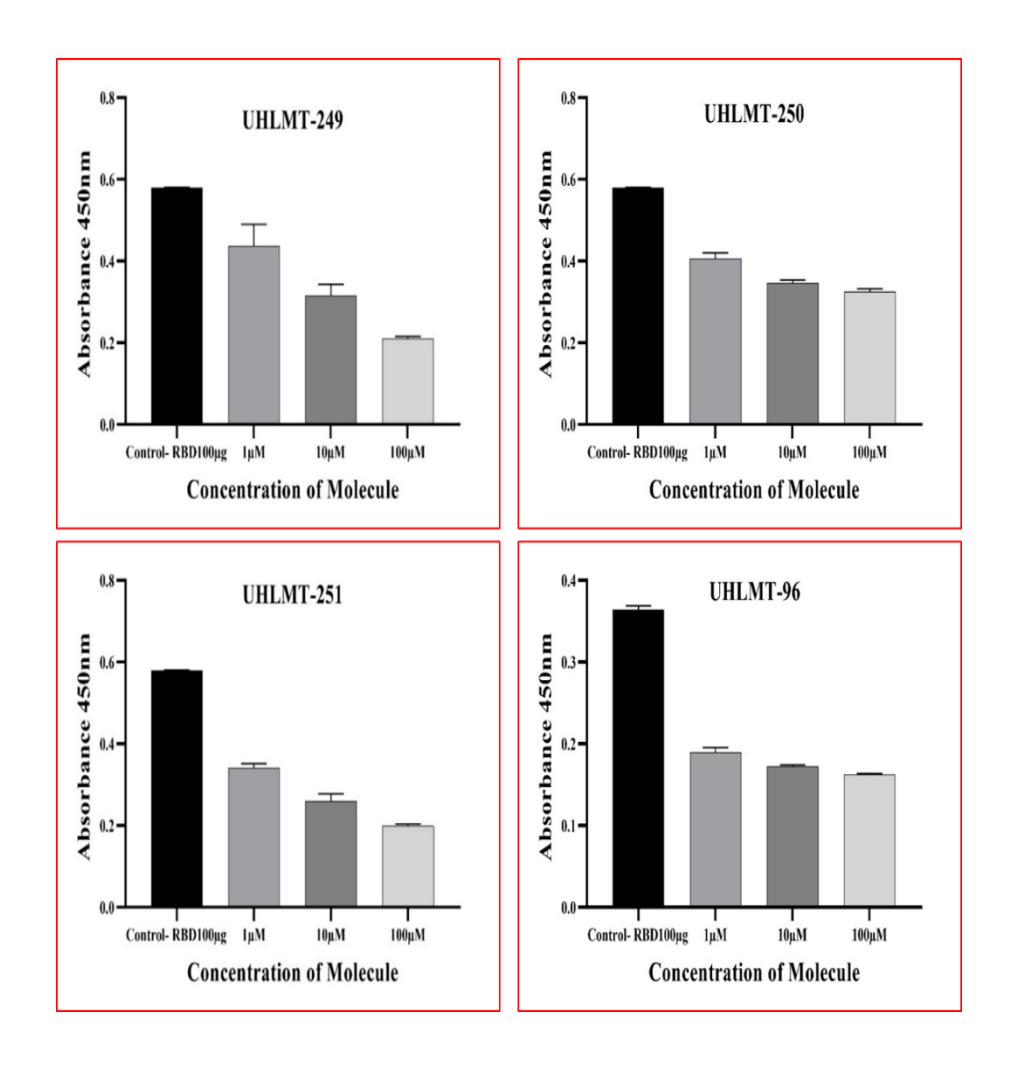


Fig 5.2.2. ELISA was performed with different concentrations of Novel (dicoumarol) small molecules ($1\mu M$, $10\mu M$, and $100\mu M$) with RBD protein ($100~\mu g$) in HEk293T cells. Results

showed that the RBD protein (100 μ g) was inhibited with increasing concentrations of small molecule mimics of Epap-1.

Novel molecules	IC50 (μM)
249	3.285±0.136
250	2.663±0.103
251	2.716±0.179
96	1.993±0.068

Table 5.2.2. Indicates the IC50 values. 96 showed higher activity, followed by the rest of the molecules.

5.2.3 Antiviral assay:

The results of Fig. 5.2.1 and 5.2.2 showed that the dicumarol derivatives possess significant affinity and inhibit RBD and ACE2 binding; this section confirmed the antiviral activity of compounds using pseudo-virus.

In an antiviral assay, HEK293T cells were incubated with pseudovirus RBD-GFP and Pseudovirus Spike-GFP in the presence of $100\,\mu\text{M}$ concentration of dicumarol derivatives, and results were analyzed in terms of GFP expression when the virus enters the cells. Cells incubated with Pseudovirus RBD/ Spike alone showed high GFP expression. While in the infection conducted in the presence of $100\,\mu\text{M}$ concentrations of dicumarol derivatives, GFP expression is observed neither in Pseudovirus RBD (Fig 5.2.3) nor Pseudovirus Spike (Fig 5.2.4), suggesting the compounds inhibit both RBD and Spike protein-mediated virus entry.

In summary, dicumarol derivatives studied in this chapter significantly affect RBD and Spike protein-mediated virus entry in ACE2 cells.

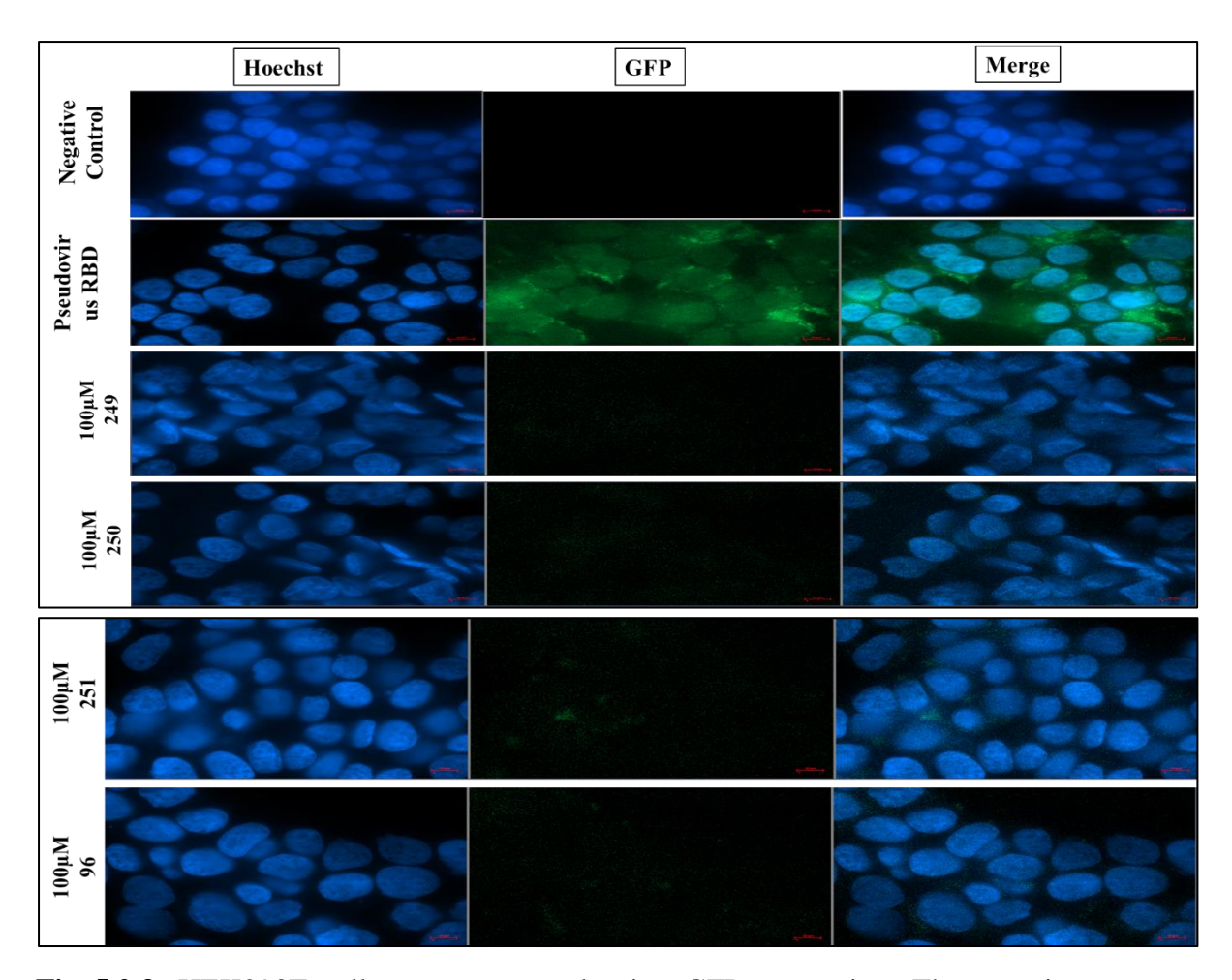


Fig 5.2.3. HEK293T cells were measured using GFP expression. The experiments were conducted in PBS in negative control cells. In Pseudovirus RBD, HEK293T cells were infected with pseudovirus without a Novel (dicoumarol) small molecule. The presence of a Novel (dicoumarol) small molecule (100μM) inhibits the pseudovirus of RBD infection in ACE2-expressing cells compared to cells infected with the pseudovirus of RBD alone.

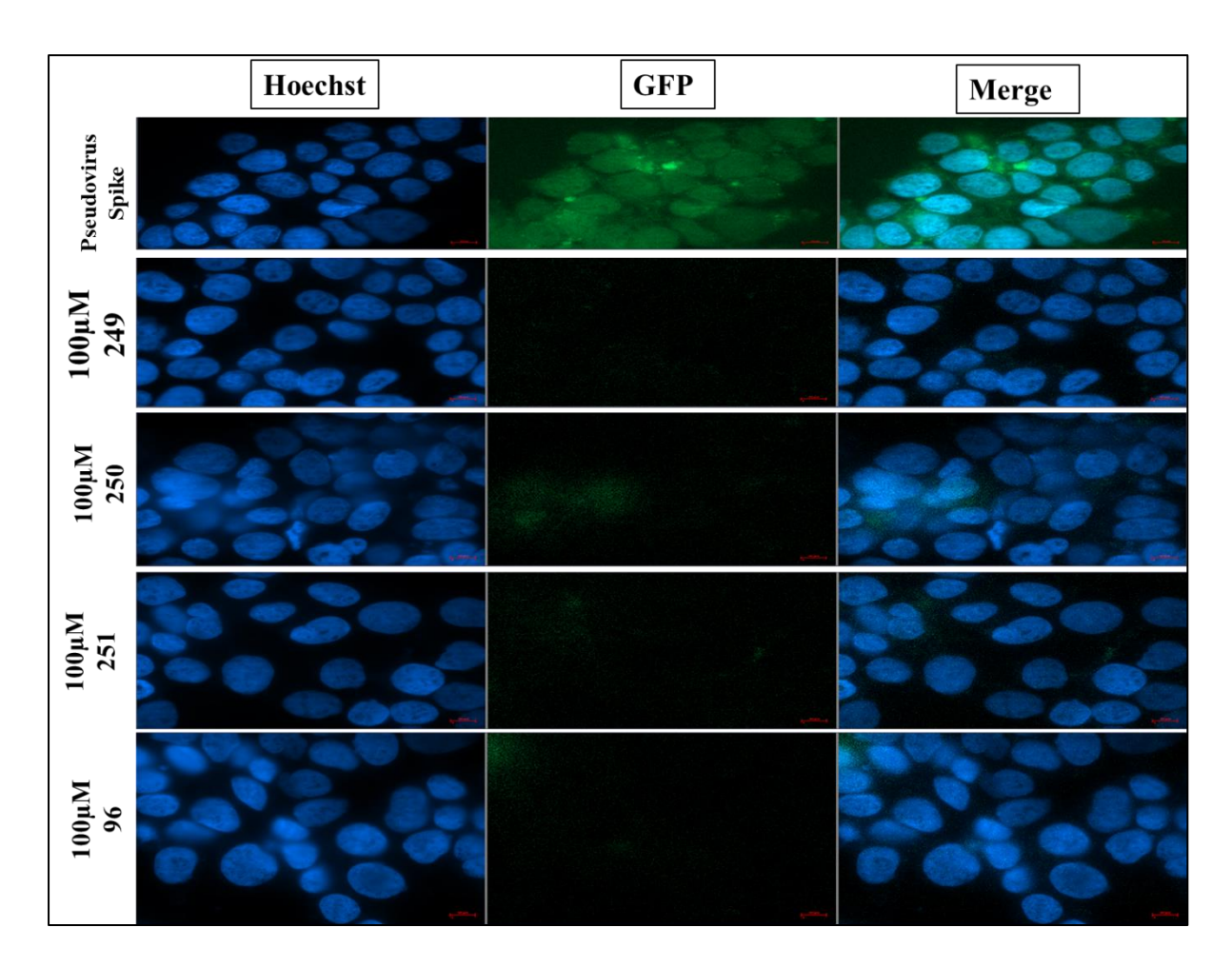


Fig 5.2.4. HEK293T cells were measured using GFP expression. The experiments were conducted in PBS in negative control cells. In Pseudovirus Spike, HEK293T cells were infected with pseudovirus without a Novel (dicoumarol) small molecule. The presence of a Novel (dicoumarol) small molecule (100μM) inhibits the pseudovirus of Spike infection in ACE2-expressing cells compared to cells infected with the pseudovirus of Spike alone.

5.2.4 <u>Analysis of Proviral DNA with SK38 and SK39 Primers for Small Molecule Mimics of</u> Epap-1 and Novel (dicoumarol) small molecules:

Antiviral analysis results are further confirmed by decreased proviral DNA Synthesis in the infection conducted in the presence of 100 µM dicumarol derivatives (249, 250, 251, 96) and Epap-1 small molecule mimics (301, 254a, 254b, 254d, 254e, 254f, 254g).

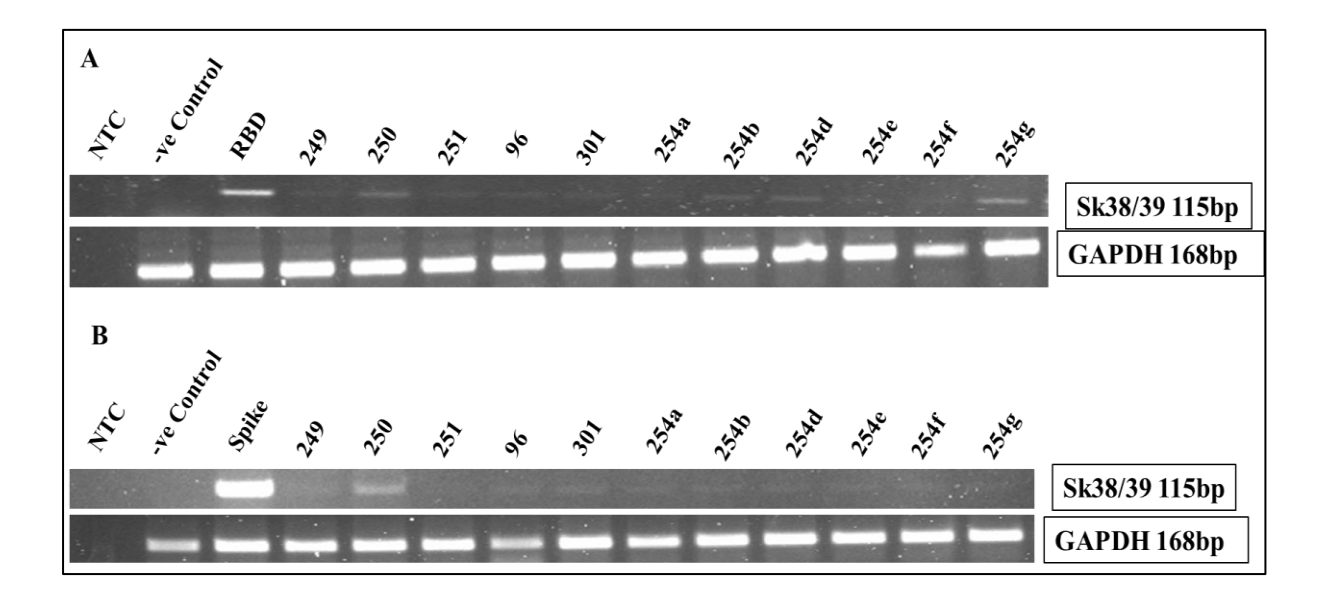


Fig 5.2.5 The HEK293T cells were collected after 6 hpi, and DNAs were extracted using phenol/chloroform. PCR was carried out according to the Thermo Fischer 2X Green Taq manufacturers' instructions, and amplified products of the gag region (115 bp), and GAPDH (168 bp, control) were visualized in 2% agarose gel stained with ethidium bromide. Panel A. RBD protein-mediated pseudovirus and Panel B. Spike protein-mediated pseudovirus. The gag synthesis was significantly reduced in small molecule Mimics of Epap-1 and Novel (dicoumarol) small molecules treated with infected HEK293T cells. These results confirm that small molecule Mimics of Epap-1 and Novel (dicoumarol) small molecule inhibit RBD and Spike protein-mediated pseudovirus infection in HEK293T cells.

5.3 Conclusion:

- Spectrofluorimetric analysis of novel small molecules of dicoumarol derivatives showed that RBD protein is completely quenched with increasing concentrations of small molecules suggesting the stronger affinity of these molecules to RBD.
- The analysis results using dicoumarol derivatives on RBD and ACE2 interaction suggest that RBD protein and ACE2 interaction are inhibited by increasing the concentration of dicoumarol derivatives. The order of activity of compounds is 96>250>251>249; methoxy substitutions at 3 and 5 may be important for the activity.
- Immunofluorescence analysis of the action of novel small molecules on viral entry suggests that both RBD and Spike protein anchored pseudovirus entry into HEK293T cells was significantly inhibited.
- The results of the analysis of proviral DNA syntheses in infected cells confirm that small molecule mimics of Epap-1, as well as dicoumarol derivatives, completely inhibit both RBD and Spike protein anchored pseudovirus entry into ACE-2 expressing HEK293T cells.

Future Perspective:

This study demonstrates that dicoumarol molecules can be a potential pharmacophore that can target Spike's RBD protein. These novel (dicoumarol) methoxy-substituted resulting compounds have shown high potential RBD protein inhibition and anti-SARS-CoV 2 activity. In this objective, we have observed that methoxy substitutions at 3 and 5 have shown the highest RBD protein inhibition and anti-SARS-CoV-2 activity.

Overall Summary:

The main aim of the thesis is to study the molecular interaction of Epap-1, small molecular mimics of Epap-1, and novel small molecules with the S-protein of SARS-CoV-2 and develop an entry inhibitor against SARS-CoV-2. The S-protein of SARS-CoV-2, a 180-200 KDa, is known to play a critical role in viral entry by binding to the PD of the ACE2 receptor on the host. Epap-1 showed inhibition against RBD and Spike protein of SARS-CoV-2 and has been evaluated for its antiviral activity. Further, various Epap-1 small molecular mimics having pyridine and dicoumarol as pharmacophores exhibited significant inhibition of the interaction between the ACE2 receptor with RBD and S-protein.

Objective 1:

An analysis of effect of Epap-1 on the SARS-Cov-2 Spike protein and ACE2 interaction and virus entry.

- Epap-1 shows a strong interaction with the ACE2 region of the Cov-2 spike protein; the region reported being involved in Cov-2 interaction with the host cells.
- Spike protein and Epap-1 complex interaction with ACE2 at position THR9 of Spike-protein and ARG4, ARG5, ARG363, SER511, TRP548, TYR555, ARG559, VAL565, ARG568, LYS683, SER684, CYS687, LYS695 of Epap-1 hydrogen bonded with ASN134, ASP136, ASN137, ASP157, TYR158, ASN159, GLU160, TYR255, SER257, LYS600, ASP609, ASP615 of ACE2 receptor.
- Spike-protein interact with ACE2 at the position Y449, Y453, N487, Y489, G496,
 T500, G502, Y505, L455, F456, F486, Q493, Q498, and N501 in the absence of Epap 1, it interacts at the position ASP553, ILE554, ARG631, MET682, GLU687, TYR692,

ASN694, GLN747, GLU745, ARG1004, GLU1016, ARG1024 in the presence of Epap-1 which indicates that the Spike-protein Epap-1 interaction may interfere the interaction of ACE2 with Spike-protein

- The results of ELISA and IF show that the RBD/Spike protein blocks ACE2 antibody
 detection; when RBD/Spike and Epap-1 protein complexes are used, the ACE2 receptor
 is exposed, as evidenced by the binding of the Anti-ACE2 antibody.
- The results of ELISA and IF show that RBD/Spike protein binding to ACE2 is significantly inhibited by Epap-1.
- The results of the anti-viral analysis confirm that Epap-1 interferes with RBD and Spike protein-mediated virus entry.
- In summary, Epap-1 binds to the RBD region of the S protein, leading to the inhibition of SARS-COV-2 entry in host cells.
- Thus, Epap-1 may be one of the host factors in regulating virus infection to highly ACE2-abundant cells in placental tissue in women during early pregnancy.

Objective 2:

Evaluation of efficacy of small molecule mimics of Epap-1 on SARS Cov-2 RBD protein and ACE2 interaction and virus entry

- RBD protein was cloned into pET23d+ and purified using NTA-Ni2+ column.
- Spectrofluorometric analysis of small molecule mimics of Epap-1 shows significant interaction of these molecules with RBD protein.
- An analysis of the action of small molecule mimics of Epap-1 on RBD and ACE2 interaction shows that these molecules inhibit in a dose-dependent manner. The compounds exhibit activity in the order of 254e>254d>254f>254g>254a>254b>301; 4-hydroxyl and 3-methoxy may be involved in interaction.

The confirmatory analysis of the action of small molecule mimics of Epap-1 on RBD /
S protein-expressed pseudovirus infection to ACE2 expressing HEK293T cells shows
that these molecules inhibit both RBD as well as S protein-mediated infection in
HEK293T cells.

Objective 3:

Development of novel dicumarol inhibitors of viral entry through RBD interaction.

- Spectrofluorometric analysis of novel small molecules of dicoumarol derivatives showed that RBD protein is completely quenched with increasing concentrations of small molecules suggesting the stronger affinity of these molecules to RBD.
- The analysis results using dicoumarol derivatives on RBD and ACE2 interaction suggest RBD protein and ACE2 interaction is inhibited with increasing concentration of dicoumarol derivatives. The order of activity of compounds is 96>250>251>249; methoxy substitutions at 3 and 5 may be important for the activity.
- Immunofluorescence analysis of the action of novel small molecules on viral entry suggests that both RBD and Spike protein anchored pseudovirus entry into HEK293T cells was significantly inhibited.
- The results of the analysis of proviral DNA syntheses in infected cells confirm that small molecule mimics of Epap-1, as well as dicoumarol derivatives, completely inhibit both RBD and Spike protein anchored pseudovirus entry into ACE-2 expressing HEK293T cells.

References:

- 1. Chan JF, To KK, Tse H, et al.. Interspecies transmission and emergence of novel viruses: lessons from bats and birds. Trends Microbiol. 2013 Oct;21(10):544–555. doi: 10.1016/j.tim.2013.05.005
- 2. Xiao, X. et al., 2013. The SARS-CoV S glycoprotein: expression and functional characterization, Biochem. Biophys. Res. Commun., 312:1159-1167.
- 3. Du, L. et al., 2009. The spike protein of SARS-CoV-a target for vaccine and therapeutic development, Nat Rev Microbiol; 7:226-236.
- 4. Anthony, J. et al., 2004. Angiotensin-converting enzyme 2. Handbook of Proteolytic Enzymes (Second Edition), Volume.
- 5. Wang Y et al., 2020. Enhanced receptor binding of SARS-CoV-2 through networks of hydrogen-bonding and hydrophobic interactions, PNAS, 1-8, www.pnas.org/cgi/doi/10.1073/pnas.2008209117
- 6. Hoffmann, M. et al., 2020. A multibasic cleavage site in the spike protein of sars-cov-2 is essential for infection of human lung cells. Mol. Cell. doi.org/10.1016/j.molcel.2020.04.022.
- 7. Li, F. et al., 2016. Structure, Function, and Evolution of Coronavirus Spike Proteins, Annu. Rev. Virol; 3:237-261.
- 8. Roberts, A. et al., 2005. Severe acute respiratory syndrome coronavirus infection of golden syrian hamsters, J Virol; 79:503-511.
- 9. Peiwen Zhou, Zonghui Li, Linqing Xie, Dong An, Yaohua Fan, Xiao Wang, Yiwei Li, Xiaohong Liu, Jianguo Wu, Geng Li, Qin Li. "Research progress and challenges to coronavirus vaccine development", Journal of Medical Virology, 2020
- 10. Velthuis, J. J. et al., 2010. The RNA polymerase activity of SARS-coronavirus nsp12 is primer dependent, Nucleic Acids Res; 38:203-214.

- 11. Pachetti M, Marini B, Benedetti F, Giudici F, Mauro E, Storici P, Masciovecchio C, Angeletti S, Ciccozzi M, Gallo RC, Zella D, Ippodrino R. Emerging SARS-CoV-2 mutation hot spots include a novel RNA-dependent-RNA polymerase variant. J Transl Med. 2020 Apr 22;18(1):179. doi: 10.1186/s12967-020-02344-6. PMID: 32321524; PMCID: PMC7174922.
- 12. Kirchdoerfer, R.N. and Ward, A.B. 2019. Structure of the SARS-CoV nsp12 polymerase bound to nsp7 and nsp8 co-factors, Nature Communications; 2342.
- 13. Snijder, E.J. et al., 2016. The nonstructural proteins directing coronavirus rna synthesis and processing, Adv Virus Res; 96:59-126.
- 14. Romano M, Ruggiero A, Squeglia F, Maga G, Berisio R. A Structural View of SARS-CoV-2 RNA Replication Machinery: RNA Synthesis, Proofreading and Final Capping. Cells. 2020 May 20;9(5):1267. doi: 10.3390/cells9051267. PMID: 32443810; PMCID: PMC7291026.
- 15. V'kovski, P., Kratzel, A., Steiner, S. *et al.* Coronavirus biology and replication: implications for SARS-CoV-2. *Nat Rev Microbiol* **19**, 155–170 (2021). https://doi.org/10.1038/s41579-020-00468-6
- 16. Nana M, Nelson-Piercy C. COVID-19 in pregnancy. Clin Med (Lond). 2021 Sep;21(5):e446-e450. doi: 10.7861/clinmed.2021-0503. PMID: 34507928; PMCID: PMC8439502.
- 17. Pierce-Williams RAM, Burd J, Felder L, Khoury R, Bernstein PS, Avila K, Penfield CA, Roman AS, DeBolt CA, Stone JL, Bianco A, Kern-Goldberger AR, Hirshberg A, Srinivas SK, Jayakumaran JS, Brandt JS, Anastasio H, Birsner M, O'Brien DS, Sedev HM, Dolin CD, Schnettler WT, Suhag A, Ahluwalia S, Navathe RS, Khalifeh A, Anderson K, Berghella V. Clinical course of severe and critical coronavirus disease 2019 in hospitalized pregnancies: a United States cohort study. Am J Obstet Gynecol MFM. 2020 Aug;2(3):100134. doi: 10.1016/j.ajogmf.2020.100134. Epub 2020 May 8. PMID: 32391519; PMCID: PMC7205698
- 18. Knight M, Bunch K, Vousden N, Morris E, Simpson N, Gale C, O'Brien P, Quigley M, Brocklehurst P, Kurinczuk JJ; UK Obstetric Surveillance System SARS-CoV-2 Infection in Pregnancy Collaborative Group. Characteristics and outcomes of pregnant women admitted to

hospital with confirmed SARS-CoV-2 infection in UK: national population based cohort study. BMJ. 2020 Jun 8;369:m2107. doi: 10.1136/bmj.m2107. PMID: 32513659; PMCID: PMC7277610.

- 19. Dong L, Tian J, He S, Zhu C, Wang J, Liu C, Yang J. Possible Vertical Transmission of SARS-CoV-2 From an Infected Mother to Her Newborn. JAMA. 2020 May 12;323(18):1846-1848. doi: 10.1001/jama.2020.4621. PMID: 32215581; PMCID: PMC7099527
- 20. Zeng H, Xu C, Fan J, Tang Y, Deng Q, Zhang W, Long X. Antibodies in Infants Born to Mothers With COVID-19 Pneumonia. JAMA. 2020 May 12;323(18):1848-1849. doi: 10.1001/jama.2020.4861. PMID: 32215589; PMCID: PMC7099444
- 21. Kondapi, A.K., Hafiz, M.A. and Sivaram, T., 2002. Anti-HIV activity of a glycoprotein from first trimester placental tissue. Antiviral research, 54(1), pp.47-57.
- 22. Newell, M. L. "Mechanisms and timing of mother-to-child transmission of HIV-1." AIDS (1998) 12(8): 831-7
- 23. Mei, C. et al., 2019. The Unique Microbiome and Innate Immunity during pregnancy, Frontiers Immunol; 10:2886.
- 24. Sessa R, Filardo S, Masciullo L, Di Pietro M, Angeloni A, Brandolino G, Brunelli R, D'Alisa R, Viscardi MF, Anastasi E, Porpora MG. SARS-CoV-2 Infection in Pregnancy: Clues and Proof of Adverse Outcomes. Int J Environ Res Public Health. 2023 Feb 1;20(3):2616. doi: 10.3390/ijerph20032616. PMID: 36767980; PMCID: PMC9915124
- 25. Sun, B. and Yeh, J. 2020. Mild and asymptomatic covid-19 infections: implications for maternal, fetal, and reproductive health, Front. Reprod. Health; https://doi.org/10.3389/frph.2020.0000.
- 26. Peng, Z. et al., 2020. Unlikely SARS-CoV-2 vertical transmission from mother to child: A case report, J Infect Public Health; 13:818–820

- 27. Alexandre, J. et al., 2020. Transplacental transmission of SARS-CoV-2 infection, Nature Communications; 11:3572.
- 28. Vivanti AJ, Vauloup-Fellous C, Prevot S, Zupan V, Suffee C, Do Cao J, Benachi A, De Luca D. Transplacental transmission of SARS-CoV-2 infection. Nat Commun. 2020 Jul 14;11(1):3572. doi: 10.1038/s41467-020-17436-6. PMID: 32665677; PMCID: PMC7360599.
- 29. Charnock-Jones, S. and Burton G.J. 2000. Placental vascular morphogenesis, Best Practice & Research Clinical Obstetrics & Gynaecology; 14:953-968.
- 30. Lovren, F. et al., 2008. Angiotensin converting enzyme-2 confers endothelial protection and attenuates atherosclerosis, Am J Physiol Heart CircPhysiol; 295:H1377–H1384.
- 31. Varga, Z. et al., 2020. Endothelial cell infection and endotheliitis in COVID-19, Lancet; 395:1417-1418.
- 32. Alice, H.A. et al., 2020. Endothelial cell dysfunction: a major player in SARS-CoV-2 infection (COVID-19)? Eur Respir J; 56:2001634.
- 33. Voina VC, Swain S, Kammili N, Mahalakshmi G, Muttineni R, Chander Bingi T, Kondapi AK. Effect of Early pregnancy associated protein-1 on Spike protein and ACE2 interactions: Implications in SARS Cov-2 vertical transmission. Placenta. 2024 May 17;152:39-52. doi: 10.1016/j.placenta.2024.05.128. Epub ahead of print. PMID: 38788480
- 34. Towbin, H., T. Staehelin, and J. Gordon. 1979. Electrophoretic transfer of proteins from polyacrylamide gels to nitrocellulose sheets: procedure and some applications. Proceedings of the National Academy of Sciences of the United States of America 76:4350-4354
- 35. Argentinian AntiCovid Consortium. Structural and functional comparison of SARS-CoV-2-spike receptor binding domain produced in Pichia pastoris and mammalian cells. Sci Rep 10, 21779 (2020). https://doi.org/10.1038/s41598-020-78711-6
- 36. Sessa Rosa, Anastasi Emanuela, Brandolino Gabriella, Brunelli Roberto, Di Pietro Marisa, Filardo Simone, Masciullo Luisa, Terrin Gianluca, Viscardi Maria Federica, Porpora Maria

- Grazia, What is the Hidden Biological Mechanism Underlying the Possible SARS-CoV-2 Vertical Transmission? A Mini Review, Frontiers in Physiology, VOLUME-13, 2022, https://www.frontiersin.org/articles/10.3389/fphys.2022.875806
- 37. Jeganathan K., Paul A.B.M. Vertical transmission of SARS-CoV-2: a systematic review. Obstet. Med. 2022;15:91–98
- 38. Alzamora, M. C., Paredes, T., Caceres, D., Webb, C. M., Webb, C. M., Valdez, L. M. La Rosa, M. (2020). Severe COVID-19 during Pregnancy and Possible Vertical Transmission. American Journal of Perinatology, 37(8), 861–865. https://doi.org/10.1055/s-0040-1710050
- 39. Zeng L, Xia S, Yuan W, et al. Neonatal Early-Onset Infection With SARS-CoV-2 in 33 Neonates Born to Mothers With COVID-19 in Wuhan, China. JAMA Pediatr. 2020;174(7):722–725. doi:10.1001/jamapediatrics.2020.0878
- 40. Wang, S., Guo, L., Chen, L., Liu, W., Cao, Y., Zhang, J. and Feng, L., 2020. A case report of neonatal COVID-19 infection in China. Clin Infect Dis, 71(15), pp.853-857.
- 41. Yu, N., Li, W., Kang, Q., Xiong, Z., Wang, S., Lin, X., Liu, Y., Xiao, J., Liu, H., Deng, D. and Chen, S., 2020. Clinical features and obstetric and neonatal outcomes of pregnant patients with COVID-19 in Wuhan, China: a retrospective, single-centre, descriptive study. The Lancet Infectious Diseases, 20(5), pp.559-564.
- 42. Oncel, M.Y., Akın, I.M., Kanburoglu, M.K., Tayman, C., Coskun, S., Narter, F., Er, I., Oncan, T.G., Memisoglu, A., Cetinkaya, M. and Oguz, D., 2021. A multicenter study on epidemiological and clinical characteristics of 125 newborns born to women infected with COVID-19 by Turkish Neonatal Society. European journal of pediatrics, 180, pp.733-742.
- 43. Cao, D., Yin, H., Chen, J., Tang, F., Peng, M., Li, R., Xie, H., Wei, X., Zhao, Y. and Sun, G., 2020. Clinical analysis of ten pregnant women with COVID-19 in Wuhan, China: A retrospective study. International Journal of Infectious Diseases, 95, pp.294-300.

- 44. Gidlöf, S., Savchenko, J., Brune, T. and Josefsson, H., 2020. COVID-19 in pregnancy with comorbidities: More liberal testing strategy is needed. Acta Obstet Gynecol Scand, pp.948-949.
- 45. Zeng, H., Xu, C., Fan, J., Tang, Y., Deng, Q., Zhang, W. and Long, X., 2020. Antibodies in infants born to mothers with COVID-19 pneumonia. Jama, 323(18), pp.1848-1849.
- 46. Hosier, H., Farhadian, S.F., Morotti, R.A., Deshmukh, U., Lu-Culligan, A., Campbell, K.H., Yasumoto, Y., Vogels, C.B., Casanovas-Massana, A., Vijayakumar, P. and Geng, B., 2020. SARS–CoV-2 infection of the placenta. The Journal of clinical investigation, 130(9), pp.4947-4953.
- 47. Patanè, L., Morotti, D., Giunta, M.R., Sigismondi, C., Piccoli, M.G., Frigerio, L., Mangili, G., Arosio, M. and Cornolti, G., 2020. Vertical transmission of coronavirus disease 2019: severe acute respiratory syndrome coronavirus 2 RNA on the fetal side of the placenta in pregnancies with coronavirus disease 2019–positive mothers and neonates at birth. American journal of obstetrics & gynecology MFM, 2(3), p.100145.
- 48. Elisheva D Shanes, MD and others, Placental Pathology in COVID-19, American Journal of Clinical Pathology, Volume 154, Issue 1, July 2020, Pages 23–32, https://doi.org/10.1093/ajcp/aqaa089
- 49. Baud, D., Greub, G., Favre, G., Gengler, C., Jaton, K., Dubruc, E. and Pomar, L., 2020. Second-trimester miscarriage in a pregnant woman with SARS-CoV-2 infection. Jama, 323(21), pp.2198-2200.
- 50. Penfield, C.A., Brubaker, S.G., Limaye, M.A., Lighter, J., Ratner, A.J., Thomas, K.M., Meyer, J.A. and Roman, A.S., 2020. Detection of severe acute respiratory syndrome coronavirus 2 in placental and fetal membrane samples. American journal of obstetrics & gynecology MFM, 2(3).
- 51. Kulkarni, R., Rajput, U., Dawre, R., Sonkawade, N., Pawar, S., Sonteke, S., Varvatte, B., Aathira, K.C., Gadekar, K., Varma, S. and Nakate, L., 2021. Severe malnutrition and anemia are associated with severe COVID in infants. Journal of tropical pediatrics, 67(1), p.fmaa084.

- 52. Vivanti AJ, Vauloup-Fellous C, Prevot S, Zupan V, Suffee C, Do Cao J, Benachi A, De Luca D. Transplacental transmission of SARS-CoV-2 infection. Nat Commun. 2020 Jul 14;11(1):3572. doi: 10.1038/s41467-020-17436-6. PMID: 32665677; PMCID: PMC7360599.
- 53. di Gioia, C., Zullo, F., Vecchio, R.C.B., Pajno, C., Perrone, G., Galoppi, P., Pecorini, F., Di Mascio, D., Carletti, R., Prezioso, C. and Pietropaolo, V., 2022. Stillbirth and fetal capillary infection by SARS-CoV-2. American Journal of Obstetrics & Gynecology MFM, 4(1), p.100523.
- 54. Dong, L., Tian, J., He, S., Zhu, C., Wang, J., Liu, C. and Yang, J., 2020. Possible vertical transmission of SARS-CoV-2 from an infected mother to her newborn. Jama, 323(18), pp.1846-1848.
- 55. Irving, W.L., James, D.K., Stephenson, T., Laing, P., Jameson, C., Oxford, J.S., Chakraverty, P., Brown, D.W.G., Boon, A.M. and Zambon, M.C., 2000. Influenza virus infection in the second and third trimesters of pregnancy: a clinical and seroepidemiological study. BJOG: An International Journal of Obstetrics & Gynaecology, 107(10), pp.1282-1289.
- 56. Szymczak A, Jędruchniewicz N, Torelli A, Kaczmarzyk-Radka A, Coluccio R, Kłak M, et al. Antibodies specific to SARS-CoV-2 proteins N, S and E in COVID-19 patients in the normal population and in historical samples. J Gen Virol. 2021;102
- 57. Yang Z and Liu Y. Vertical Transmission of Severe Acute Respiratory Syndrome Coronavirus 2: A Systematic Review. Am J Perinatol. 2020 Aug;37(10):1055-1060. doi: 10.1055/s-0040-1712161. Epub 2020 May 13. PMID: 32403141; PMCID: PMC7416189
- 58. Zeng H, Xu C, Fan J, et al. Antibodies in Infants Born to Mothers With COVID-19 Pneumonia. JAMA. 2020;323(18):1848–1849. doi:10.1001/jama.2020.4861
- 59. Jing, Y., Run-Qian, L., Hao-Ran, W., Hao-Ran, C., Ya-Bin, L., Yang, G. and Fei, C., 2020. Potential influence of COVID-19/ACE2 on the female reproductive system. Molecular human reproduction, 26(6), pp.367-373.

- 60. Vaz-Silva, J., Carneiro, M.M., Ferreira, M.C., Pinheiro, S.V.B., Silva, D.A., Silva, A.L., Witz, C.A., Reis, A.M., Santos, R.A. and Reis, F.M., 2009. The vasoactive peptide angiotensin-(1–7), its receptor Mas and the angiotensin-converting enzyme type 2 are expressed in the human endometrium. Reproductive sciences, 16, pp.247-256.
- 61. Valdés, G., Neves, L.A.A., Anton, L., Corthorn, J., Chacon, C., Germain, A.M., Merrill, D.C., Ferrario, C.M., Sarao, R., Penninger, J. and Brosnihan, K.B., 2006. Distribution of angiotensin-(1-7) and ACE2 in human placentas of normal and pathological pregnancies. *Placenta*, 27(2-3), pp.200-207.
- 62. Wu, C., Chen, X., Cai, Y., Zhou, X., Xu, S., Huang, H., Zhang, L., Zhou, X., Du, C., Zhang, Y. and Song, J., 2020. Risk factors associated with acute respiratory distress syndrome and death in patients with coronavirus disease 2019 pneumonia in Wuhan, China. JAMA internal medicine, 180(7), pp.934-943.
- 63. Cui, D., Tang, Y., Jiang, Q., Jiang, D., Zhang, Y., Lv, Y., Xu, D., Wu, J., Xie, J., Wen, C. and Lu, L., 2021. Follicular helper T cells in the immunopathogenesis of SARS-CoV-2 infection. Frontiers in Immunology, 12, p.731100.
- 64. Senapathi, J., Bommakanti, A., Vangara, S., & Kondapi, A. K. (2021). Design, synthesis, and evaluation of HIV-1 entry inhibitors based on broadly neutralizing antibody 447-52D and gp120 V3loop interactions. Bioorganic Chemistry, 116. https://doi.org/10.1016/j.bioorg.2021.105313

Molecular interactions of Epap-1 and small molecules with spike protein: Development of SARS Cov-2 entry inhibitors

by Vidya CV

Librarian

Indira Gandhi Memorial Library
UNIVERSITY OF HYDERABAD
Central University P.O.
HYDERABAD-500 046.

Submission date: 25-Jun-2024 03:01PM (UTC+0530)

Submission ID: 2408383450 File name: Vidya_C_V.pdf (5.12M)

Word count: 13939 Character count: 73318

Molecular interactions of Epap-1 and small molecules with spike protein: Development of SARS Cov-2 entry inhibitors

49 _%	13%	48%	8%
SIMILARITY INDEX	INTERNET SOURCES	PUBLICATIONS	STUDENT PAPERS
PRIMARY SOURCES			
Kammili pregnar	nitta Voina, Sarit , G. Mahalakshr ncy associated p and ACE2 intera ov-2 vertical tran	ni et al. "Effect rotein-1 on Sp ections: Implic esmission", Pla	ations in
2 dspace. Internet Sour	uohyd.ac.in		Gachibowii, Hyderasa 2%
3 Submitt Hyderak Student Pape		of Hyderabad	1 %
4 journals Internet Sour	.plos.org		1%
5 www.nc	bi.nlm.nih.gov		1 %
6 www.na	iture.com		<1%

www.frontiersin.org

15	www.mdpi.com Internet Source	<1%
16	journals.viamedica.pl Internet Source	<1%
17	Submitted to UC, San Diego Student Paper	<1%
18	pure.uva.nl Internet Source	<1%
19	baadalsg.inflibnet.ac.in Internet Source	<1%
20	Peiwen Zhou, Zonghui Li, Linqing Xie, Dong An, Yaohua Fan, Xiao Wang, Yiwei Li, Xiaohong Liu, Jianguo Wu, Geng Li, Qin Li. "Research progress and challenges to coronavirus vaccine development", Journal of Medical Virology, 2020 Publication	<1%
21	www.biorxiv.org Internet Source	<1%
22	www.thermofisher.com Internet Source	<1%
23	link.springer.com Internet Source	<1%
24	www.degruyter.com Internet Source	<1%

25	Submitted to Imperial College of Science, Technology and Medicine Student Paper	<1%
26	benthamscience.com Internet Source	<1%
27	Sanjay Kumar Mishra, Timir Tripathi. "One year update on the COVID-19 pandemic: Where are we now?", Acta Tropica, 2021	<1%
28	dspace.mit.edu Internet Source	<1%
29	Submitted to University of Kent at Canterbury Student Paper	<1%
30	d-nb.info Internet Source	<1%

Exclude quotes

On

Exclude matches

< 14 words

Exclude bibliography On



University of Hyderabad Hyderabad-500046. Telangana, India.

Plagiarism free certificate

This is to certify that the similarity index of the thesis entitled "Molecular interaction of Epap-1 and small molecules with Spike protein: Development of SARS-CoV-2 entry inhibitors" by C V Vidya, as checked by the library of the University of Hyderabad is 49%.

Out of this, 40%similarity has been identified by candidate C V Vidya's own publication. The publication of C V Vidya is a part of the thesis and has been mentioned there. The remaining 9% similarity, much is generic in nature and pertains to standard notations and definitions of the subject matter.

Hence, the present thesis may be considered plagiarism-free.

Publication details:

Voina VC, Swain S, Kammili N, Mahalakshmi G, Muttineni R, Chander Bingi T, Kondapi AK. Effect of Early pregnancy associated protein-1 on Spike protein and ACE2 interactions: Implications in SARS Cov-2 vertical transmission. Placenta. 2024 May 17;152:39-52. doi: 10.1016/j.placenta.2024.05.128. Epub ahead of print. PMID: 38788480

Prof. Anand K Kondapi

PrSpervisor
Senior Professor
Dept. of Biotechnology & Bioinformatics
School of Life Sciences
University of Hyderabad
Gachibowil, Hyderabad-500 046.



Contents lists available at ScienceDirect

Placenta

journal homepage: www.elsevier.com/locate/placenta





Effect of Early pregnancy associated protein-1 on Spike protein and ACE2 interactions: Implications in SARS Cov-2 vertical transmission

Vidya Chitta Voina ^a, Sarita Swain ^a, Nagamani Kammili ^b, G. Mahalakshmi ^c, Radhakrishna Muttineni ^d, Thrilok Chander Bingi ^e, Anand K. Kondapi ^a, *

- ^a Department of Biotechnology and Bioinformatics, School of Life Sciences, University of Hyderabad, Hyderabad, 500046, India
- b Department of Microbiology, Gandhi Medical College and Hospital, Secunderabad, India
- c Department of Obstetrics and Gynecology, Gandhi Medical College and Hospital, Secunderabad, India
- ^d Virus Research Laboratory, Department of Zoology, Osmania University, Hyderabad, India
- e Department of General Medicine, Gandhi Medical College and Hospital, Secunderabad, India

ARTICLE INFO

Handling Editor: Dr A Perkins

Keywords:
Early pregnancy
SARS Cov-2
Spike protein
Receptor binding domain protein
Early pregnancy-associated Protein-1
ACE2
Anti-viral

ABSTRACT

Introduction: Several factors influence transmission of 2019-nCoV from mother to fetus during pregnancy, thus the dynamics of vertical transmission is unclear. The role of cellular protective factors, namely a 90 KDa glycoprotein, Early pregnancy-associated protein (Epap-1), expressed by placental endothelial cells in women during early pregnancy would provide an insight into role of placental factors in virus transmission. Since viral spike protein binding to the ACE2 receptors of the host cells promotes virus invasion in placental tissue, an analysis of effects of Epap-1 on the Spike-ACE2 protein binding was studied.

Methods: Epap-1 was isolated from MTP placental tissue. Molecular interaction of Epap-1 and variants of the spike was analyzed in silco. The interaction of Epap-1 with Spike and RBD were analyzed using ELISA and immunofluorescence studies.

Results: The results in silico showed an interaction of Epap-1 with S-protein at RBD region involving K417, Y449, Y453, Y456, Y473, Q474, F486, Q498, N501 residues of spike with Y61, F287, I302, N303, N305, S334, N465, G467, N468 residues of Epap-1 leading to interference of S-protein and ACE2 interaction [1]. Further, the interaction is conserved among the variants. The studies *in vitro* confirm that Epap-1 affects S protein-ACE2 and RBD- ACE2 binding, thus suggesting that during early pregnancy, SARS CoV-2 infection may be protected by Epap-1 protein present in placental tissue. The results were further confirmed by pseudovirus expressing Spike and RBD in an infection assay.

Discussion: Epap-1 interferes with Spike and RBD interaction with ACE2, suggesting a possible mechanism of the antiviral environment during pregnancy.

1. Introduction

Severe acute respiratory syndrome Coronavirus-2 (SARS-CoV-2) was reported in the Wuhan region, China, on December 31, 2019, with an exponential expansion of the infection all over the world (WHO, 2020). The virus is prone to several mutations, evolving into variants classified in terms of mutations observed in Spike protein (S-protein), Omicron being the current variant (WHO, 2021). Based on susceptibility to the virus infection, pregnant women reported an increase in mortality rate due to serious complications [2,3]. Abnormalities in the placenta have been reported in pregnant women infected with SARS-CoV-2 in terms of

extensive intervillous fibrin deposition, maternal vascular malperfusion of the placental, and choriohemangioma [4–6]. An increased risk of preeclampsia, onset gestational diabetes, hypertensive disorders, fetal malformations, etc., were reported in women infected with SARS-CoV-2 compared to women without infection [7–11], in addition, maternal mortality was reported to be high among women admitted with SARS-CoV-2 infection 1.5 per 1000, compared to non-pregnant women, i.e., 1.2 per 1000 [12].

Studies on vertical transmission of the virus reported mixed results, though the majority of studies were during the third trimester of pregnancy [13,14]. Neonates from Cov-2 infected women showed positive

https://doi.org/10.1016/j.placenta.2024.05.128

Received 30 November 2023; Received in revised form 24 March 2024; Accepted 15 May 2024 Available online 17 May 2024

0143-4004/© 2024 Elsevier Ltd. All rights are reserved, including those for text and data mining, AI training, and similar technologies.

^{*} Corresponding author. E-mail address: akondapi@gmail.com (A.K. Kondapi).